

NATURE OF DEFORMATION ACROSS THE GRENVILLE FRONT, ONTARIO.

CHARACTERIZATION OF THE NATURE OF DEFORMATION
AND METAMORPHIC GRADIENT ACROSS THE GRENVILLE FRONT
TECTONIC ZONE IN CARLYLE TOWNSHIP, ONTARIO.

By

LYNN LOUISE O'DONNELL

A Thesis

Submitted to the School of Graduate Studies
in Partial Fulfilment of the Requirements
for the Degree
Master of Science

McMaster University

September 1986

MASTER OF SCIENCE (1986)

McMASTER UNIVERSITY

(Geology)

Hamilton, Ontario

TITLE: Characterization of the Nature of Deformation and
 Metamorphic Gradient Across the Grenville Front
 Tectonic Zone in Carlyle Township, Ontario

AUTHOR: Lynn Louise O'Donnell, B.Sc. (McMaster University)

SUPERVISOR: Professor P.M. Clifford

NUMBER OF PAGES: xii, 199

ABSTRACT

The last major episode of deformation occurred in the area studied during the Grenville orogeny (~1000 Ma ago). Deformation of this zone is characterized by a northeast trending penetrative foliation and southeast plunging mineral lineation which increase in intensity and decrease in inclination from northwest to southeast. The deformation was imposed during reverse fault movement in which the southeastern block (the Grenville province) was vertically displaced on the order of 20 kilometers above the adjacent block (the Southern province). The Killarney belt of granites, which separate the Grenville province from the Southern province in this area, are intrusive into the Huronian metasediments and predate the Grenville orogeny. These granites also show evidence of Grenvillian deformation.

Paleopiezometry has shown that the differential stress during deformation increases from less than 1 Kbar to more than 6 Kbar from southeast to northwest. The microstructural strain features in quartz and feldspar and the mineralogy indicate that a temperature change of 400 C is associated with this change in differential stress. Kinematic analysis of mylonites supports the reverse fault model of the Grenville Front.

ACKNOWLEDGMENTS

Dr. P.M. Clifford, who has supported me wholeheartedly throughout my years at McMaster, suggested the topic and enthusiastically supervised the research. Dr. A. Davidson, provided field support and helpful discussions in the field. Field assistance was provided by Mr. C. Rice. I would like to thank Frank Fueten and Andy Fyon for their helpful comments, Jack Whorwood for his expert photography, and Len Zwicker for preparing thin sections of my very hard samples. I would also like to thank my husband, Dave, for moral support and much needed assistance with drafting and editing.

Financial assistance for the 1984 field season was supplied by the Geological Survey of Canada. Scholarship funding was supplied by NSERC.

TABLE OF CONTENTS

CHAPTER	PAGE
1. INTRODUCTION	1
Location and Access	4
Physical Features and General Geology	5
Previous Work	6
2. PETROGRAPHY	
Introduction	12
Bell Lake Granite	13
Terry Lake Diorite	26
Killarney Granite	27
Fine Grained Granite	29
Tonalite	30
Augen Gneiss	33
Paragneiss	37
Breccia	41
Pegmatites	42
3. STRUCTURAL ANALYSIS: MACROSCOPIC	
Introduction	46
Structural Geometry	47
Geometry of Area 1	49
Geometry of Area 2	52

CHAPTER	PAGE
Geometry of Area 3	57
Geometry of Area 4	65
Geometry of Area 5	66
Geometry of Area 6	71
Regional Shear Zone Geometry: Introduction	73
Regional Development of Shear Zones: Relationships Between Deep Level Ductile and High Level Brittle	75
Distribution of Brittle/Ductile Strain	79
Regional Trends in Fabric	83
4. MICROSTRUCTURES	
Introduction	90
Mylonites	91
QUARTZ MICROSTRUCTURES	
Progressive Development of Microstructural Strain Features	94
Variations in Microscopic Strain Features	99
Discussion of Quartz Microstructures	108
FELDSPAR MICROSTRUCTURES	
Progressive Development of Microstructural Strain Features	116
Variations in Strain Features in Feldspar	120
Feldspar Fracture Distribution	134
Discussion of Feldspar Microstructures	142

CHAPTER	PAGE
KINEMATIC ANALYSIS	
Introduction	148
C & S Fabrics	148
5. STRESS, STRAIN AND METAMORPHISM	
Theory and Application of Paleopiezometers	160
Introduction	160
Energy Controls	161
Diffusion of Point Defects	162
Derivation of the Paleopiezometer	163
Limitations	164
STRAIN ESTIMATE	169
METAMORPHISM	172
Quartz	176
Feldspar	177
DISCUSSION	178
6. CONCLUSIONS	
Suggestions for Further Research	185
REFERENCES	186
APPENDIX	194

LIST OF FIGURES

FIGURE	PAGE
1. Subprovinces of the Southwestern Grenville Province	3
2. Lithologic Map	pocket
3. Triangular Plot of Modal Analyses	15
4a. Bell Lake Granite, Biotite Foliation	18
b. Bell Lake Granite, Primary Foliation	18
c. Compositional Variation	19
5. Quartzite-Bell Lake Granite Contact	20
6. Augen Mylonite	21
7ab. Quartzite Xenoliths	22
c. Folded Quartzite Xenolith	23
d. Dent du Cheval Texture	23
ef. Argillite Xenoliths	24
gh. Mafic Xenoliths	25
8ab. Tonalite	31
c. Tonalite	32
9a. Augen Gneiss	35
b. Ptygmatic Folding in a Pegmatite	35
c. Folded Megacrystalline Pegmatite	36
10ab. Streaky Biotite Gneiss	38
11ab. Quartz-Feldspar-Biotite Paragneiss	39
c. Quartz-Feldspar-Biotite Paragneiss	40
d. Folded Migmatite	40

FIGURE	PAGE
12ab. Breccia	44
cd. Breccia	45
13. Structural Divisions Map	50
14. Fabric Diagrams for Area 1	55
15. Fabric Diagrams for Area 2	56
16a. Mineral Lineation	60
b. Interlayering of Units	60
c. Crosscutting Relationship of Mylonite Zones	61
17. Fabric Diagrams for Area 3	62
18. Fabric Diagrams for Area 4	68
19. Fabric Diagrams for Area 5	69
20. Fabric Diagrams for Area 6	72
21. Brittle/Brittle-Ductile/Ductile Fault Geometry	77
22a. Offset Dyke in Bell Lake Granite	81
22b. En Echelon Tension Fractures	81
23. Foliation Map	pocket
24. Lineation Map	pocket
25. Trend in Fabric	84
26a. Deformation Bands in Quartz	97
b. Strain Features in Quartz	97
c. Quartz Ribbon Aggregate	98
d. Quartz-Feldspar Mylonite	98
27. Microfault with Fault Gouge	102
28a. Recrystallized Quartz Aggregate	103

FIGURE	PAGE
28b.Quartz Ribbon	103
28cd.Core and Mantle Structure in Quartz	104
29. Quartz Ribbon	113
30. Dynamically Recrystallized Quartz Ribbon	113
31. Deformation Textures in Granite	114
32. Deformed Quartz Grain	115
33a.Deformation Twins in Plagioclase	121
b.Kink Band	121
c.Plagioclase Porphyroblast in Ultramylonite	122
d.Core and Mantle Structure in Feldspar	122
34. Fractures in Feldspar	128
35. Strain Features in Feldspar	129
36. Perthite Flames	130
37. Fracture and Separation of Feldspar	130
38. Deformation Textures; Area 3A	131
39. Recrystallization Textures in Feldspar	132
40. Deformation Textures; Area 6	133
41. Feldspar Fracture Diagrams	136-140
42. Feldspar Fracture and Rotation	141
43. C & S Fabric	156
44. Sigmoidal Quartz Aggregate	157
45. Fabric Asymmetry in Micas	157
46. Mica Fish	158
47. Ultramylonite; Polished Slab	159

FIGURE

PAGE

48. Symmetrical Biotite in XY Section

171

49. Isograd Map

175

LIST OF TABLES

TABLE	PAGE
1. Modal Analyses	14
2. Foliations from Fabric Diagrams	85
3. Lineations from Fabric Diagrams	86
4. Paleopiezometers for Quartz	167
5. Differential Stress from Paleopiezometry	168
6. Mineral Assemblages	174

CHAPTER 1

Introduction

The Grenville Front, which marks the northwest boundary of the Grenville Province (Figure 1), manifests itself in many places as a zone of intense deformation, ranging in style from cataclastic to ductile. This deformation was, in part, the result of reverse fault movement along the Front during the Grenville Orogeny (~1000Ma; e.g. Wynne-Edwards, 1972). Deformation associated with this displacement, however, is not restricted to a single fault plane, but becomes increasingly penetrative southeastward from the Grenville Province boundary, and has produced several zones of sheared and mylonitized rocks. Due to the complex history of the Grenville Province, and adjacent structural provinces of the Canadian Shield, recognition of Grenvillian

deformation is not straightforward.

The northwest boundary of the area mapped is defined by the contact between Huronian sedimentary rocks, to the northwest, and granitoid rocks that form a number of northeast-elongate bodies referred to as the 'Grenville Front Granites' by Frarey and Cannon (1968). This contact follows a line connecting Kakakise, Ruth-Roy and Bell Lakes, and, according to Frarey (1985) and Frarey and Cannon (1968), separates the Southern and Grenville Provinces, characterized respectively by east-trending steeply folded Huronian strata and adjacent northeast trending, southeast dipping gneissic rocks. Card and Lumbers (1977), however, placed the Grenville Front farther east, passing through Carlyle Lake and the southeast part of Johnny Lake: this is within the Grenville Front Tectonic Zone of Lumbers (1978).

A small segment of the Grenville Front southwest of Sudbury, Ontario, has been studied in order to characterize the nature of the deformation which has occurred within part of the Tectonic zone adjacent to the Southern Province. The area is underlain by various granitoid phases and metasedimentary xenoliths and screens, all cut by dykes of diabase, pegmatite and fine grained granite. The development of the structural fabric, sense of movement along shear planes, metamorphic gradient and the petrography of granites and gneisses have also been studied.

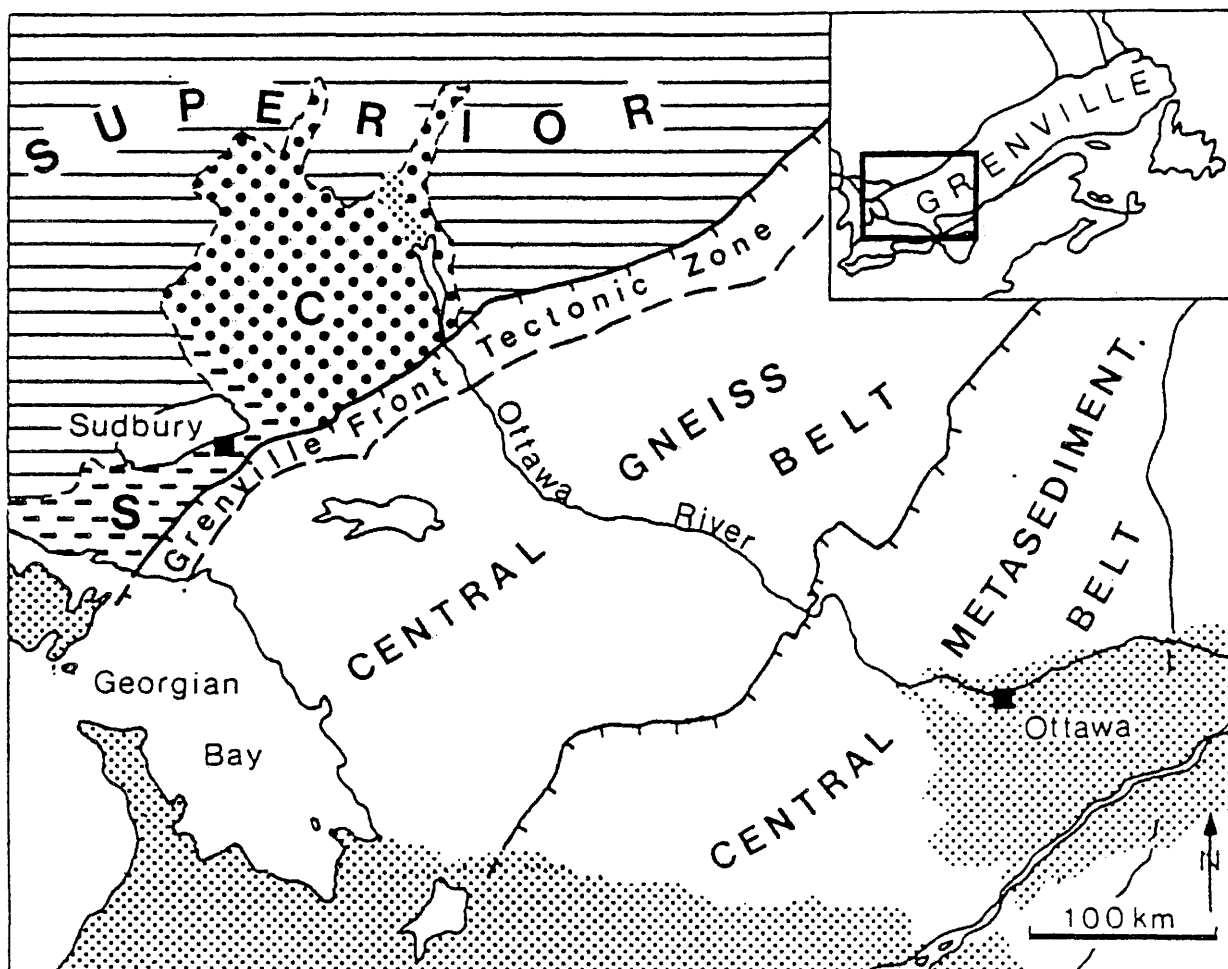


Figure 1. Subprovinces of the southwestern Grenville Province, after Wynne-Edwards (1972). S - Southern Province, C - Huronian cover on the Superior Province (Cobalt Plate). Paleozoic cover is stippled.

Location and Access

The study area is located approximately 60 km southwest of Sudbury, Ontario, where the Grenville Front follows Carlyle, Johnny and Bell Lakes (Figure 2, pocket) in Carlyle Township. The area mapped is triangular in shape and is bounded by Ontario Highway 637 to the south, the Carlyle Township Lines to the east and west and the Huronian-granite contact to the north. The total area mapped encompasses 50 square kilometers.

The area is easily reached by vehicle from highway 637, the Bell Lake Road and small cottage roads. These roads also provide access to a large number of inter-connected lakes which span the length of the study area.

Mapping of the area was carried out by road, canoe and foot traverses at a scale of 1:10,000 or less. Foot traverses were planned based on outcrop location in air photographs such that all sizable outcrops were observed. Road and lakeshore outcrops were mapped in detail. Accomodation was provided by cottages on Carlyle Lake.

Physical Features and General Geology

The northwest boundary of the area is flanked by the Lorrain and Bar River Quartzites of the Huronian Supergroup. These very resistant units create a rugged topography of prominent bare white hills and broad east-west trending ridges which together form the eastern most and highest part of the La Cloche Mountains.

The rocks of the Grenville terrain are much less resistant to erosion than the quartzites. The topography consists of low lying narrow ridges separated by narrow swamp filled valleys . This topography is largely bedrock controlled such that the general trend of the ridges is in a northeasterly direction.

Adjacent to, and intruding the Huronian metasediments, and bounded to the southeast by the Grenville gneisses, is the strip of granitic rocks referred to by Frarey and Cannon (1968) as the "Grenville Front Granites". This strip is composed of a suite of deep red to pink granitic bodies aligned in a northeasterly direction. The sharp colour contrast between these units and the white rocks of the Southern Province makes this a dramatic and easily recognized contact. The granites have an intermediate resistance to erosion relative to the gneisses and the quartzites and form smooth rounded hills separated by narrow, deep lakes.

Previous Work

The Grenville Province which passes through Ontario, Quebec and Labrador, is the youngest structural province of the Canadian Shield. It extends for 2000 kilometers in a northeasterly direction, from northern Georgian Bay in Ontario to the coast of Labrador. The exposed width of the Province varies from 300 to 450 kilometers.

The northwest boundary of the Grenville Province is a structural discontinuity known as the Grenville Front. Along this boundary, Grenville Province rocks abut rocks of the Southern, Superior, Churchill and Nain structural provinces. To the southeast, The Grenville Province is buried beneath Paleozoic cover.

Geological investigations have been carried out in the Grenville Province for over a century. In spite of this, progress toward improving our understanding of the origin of the province has been slow. Due to the complex nature of the Grenville Province as a whole, any straight forward interpretation of origin cannot be made. Several regional studies have been published in the past two decades, the best known being that of Wynne-Edwards (1972). Others include Lumbers (1978) and Stockwell (1982). For a complete review of the literature on the Grenville Province prior to 1972, the

reader is referred to Wynne-Edwards.

Wynne-Edwards (1972) has divided the Grenville Province into seven major subdivisions with subsidiary segments based on differing structural and metamorphic styles. These are:

- I Grenville Foreland Belt
 - Ia) Southern Foreland Zone
 - Ib) Superior Foreland Zone
 - Ic) Churchill Foreland Zone
 - Id) Nain Foreland Zone
- II Grenville Front Tectonic Zone
- III Central Gneiss Belt
- IV Central Metasedimentary Belt
- V Central Granulite Terrain
- VI Baie Comeau Segment
- VII Eastern Grenville Province

For the purposes of this study, only Ia and II are discussed.

I Grenville foreland Belt

The Grenville foreland belt lies to the northwest of the Grenville Front. It is a zone 20 to 60 kilometers wide which has a northwest boundary defined by the limit of northeast trending southeast dipping cleavage, faults and folds commonly associated with the Grenville Orogeny.

Ia) Southern Foreland Zone

The Southern foreland zone lies within the Penokean Fold Belt of the Southern Province. In this zone rocks of the Huronian Supergroup have been deformed during the Hudsonian Orogeny (~1850Ma). Superimposed on the east-west trending folds are northeast trending structures believed to be the result of the Grenville Orogeny. Radiometric K-Ar dates determined for rocks of the Southern foreland zone have not been reset to Grenvillian ages.

II Grenville Front Tectonic Zone

The Grenville Front Tectonic Zone forms a belt 15 to 80 kilometers wide, having a strong and persistent northeast trending foliation and southeast plunging lineation. The dominant rock type in the zone is quartzo-feldspathic gneiss of high metamorphic grade (commonly upper amphibolite to granulite grade). The belt has conspicuously low magnetic relief and no magnetic texture which is in sharp contrast to the complicated and detailed pattern of the rest of the Grenville Province. A negative Bouguer anomaly, 50 to 80 kilometers wide and extending for more than 1100 kilometers along strike also coincides with this zone. Seismic profiles across the Grenville Front Tectonic Zone suggest that the underlying crust is 5 to 8 kilometers thicker than elsewhere in the Shield (normal thickness: 34 to 36 kilometers). The Grenville Front Tectonic Zone is also the locus of numerous

parallel zones of cataclasis and mylonitization.

The Grenville Front which marks the northwest limit of the Grenville Province has long been recognized as a major tectonic feature of the Canadian Shield but the exact definition of the Grenville Front is still an issue of controversy. The term "Grenville Front" was first used by Derry (1950) on a Tectonic Map of Canada but the feature was not defined in that publication. Part of the problem arises from the fact that the structural nature of the Front changes along its length. Different segments are marked by any one of the following: a fault, a fault zone, a metamorphic boundary, a locus of mylonites or shear zones, intrusive igneous activity.

Wynne-Edwards (1972) defined the boundary on the basis of geochronology as the line across which K-Ar ages were reset to 1000 Ma. Stockwell (1982) used a combination of geochronological, structural and metamorphic criteria to define the boundary. Other definitions have also been proposed.

The southwestern Grenville Front has been of particular interest since the mid 1800's. Nineteenth century investigators included Murray (1849,1857), Bell (1878,1891,1898) and Barlow (1893). Bell (1898) produced the first map showing all the major rock units. He recognized the

post-Huronian age of the granites which separate the metasedimentary rocks of the Southern Province from the gneisses of the Grenville Province, which he called "the Killarney belt of granites". The abrupt change in lithology from supracrustals to quartzofeldspathic gneisses across the Grenville Front in the Sudbury region and the prevailing high grade of regional metamorphism in the Grenville Province was recognized by Wilson in 1918.

Systematic mapping in the southwestern Grenville Province and the adjacent area in the Southern Province was first done by Quirke (1917), Collins (1916) and Eskola (1922, in Collins, 1925). In Collins (1925), the stratigraphic and structural relationships of the Huronian rocks of the Southern Province were established as well as the marked change in structural trend across the southwest segment of the Grenville Front. This boundary Collins referred to as "the limit of Huronian strata". A few years later, Quirke and Collins (1930) published their conclusions on specific relationships between the Huronian sediments and the Grenville gneisses. The "Killarney belt of granites" were thought to be melted and remobilized or metasomatized Huronian sediments and the gneisses, the result of wholesale granitization, the large contrast in metamorphism on either side of the granites being the result of great vertical displacement along the structural break. Lawson (1929) after visiting the area,

agreed on the post-Huronian age of the granites but gave evidence for the intrusive nature of the granites.

Until Frarey and Cannon (1968) and Frarey (1985), no comprehensive study had been done in this area since 1926 but many specialized studies have been carried out. These include Jones (1930), Dollase (1962), Brooks (1967,1976) and Henderson (1967,1972). Even with the restricted areas covered by these studies, the precise location of the southwest Grenville Front has yet to be agreed upon.

CHAPTER 2

PETROGRAPHY

Introduction

The areal distribution of units, as they have been defined in this study, is shown in figure 2. Most of these units have previously been described by other authors who have worked along this section of the Grenville Front (eg. Brooks, 1964; Frarey, 1985). Some of the contacts between units which were determined through detailed mapping vary slightly from that published by Frarey (1985). A large number of contacts were covered by swamps or overburden and had to be inferred and the nature of these contacts could not generally be determined. The nature of those contacts that were observed directly includes intrusive, sheared or faulted, and gradational. The division of the units

described is based largely on field descriptions. A more detailed petrographic study of the area may result in modifications to many of the boundaries.

The modal proportions of various samples were determined by point counting of thin sections on the petrographic microscope using a mechanical stage with a point spacing of 0.3 millimeters. The results of this are shown in table 1. The location of each sample counted is shown in figure 2. Each of these has also been plotted on a quartz-feldspar triangular diagram (Figure 3).

Bell Lake Granite

The Bell Lake Granite is the largest and most distinctive unit in the area and is one member of the "Killarney Belt of Granites". It is a lenticular body, extending from Carlyle Lake northeastward for 17.6 kilometers to Annie Lake (located 10 kilometers northeast of the study area), and has a maximum width of approximately 2 kilometers. This unit underlies approximately one third of the study area which accounts for the southwestern half of the of its total extent.

The Bell Lake Granite is a coarse grained light pink to red porphyritic granite to granodiorite with a black biotitic matrix. The unit can range from massive to very well foliated with the foliation commonly being marked by the

Sample	Quartz	K-sper	Plag.	Bio.	Epidote	Musc.	Hbd.	Cht.	Cte.	Sphene	Mte.	Garnet	TOTAL	* Qtz,Ksp, Plag	Rock Type
P10	34.0	17.8	41.5	4.7	-	0.6	0.3	-	-	-	0.3	0.1	3290	93.3	Granodiorite
P35-1	20.7	29.5	40.5	4.9	-	-	0.8	1.5	-	1.8	0.3	-	2052	90.7	Qtz Monzonite
P35	25.2	16.5	51.8	3.9	0.5	-	0.2	1.1	-	0.5	0.2	-	2058	93.5	Granodiorite
P35a	22.5	18.1	46.6	9.5	0.8	1.5	-	trace	-	0.3	0.3	-	4109	87.2	Granodiorite
P45	27.6	6.3	59.4	3.4	-	1.9	-	-	0.2	0.3	0.5	trace	1134	93.3	Tonalite
P54	26.5	33.1	32.9	6.1	-	0.1	-	-	-	-	0.9	-	2113	92.5	Granite
P102	26.6	43.0	28.1	0.2	0.2	1.2	-	-	-	-	0.6	-	2035	97.7	Granite
P109	16.5	23.6	41.5	9.3	4.1	2.4	-	-	-	1.3	1.2	-	1206	81.6	Granite
P113	0.1	5.1	50.6	8.2	4.4	-	29.4	-	-	0.7	0.8	-	1054	55.8	Diorite
P115	15.2	26.1	45.0	7.2	2.8	1.7	-	-	0.1	1.1	0.8	-	4093	86.3	Qtz Monzonite
P121	22.2	26.3	32.2	9.0	4.6	1.5	-	-	-	0.5	0.1	-	788	80.7	Granite
P139	24.7	29.0	29.4	8.3	3.8	2.5	-	-	trace	0.3	0.4	0.1	5160	83.1	Granite
P204	25.6	35.6	11.1	0.4	12.6	2.6	-	10.2	-	1.6	0.1	-	1200	72.3	Granite
P244	20.8	44.8	28.8	0.8	-	-	2.5	-	-	-	0.9	0.5	2078	94.4	Granite
P245	16.9	42.3	24.0	-	-	-	15.1	-	-	-	1.0	0.4	2084	83.2	Granite
P268	26.7	16.3	41.8	5.7	1.4	1.9	-	4.0	-	0.2	1.2	0.6	2059	84.8	Granodiorite
P269	30.9	29.3	28.1	8.0	1.2	2.5	-	-	-	-	-	0.5	1021	88.3	Granite
P283	32.3	28.6	35.6	0.7	0.1	trace	-	1.5	-	0.1	0.7	-	2062	96.5	Granite
P286	28.5	29.4	37.0	0.05	-	0.05	-	3.9	-	0.1	0.8	0.1	2051	94.9	Granite
P347	32.4	30.6	30.7	1.6	1.9	2.5	-	0.1	-	-	0.2	trace	6183	93.7	Granite
P361	32.6	20.0	35.1	3.3	3.2	5.6	-	-	-	-	0.1	-	6016	87.7	Granite
P368	31.0	25.5	31.6	1.4	2.5	7.7	-	-	-	-	0.3	-	4102	88.1	Granite
R95	26.6	28.3	35.7	5.5	0.4	2.0	-	-	-	-	0.3	0.4	1167	90.6	Granite
P10-1	7.1	20.8	45.9	20.0	-	-	-	0.8	-	1.7	1.5	0.2	2638	73.8	Qtz Monzodiorite
P10b	22.3	29.4	37.6	-	2.7	-	-	7.1	-	-	0.6	trace	524	89.3	Granite
P52	20.6	7.3	60.3	10.8	-	-	-	trace	-	-	0.3	-	2042	88.2	Granodiorite
P53	32.9	13.9	50.7	2.2	-	0.1	-	-	-	-	trace	-	2726	97.5	Granodiorite
P460	16.4	5.1	45.9	18.3	4.4	7.5	-	0.1	-	0.6	0.1	0.2	1485	77.4	Granodiorite
P527	13.5	15.6	45.6	23.0	1.1	-	-	0.3	-	0.1	0.7	-	1071	74.7	Qtz Monzodiorite
P529	22.6	20.4	47.0	5.2	0.1	-	3.7	-	-	0.3	0.5	-	1019	90.0	Granodiorite
P602	21.1	21.1	40.1	16.4	-	-	-	0.6*	-	-	0.3	-	2136	82.3	Granodiorite

TABLE 1: Modal Analyses.

* - Serpentine

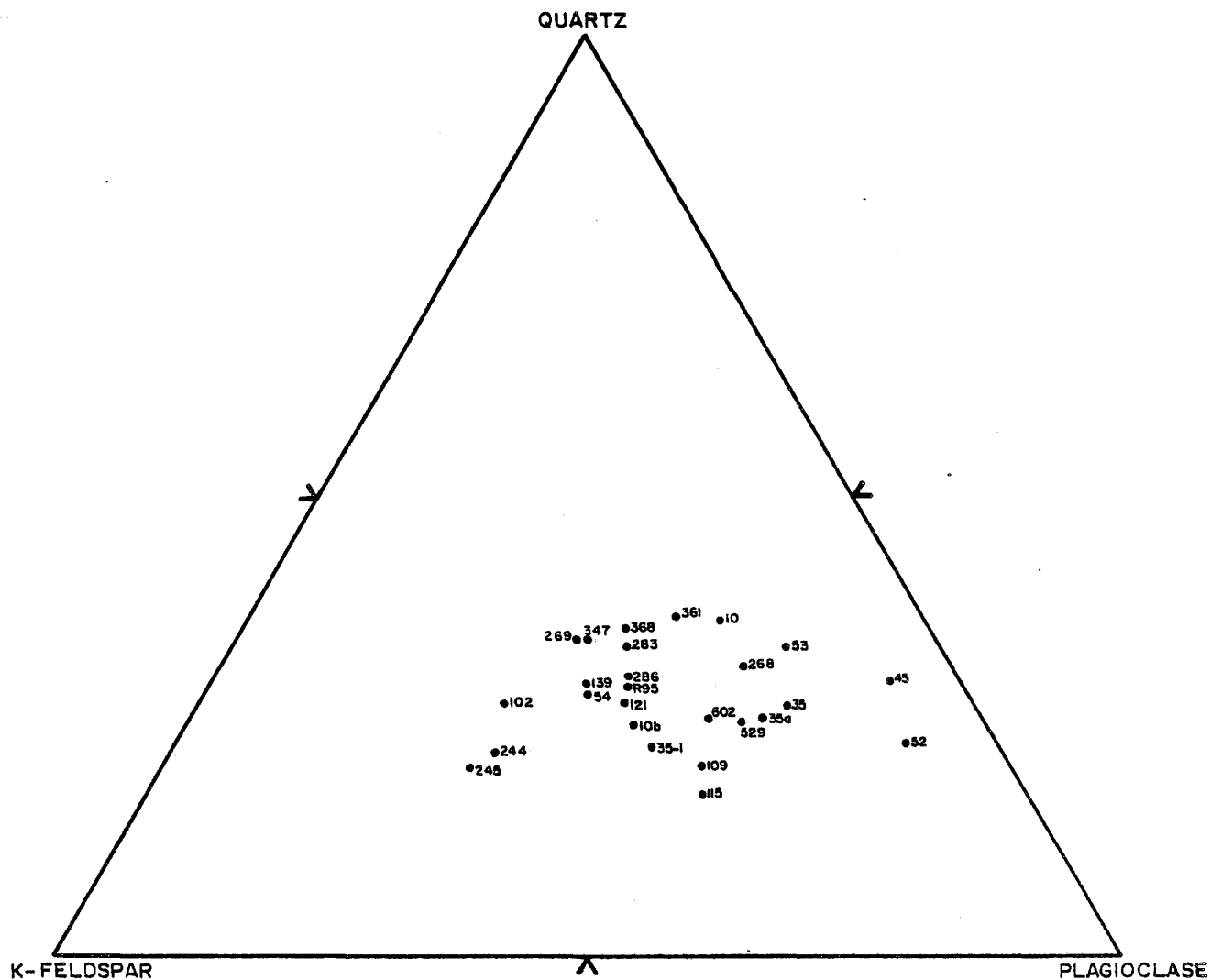


Figure 3. Triangular plot of modal analyses of batholithic rocks discussed in the text and listed in Table 1 with more than 80% Quartz + Plagioclase + K-Feldspar. Classification based on that of Streckeisen (1976).

parallel alignment of biotite flakes (Figure 4a). The phenocrysts range from 0.5 to 6 centimeters in length with the average being 2 centimeters. These are locally arranged in parallel alignment which is most likely a primary feature (Brooks, 1976; Figure 4b). The modal abundance of phenocrysts varies widely, from 10 to 75 percent, but is normally close to 50 percent.

The matrix is generally coarse grained, phaneritic, hypidiomorphic granular having an average grain size of 5 millimeters. The matrix consists of quartz, microcline, perthite, oligoclase-andesine and biotite. Minor components and accessories include hornblende, muscovite, magnetite, allanite, sphene, epidote, garnet, sulphides, chlorite and calcite. The modal composition of the Bell Lake Granite locally varies widely (Figure 4c) in all of the major, minor and accessory components.

The northwest contact of the Bell Lake Granite is intrusive into the Huronian metasediments from the northeast tip of Bell Lake to the southwest tip of Ruth-Roy Lake. This contact is generally marked by a zone a few tens of meters wide in which Bell Lake Granite has intruded along bedding planes of the quartzite. As this zone is crossed to the southeast, the proportion of granite to quartzite increases until the quartzite occurs as definable xenoliths in a granitic body (Figure 5a,b). From the southwest tip of

Ruth-Roy Lake the Bell Lake Granite, no longer in contact with the Huronian metasediments, begins to taper down toward Carlyle Lake where it is drawn out into a thin band or zone interlayered with non-porphyrific coarse grained granite, pegmatites, fine grained porphyritic felsite dykes and mylonite.

The southeast boundary of the Bell Lake Granite is a sheared contact which follows a line extending from the northeast at Turbid Lake to the southwest tip of Carlyle Lake. Along this contact the Bell Lake Granite is strongly deformed and can generally be recognized as a black augen mylonite (Figure 6a,b).

A large number of sedimentary xenoliths are found within the body of the Bell Lake Granite. These include large quartzite or quartz-arenite xenoliths ranging in size from one to a few tens of meters (Figure 7a,b,c), small, elliptical, fine grained, black quartz-biotite xenoliths which generally possess 'dents du cheval' texture (Figure 7d) and a large argillaceous xenolith which extends for ~200 meters along the west shore of the central section of Johnny Lake (Figure 7e,f).

Figure 4a. Foliated Bell Lake Granite. The foliation can be seen to be defined by the parallel alignment of biotite flakes which are concentrated into narrow zones. Bell Lake Road, south of Bell Lake.

Figure 4b. Primary foliation in the Bell Lake Granite defined by the parallel alignment of feldspar phenocrysts. Bell Lake Road, east of Bell Lake.



Figure 4c. Compositional variations in the Bell Lake
Granite. Bell Lake Road, East of Bell Lake.



© 2017



Figure 5. Interlayering of quartzite and Bell Lake Granite along the northwestern contact a) at Johnnie Lake (hammer rests on an inclusion of amphibolite), b) at Ruth-Roy Lake. Hammer aligned north-south, head to the south.



Figure 6. Augen mylonite produced from a Bell Lake Granite parent. a) Johnnie Lake, 5cm lens cap for scale. b) Carlyle Lake, 4cm wooden match for scale.

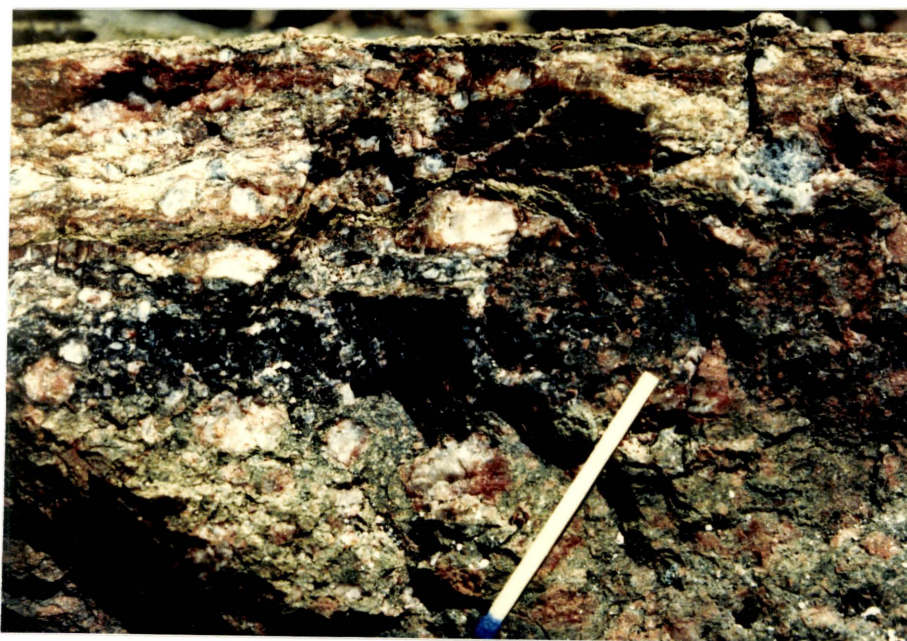
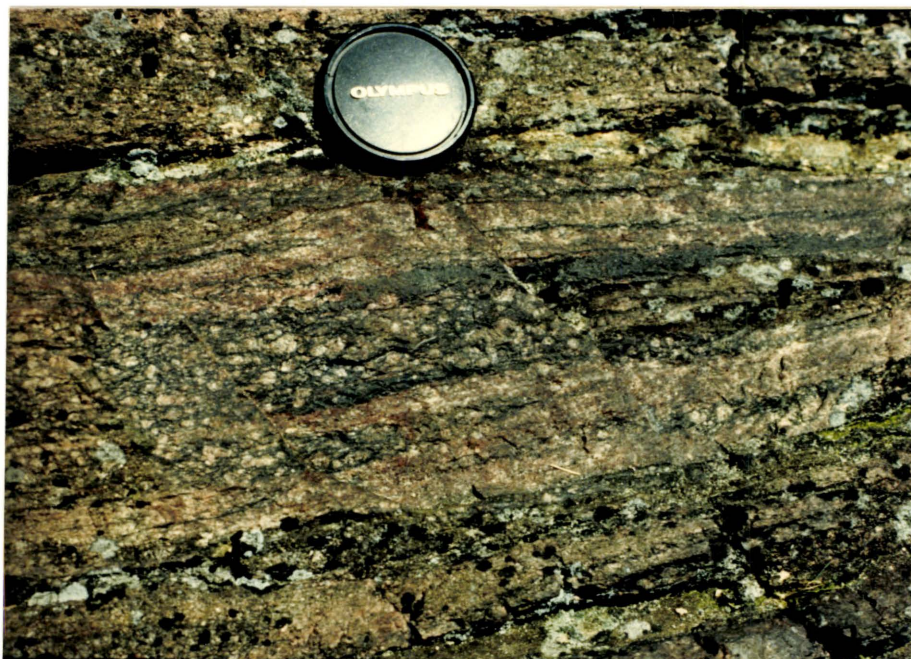


Figure 7a. Bell Lake Granite enclosing a xenolith of Lorrain Quartzite (foreground). White quartzite peak in the background (Silver Peak) is in the Huronian proper.

Figure 7b. Close-up of the xenolith in figure 7a. Johnnie Lake.



Figure 7c. Folded Quartzite xenolith in Bell Lake Granite. The fold axial surface is oriented parallel to the local foliation. Johnnie Lake.

Figure 7d. "Dent du Cheval" texture in an argillaceous xenolith enclosed by Bell Lake Granite. Light crystals are feldspar, black crystals are quartz. Bell Lake Road, east of Bell Lake.

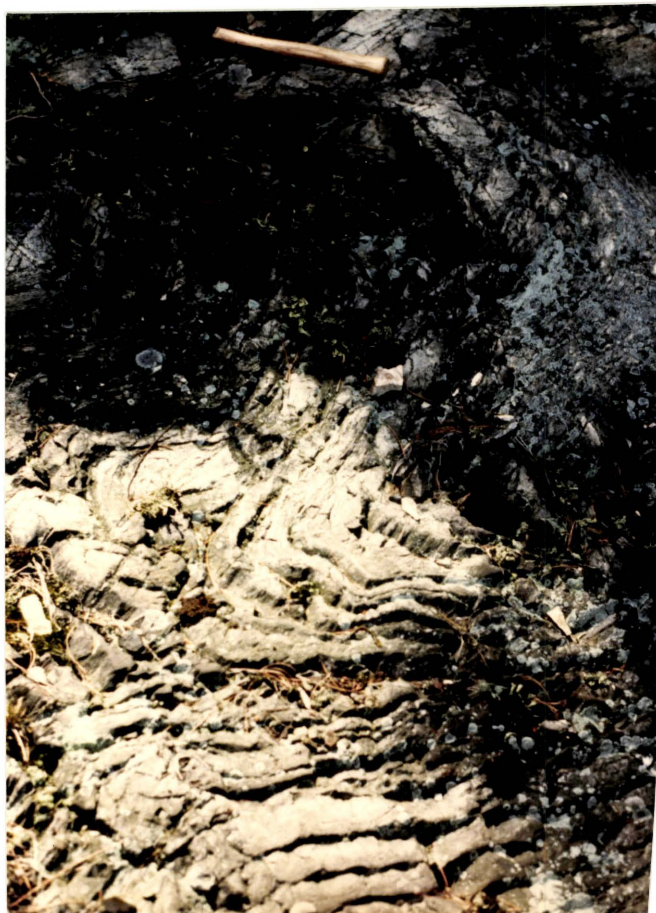


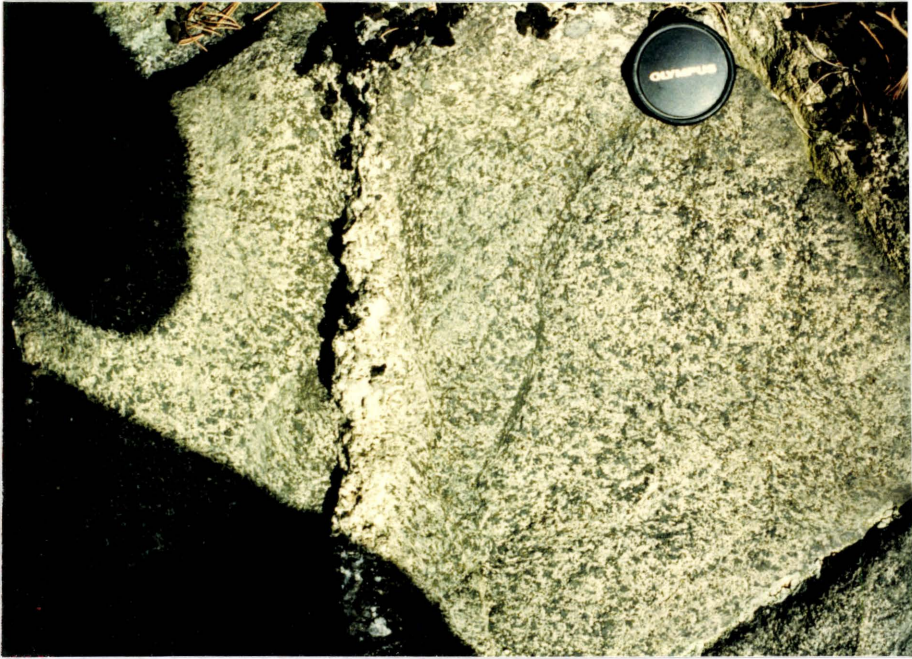
Figure 7e. Deformed relict sedimentary structures in an argillaceous xenolith in the Bell Lake Granite. Johnnie Lake.

Figure 7f. Migmatite and boudinage developed in the argillaceous xenolith at Johnnie Lake. Pencil tip points north.



Figure 7g. Diorite xenolith enclosed in Bell Lake Granite. Johnnie Lake.

Figure 7h. Fractured xenolith of diabase enclosed in Bell Lake Granite. Johnnie Lake.



Many of the quartzite xenoliths still retain their primary sedimentary features. When the bedding planes of these xenoliths are oriented parallel to the northeast trending regional fabric, the internal structure remains relatively undeformed. Those xenoliths which have bedding oriented normal or oblique to the regional foliation are invariably folded such that their fold axial surfaces follow the regional planar fabric (Figure 7c). Other inclusions include diorite (Figure 7g) and amphibolite or diabase (Figure 7h).

The Bell Lake Granite is intruded by a number of dykes the most abundant of which are thin, fine grained, locally porphyritic pink or purple felsite dykes. As well as these there are more rarely pegmatite and diabase dykes.

Terry Lake Diorite

The Terry Lake Diorite is an irregular shaped body located north of Carlyle Lake between Terry Lake and the Huronian. It extends for approximately four kilometers from the southwest end of Ruth-Roy Lake southwestward to Kakakise Lake. The texture of the diorite is phaneritic, hypidiomorphic granular with an average grain size of 5 millimeters. The unit has a black and white speckled appearance and is composed of plagioclase and blue-green hornblende with minor biotite, epidote and potassium

feldspar. Accessory minerals include quartz, sphene, magnetite, zircon and apatite. It locally has developed within it short thin discontinuous shears or a weak foliation. It also contains pods of essentially pure hornblende.

The boundary of the Terry Lake Diorite is not exposed but, like the Bell Lake Granite, it contains large xenoliths of quartzite near its contact with the Huronian metasediments. Its northwestern contact is therefore believed to be an intrusive one. Xenoliths of Terry Lake Diorite are found within both the Bell Lake Granite and the Killarney Granite implying that it is the oldest unit of the Killarney Complex.

Killarney Granite

The main body of the Killarney Granite is located near the village of Killarney from which it continues northeastward into the southwestern end of the study area. It was previously mapped by Frarey (1985) and Frarey and Cannon (1969) as such where it occurs north of Carlyle Lake. Other bodies occurring south of Carlyle Lake and across the study area to the east have a similar character and composition and have therefore included as part of this unit.

The Killarney Granite is a coarse grained, phaneritic,

hypidiomorphic granular, red to pink granite, granodiorite or quartz-monzonite. The largest systematic occurrence of quartz-monzonite is indicated in figure 2. The Killarney Granite is massive or moderately foliated and has a distinctive deep red weathered surface. Where a foliation is developed, it is marked by the parallel alignment of biotite flakes and can be either planar and consistent or short and discontinuous, depending largely on the abundance of biotite. Where transected by major shear zones (eg. southwest tip of Carlyle Lake) it forms a deep red glassy mylonite.

The Killarney Granite is composed of orthoclase, microcline, oligoclase, quartz, biotite and locally contains one or more of chlorite, muscovite or hornblende. Accessory minerals include sphene, magnetite, allanite, calcite, pyrite and zircon. It is generally leucocratic with mafic minerals accounting for less than 15 percent of the rock. The plagioclase in the Killarney Granite is finely twinned and sericitized. Crystals are irregular to well formed euhedra and may show zoning. Sericitized plagioclase is often surrounded by a potassium feldspar rim. The quartz occurs as irregular grains filling interstices between feldspars. The quartz content of this unit varies from 10 to 25 percent.

The Killarney Granite is intruded by diabase dykes; where it occurs south of Carlyle and Johnny Lakes, it contains numerous pegmatite dykes.

Fine Grained Granite

The fine grained granite occurs in the study area as a thin strip which trends northeasterly along the south shores of Carlyle and Johnny Lakes. It also occurs interlayered with the Bell Lake Granite on the north shore of Carlyle Lake. The unit is dominantly fine grained pinkish-grey to red, its weathered surface developing an orange hue. It is leucocratic, composed of quartz, potassium feldspar and plagioclase with minor amounts of biotite, muscovite and chlorite. Accessories include epidote, sphene, allanite, zircon, apatite and magnetite. The texture of the granite is massive to foliated, hypidiomorphic granular to porphyritic. Where porphyritic, 1 to 5 millimeter euhedral potassium feldspar phenocrysts are apparent in outcrop by their paler pink to white weathering. The foliation that develops in the granite is expressed by the parallel alignment of biotite flakes. Foliation surfaces are generally closely spaced (1-5mm) and are best developed where the biotite content locally increases. The granite has been intruded by thin pegmatite dykes.

Tonalite

Tonalite, which occurs southeast of Johnny Lake, extends in a northeasterly direction from highway 637 to the eastern boundary of the map area. This unit is a fine grained purple rock in fresh exposure which weathers deeply to a paler pink colour. It is composed of quartz, plagioclase (~60%), potassium feldspar and biotite with minor muscovite. Accessories include calcite, spinel, magnetite, allanite and zircon. Sillimanite was also observed in thin section. The unit was seen everywhere to have a well developed planar and persistent foliation, parallel to the regional trend, which is locally folded. It is invariably cut by a large number of pegmatite dykes which, in some outcrops, account for 60 percent of the exposed rock. The boundaries of the pegmatites are sharp to gradational and inclusions of country rock are locally found within the dykes. The foliation within these inclusions conforms with that surrounding the pegmatites. Pegmatites which crosscut the foliation are generally folded such that their fold axial surfaces parallel the local foliation. In many cases, deformation during folding has reduced the pegmatites to a string of large tailed feldspar augen surrounded by a matrix of recrystallized quartz.

Figure 8. Biotite pods surrounded by halos of mafic free country rock. a) Elliptical pods, Johnnie Lake Road. b) Pink folded vein containing elongated biotite pods, Highway 637 south of Carlyle Lake.

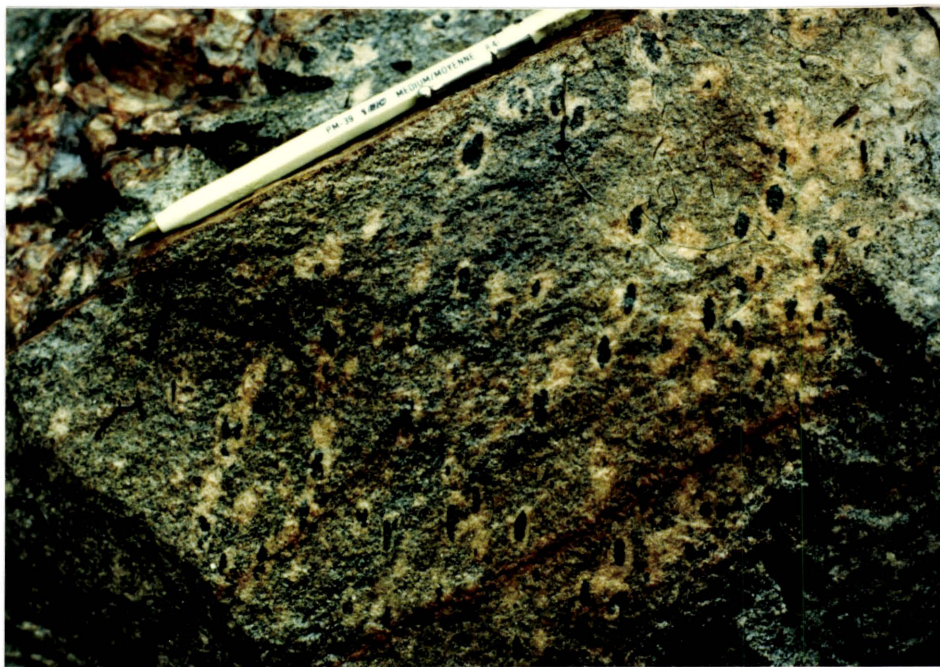


Figure 8c. Slab of Tonalite containing the pink segregation bands. Sample is cut normal to that shown in figure 8b. Highway 637, south of Carlyle Lake.



One characteristic feature of this unit, on which the field classification was based, is the development of pink bleached halos surrounding equant or elongated to linear pods of biotite or magnetite (Figure 8a,b). Within these pods, preferentially oriented books of biotite are surrounded by a rim of essentially mafic free country rock. These pods may develop into bands which vary from a few millimeters to 2 centimeters wide (Figure 8c). These bands also appear folded but show little to no internal deformation. This may be a precursor to the pink and black banded gneiss which occurs just east of this unit along highway 637.

Augen Gneiss

The augen gneiss occupies the southeast corner of the map area. It is a very coarse grained granite, granodiorite or quartz-monzonite which ranges in colour from black and white to pale pink to deep red and weathers grey to pale pink or purple. It consists mainly of closely packed polycrystalline potassium and plagioclase feldspar augen, 0.5 to 1 centimeter in diameter, surrounded by a black matrix of fine grained quartz, feldspar and biotite or hornblende giving it a bimodal appearance (Figure 9a). The augen contain inclusions of biotite, magnetite hornblende and quartz. Accessories include allanite, sphene, magnetite, garnet and serpentine.

The abundance of magnetite increases locally to the point where it becomes an important constituent of the rock. This unit may be responsible in this area for the strong positive aeromagnetic anomaly which occurs along the Grenville Front Tectonic Zone.

The foliation, defined by the matrix and the elongation of feldspars, is generally wavy or anastomosing around closely spaced feldspar augen and often displays a C and S fabric (see Figure 9a). Where the level of deformation increases to that of a protomylonite, the grain size reduces to a point where the foliation becomes rectiplanar. The unit locally develops into a grey to purple mylonite.

The augen gneiss is intruded by pegmatite dykes which are generally oriented parallel to the local and regional foliation. Those that crosscut the foliation are folded irregularly about axial surfaces that trend parallel to the foliation (figure 9b,c). The foliation is commonly observed to penetrate the outer few centimeters of the pegmatite boundary. The dykes are seen to crosscut one another with the later, often thinner, dykes being much less deformed than those they crosscut. The augen gneiss is also intruded by thin, fine grained granitic dykes which generally trend parallel to the local foliation and large but discontinuous dark green amphibolite dykes which locally contain up to meter sized blocks of deformed country rock.

Figure 9a. Red and black augen gneiss which displays a well developed C and S fabric (surfaces indicated). Highway 637.

Figure 9b. Ptygmatic folding of a pegmatite dyke enclosed in augen gneiss. North of highway 637, west of the Bell Lake Road.

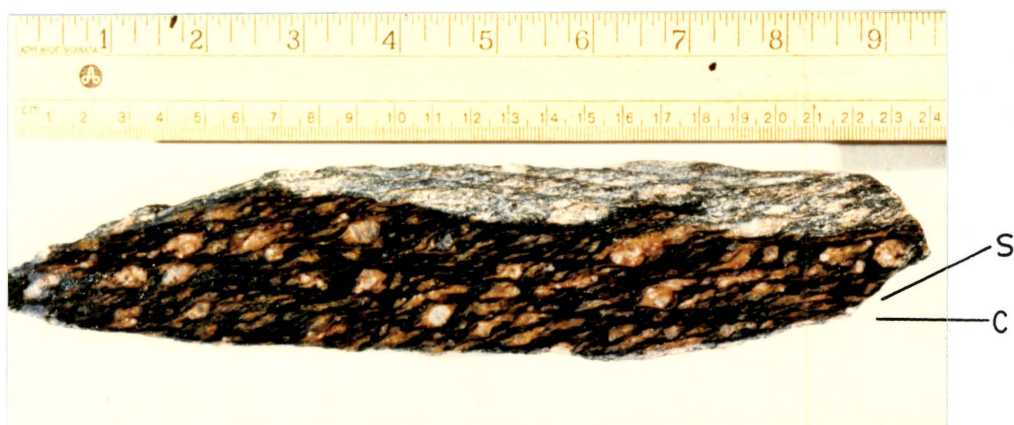
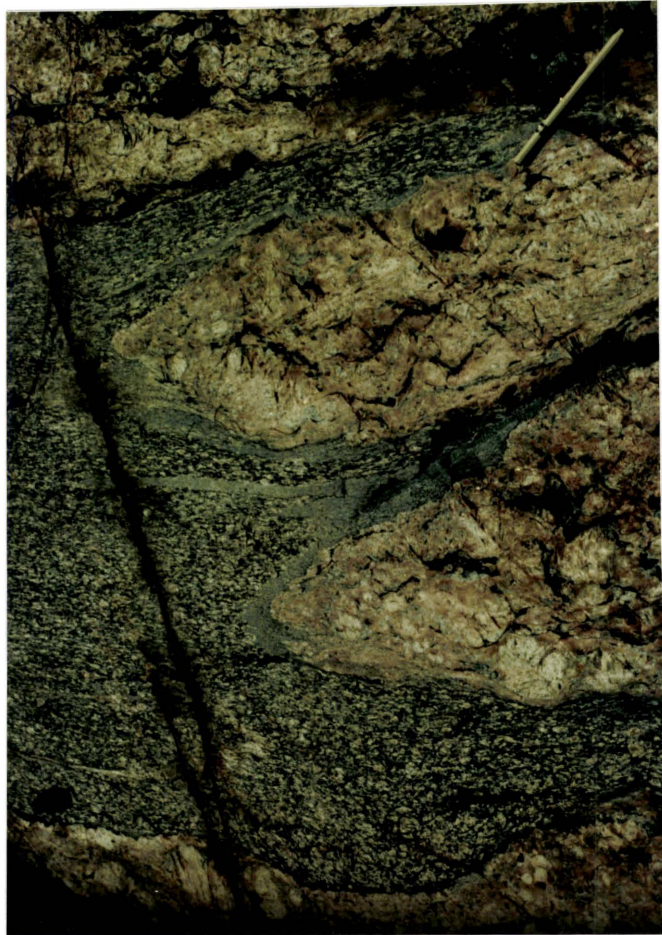


Figure 9c. Megacrystalline pegmatite, folded within
augen gneiss. Bell Lake Road.



Paragneiss

Along the northwestern boundary of the Bell Lake Granite at Ruth-Roy and Johnny Lakes is a strip of gneiss referred to by Cannon as "Streaky Biotite Gneiss" (see Frarey, 1985) which occurs in close association with large outcrops of cataclastic breccia. Other occurrences of paragneiss exist southeast of the Bell Lake Granite, east of Johnny Lake.

Streaky Biotite Gneiss

The Streaky Biotite Gneiss (Figure 10a) has a granular texture and consists of quartz, biotite, muscovite, potassium feldspar and accessories. Tourmaline stars are locally developed. It possesses a planar to wavy or irregular foliation which is defined by the concentration of randomly oriented, 3 millimeter flakes of biotite and muscovite into thin layers separated by bands of quartz and feldspar. The spacing in the layering ranges from 2 millimeters to a few centimeters. It is bounded on the south side by Bell Lake Granite and on the north side by Lorrain Quartzite. Within the gneiss occur xenoliths of quartzite and amphibolite which are themselves foliated and which cause the fabric in the gneiss surrounding them to be disrupted. The gneiss can also be seen locally as interlayered with both Bell Lake Granite and quartzite. The assemblage has been intricately folded (Figure 10b) but evidence of this is only apparent locally.

Figure 10. Streaky Biotite Gneiss. Northwest contact of the Bell Lake Granite at Ruth-Roy Lake.

a) Vertical section showing the strong foliation.

b) Horizontal surface showing the irregular fold pattern.

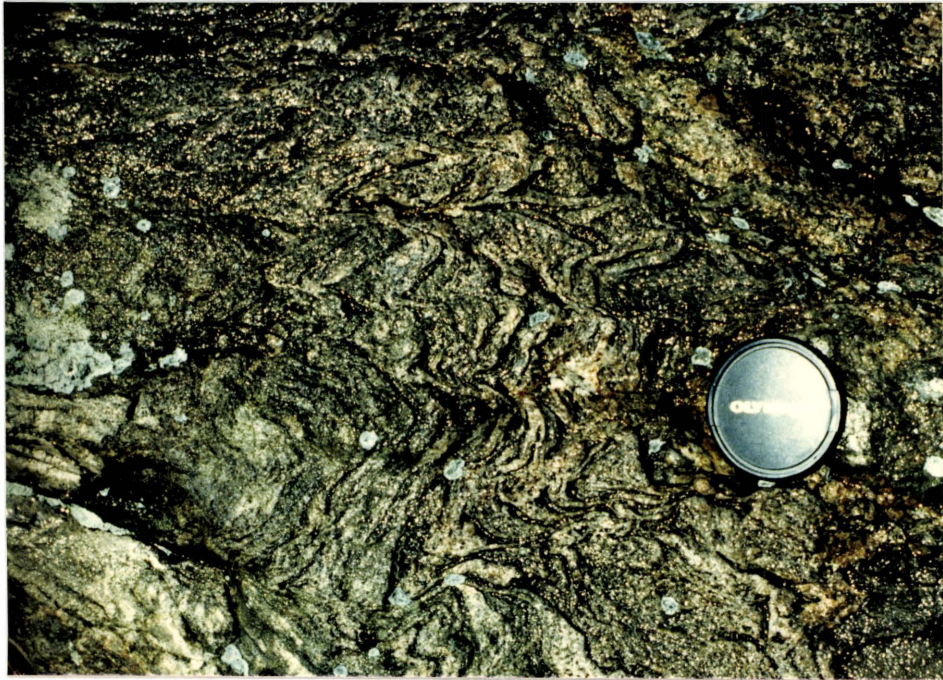
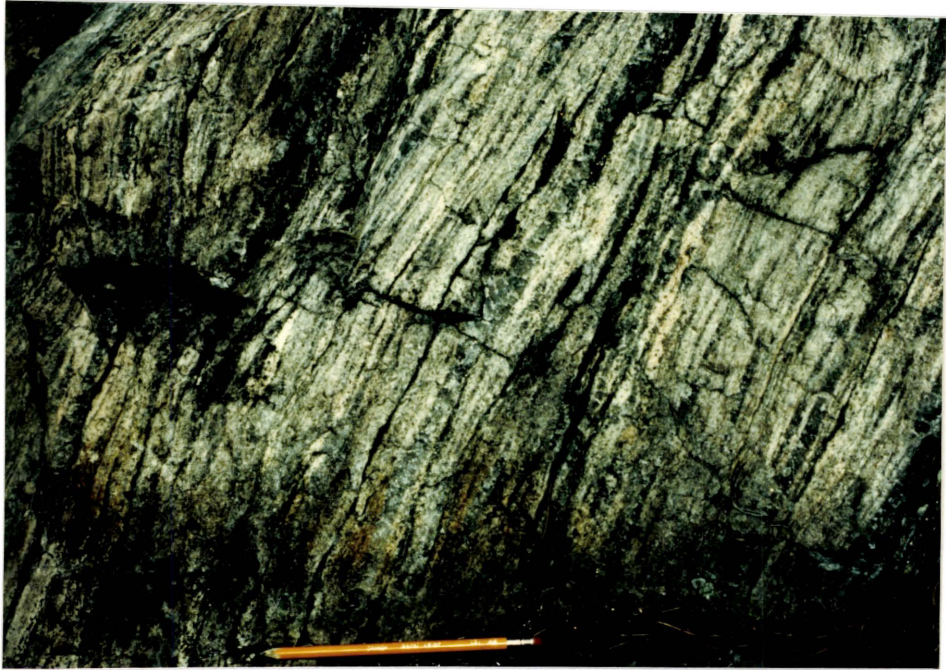
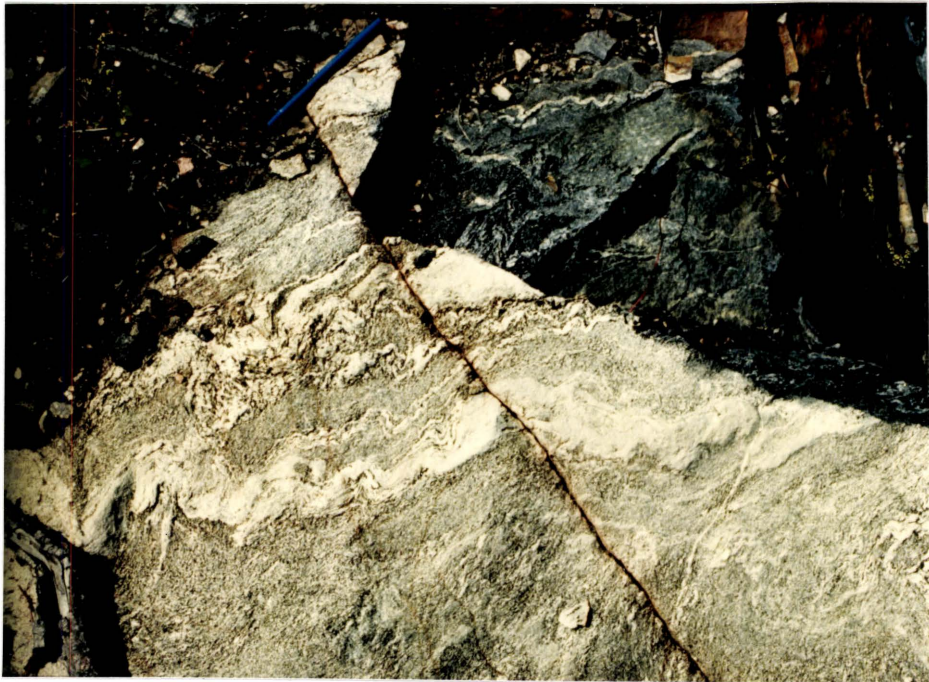


Figure 11. Quartz-feldspar-biotite paragneiss with crosscutting pegmatite vein. a) Vertical section. b) Horizontal section. Bell Lake Road, east of Johnnie Lake.



Figure 11c. Isoclinal folding in the quartz-feldspar
-biotite paragneiss. Bell Lake Road, east of Johnnie
Lake.

Figure 11d. Folded migmatite in argillite. Bell Lake
Road, east of Johnnie Lake.



Other Paragneisses

The other supracrustal gneisses (Figure 11a,b,c,d), which occur east of Johnny Lake, include biotite paragneiss or argillite, various phases of quartzite gneiss and an intermediate paragneiss similar to the Streaky Biotite Gneiss. Within this block of metasedimentary gneisses, which extends eastward to Tyson Lake (~3 kilometers east of Turbid Lake), occur what appear to be the deformed equivalents of some of the units occurring in the Huronian Supergroup. Some of these have been described as "unmistakably Lorrain" by Frarey (1985), while the more argillaceous units appear to be Gowganda equivalents including a small outcrop on the Bell Lake Road of paraconglomerate. Wherever primary bedding is seen in these units it is invariably intricately folded but is generally unrecognizable.

Breccia

As was mentioned previously, the streaky gneiss occurs in close association with a large volume of cataclastic breccia. The composition of the breccia varies locally and is largely dependent on the host rock. Clast composition ranges from quartzite to quartz-arenite where it is in contact with Lorrain Quartzite to the northwest. As it is traversed across strike, the clast composition changes to include clasts of

granitic schist, green chlorite-muscovite schist, amphibolite, and Bell Lake Granite (Figure 12a,b,c,d). Clast sizes range from a few centimeters to as large as 8 square meters and shapes vary from angular to rounded. Planar features within the clasts are randomly oriented. The matrix of the breccia is also highly variable. Within the quartzite breccia which occurs on the point along the south shore of the north section of Johnny Lake, the matrix is void filling euhedral quartz with crystals as large as 8 centimeters in length. More generally the matrix is fine grained quartz, quartz-chlorite or quartz-muscovite. Where the breccia is in contact with the Bell Lake Granite, the clasts are largely composed of Bell Lake Granite and the matrix appears granitic. The breccia grades over a short distance into massive Bell Lake Granite which is locally cut by small brittle faults, some of which contain pseudotachylitic material.

Pegmatites

A large volume of pegmatite occurs within the study area. Southeast of Carlyle and Johnny Lakes, pegmatites are ubiquitous. To the northwest of these lakes pegmatites are generally thinner and much less abundant. Pegmatites occur as dykes, sheets or irregular masses which individually are

rarely more than a few meters in width. The composition of the pegmatites which varies only in its mafic component, is normally quartz, microcline and one or more of biotite, hornblende, magnetite or muscovite. Graphic intergrowth of quartz and feldspar is common. Garnet is also found in some pegmatites. The mafic mineral which occurs appears to be controlled by the host rock suggesting local development or migmatization. The crystal size ranges from 1 to 50 centimeters with an average size of 5 to 10 centimeters. The very large crystals are found in the large mass of pegmatite which occurs midway along the Bell Lake Road within the block of metasedimentary gneisses.

All pegmatites observed have undergone some deformation but the amount of deformation varies, not only between outcrops but also from one pegmatite to the next within the same outcrop. This range in deformation coupled with crosscutting relationships suggests that there has been more than one episode of pegmatite generation or continuous production through a long deformational history. Deformational styles include cataclasis, shearing and concordant folding. The limbs of folded dykes which are oriented subparallel to the foliation are generally thinner than those in an oblique orientation. Boudinaged limbs are also common.

Figure 12. Cataclastic breccia. a) Angular to rounded quartzite fragments in a quartz-chlorite matrix. Johnnie Lake. b) Quartzite and Bell Lake Granite clasts in a crushed granitic matrix. Ruth-Roy Lake.

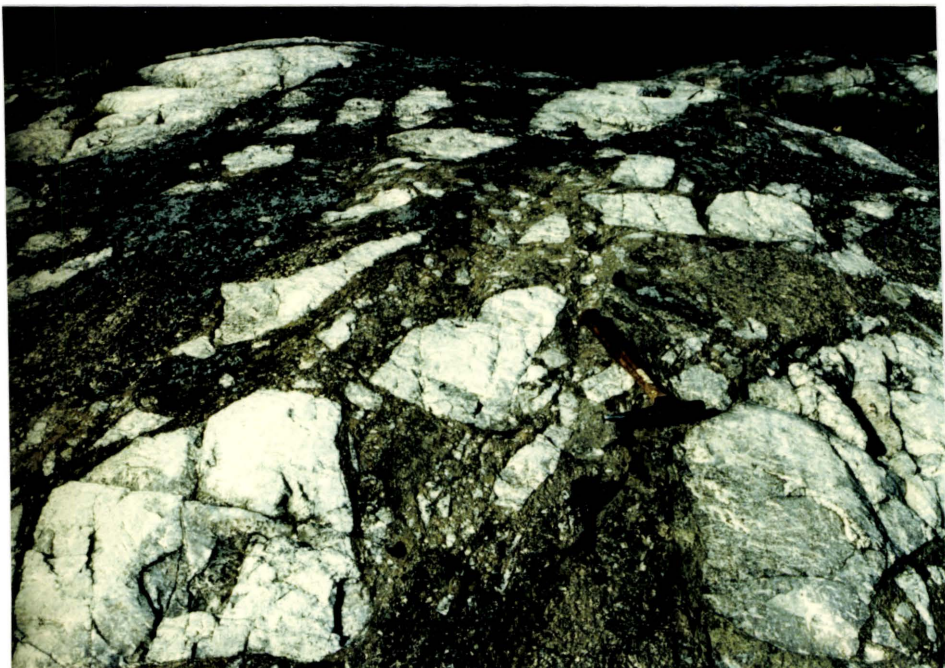
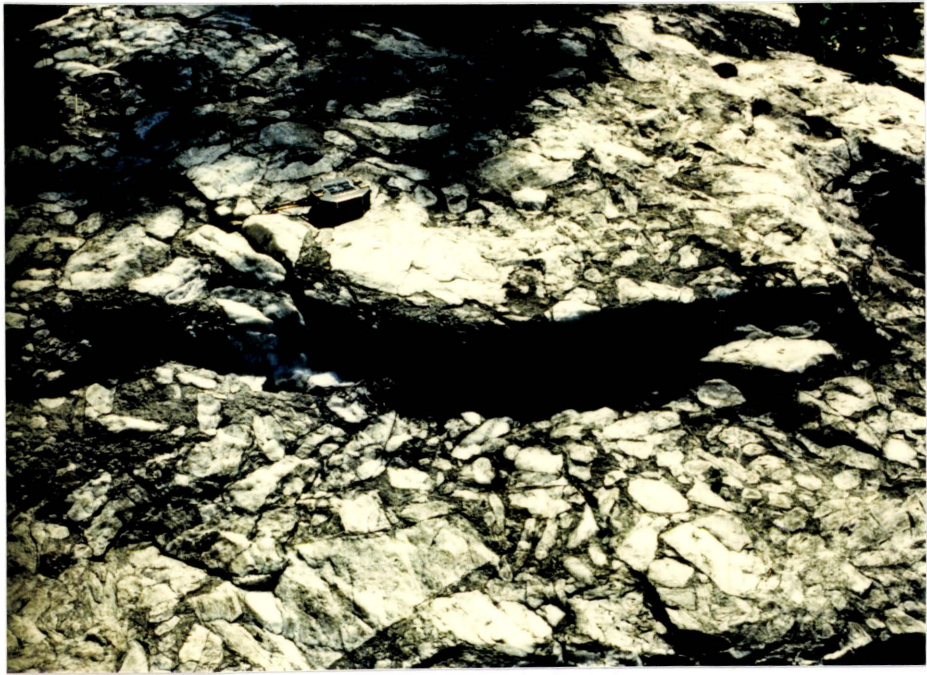
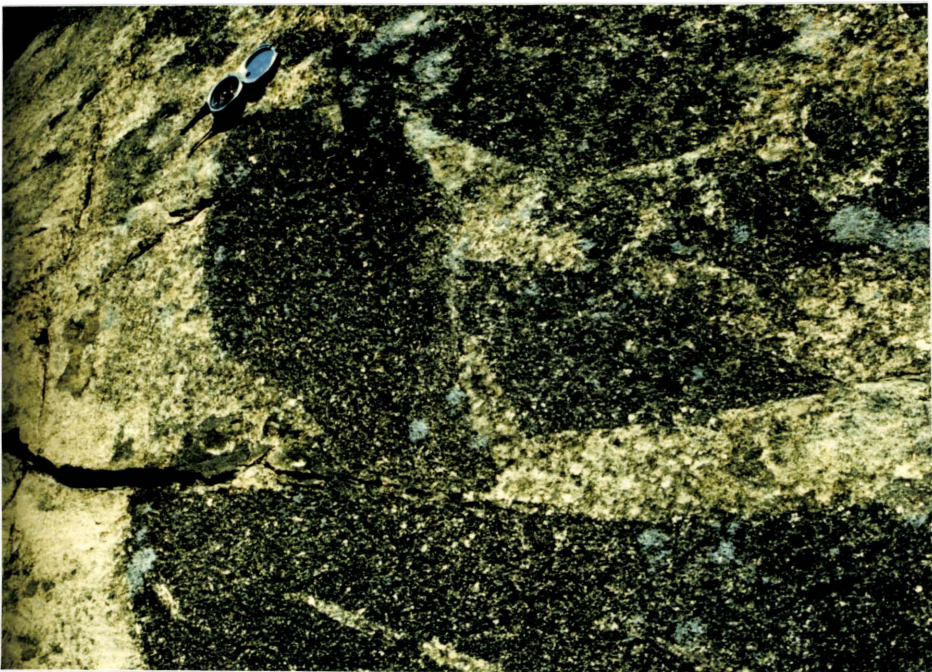
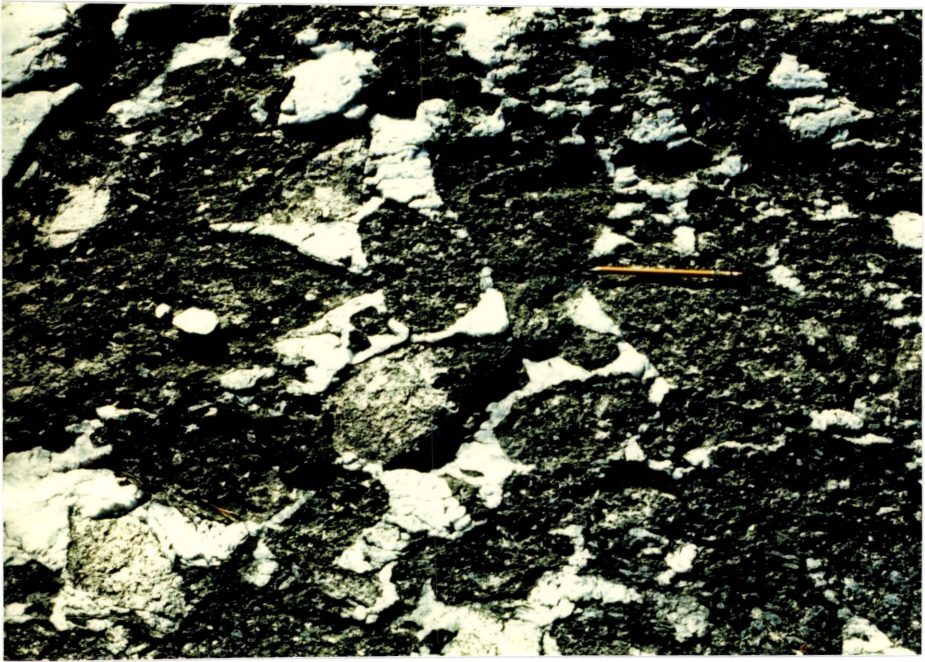


Figure 12. Cataclastic breccia. c) Rounded Bell Lake Granite clasts in a crystalline quartz matrix. Ruth-Roy Lake. d) Angular Bell Lake Granite clasts in a granitic matrix. Johnnie Lake.



CHAPTER 3

STRUCTURAL ANALYSIS: MACROSCOPIC

Introduction

Structural analysis has two main objectives. The first objective is to describe the nature, orientation and relationships between the various structural elements observed, i.e. geometric analysis. The second objective is to interpret these data based on existing theoretical and empirical observations in order to determine principal stress and strain directions as well as those mechanisms responsible for the development of the observed fabric. The second objective constitutes a kinematic and dynamic analysis.

The structural analysis of the study area has been divided into two sections. The first section, on macroscopic structure, deals with those structures observable, both

directly and indirectly, on the scale of an outcrop or larger. The second section will deal with microscopic structure, observable in thin section.

The structural fabric of the Grenville Front Tectonic Zone, including the area studied, is characterized by a penetrative northeast trending foliation and southeast plunging lineation, (eg. Davidson, 1986). This fabric is observed in all rock types which occur in the area but the nature and intensity of this fabric tend to vary with both location and lithology.

Structural Geometry

The orientation of planar and linear elements were measured in the field. Planar elements are generally expressed as a preferential alignment of minerals, normally biotite, forming a foliation or schistosity. In many outcrops there exist two measurable foliation surfaces, these being a schistosity (S) and a shear (C) foliation. When both of these planar elements form in response to the same tectonic event or stress field they define a C & S fabric (Berthe et al, 1979), which can be used as a kinematic indicator. Other planar elements measured include:

- 1) minor fold axial surfaces, which occur mainly in sedimentary xenoliths, dykes and metasedimentary gneisses,

2) joints, and

3) gneissic banding, which occurs in the paragneisses and rarely within other units.

Linear elements are generally expressed as a mineral lineation which can be seen on foliation surfaces. The mineral lineation is defined by aggregates of quartz or quartz and feldspar, forming rods or ribbons, or, where less strongly developed, by the parallel alignment of biotite, muscovite, magnetite or hornblende. Where fold axes could be defined they were also measured.

Several shear zones were mapped which were expressed as either faults with associated breccia, or mylonite zones, recognized by the reduction in grain size and intense development of both a foliation and mineral lineation.

The area has been divided into six structural sub-areas based largely on lithology and internal structural homogeneity (Figure 13). These are:

Area 1: The northwest contact of the Bell Lake Granite;

Area 2: The main body of the Bell Lake Granite, the Killarney granite north of Carlyle Lake and the Terry Lake Diorite;

Area 3: The southeastern contact of the Bell Lake granite; Area 3A: The granite-granite contact along Carlyle and Johnny Lakes (the Johnny Lake Shear Zone); Area 3B: The extension of this zone along the granite-paragneiss contact

at Turbid Lake;

Area 4: Metasedimentary gneisses east of Johnny Lake;

Area 5: Granitic units south of Johnny Lake bounded to the southeast by the augen gneiss contact;

Area 6: Augen gneiss.

Geometry of Area 1

Area 1 is underlain by the contact between the Bell Lake Granite and the Huronian metasediments. Due to a lack of exposure southwest of Ruth-Roy Lake, the Huronian contact with the other intrusive units of the Killarney Complex, which likely fall within this zone as well, will not be discussed. The intrusive nature of this contact is best exposed along the southeast shore at the northeast end of Bell Lake. Over a strike normal distance of ~100 meters, the proportion of quartzite to Bell Lake Granite changes from 90:10, the Bell Lake Granite occurring as dykes intruded along bedding planes of the quartzite, to 10:90, the quartzite occurring as xenoliths within the Bell Lake Granite. A similar contact has been documented by Henderson (1967) for the Chief Lake Batholith which occurs northeast of the study area. Southwestward along this shore the Bell Lake Granite contains numerous xenoliths of argillaceous material and quartzite.

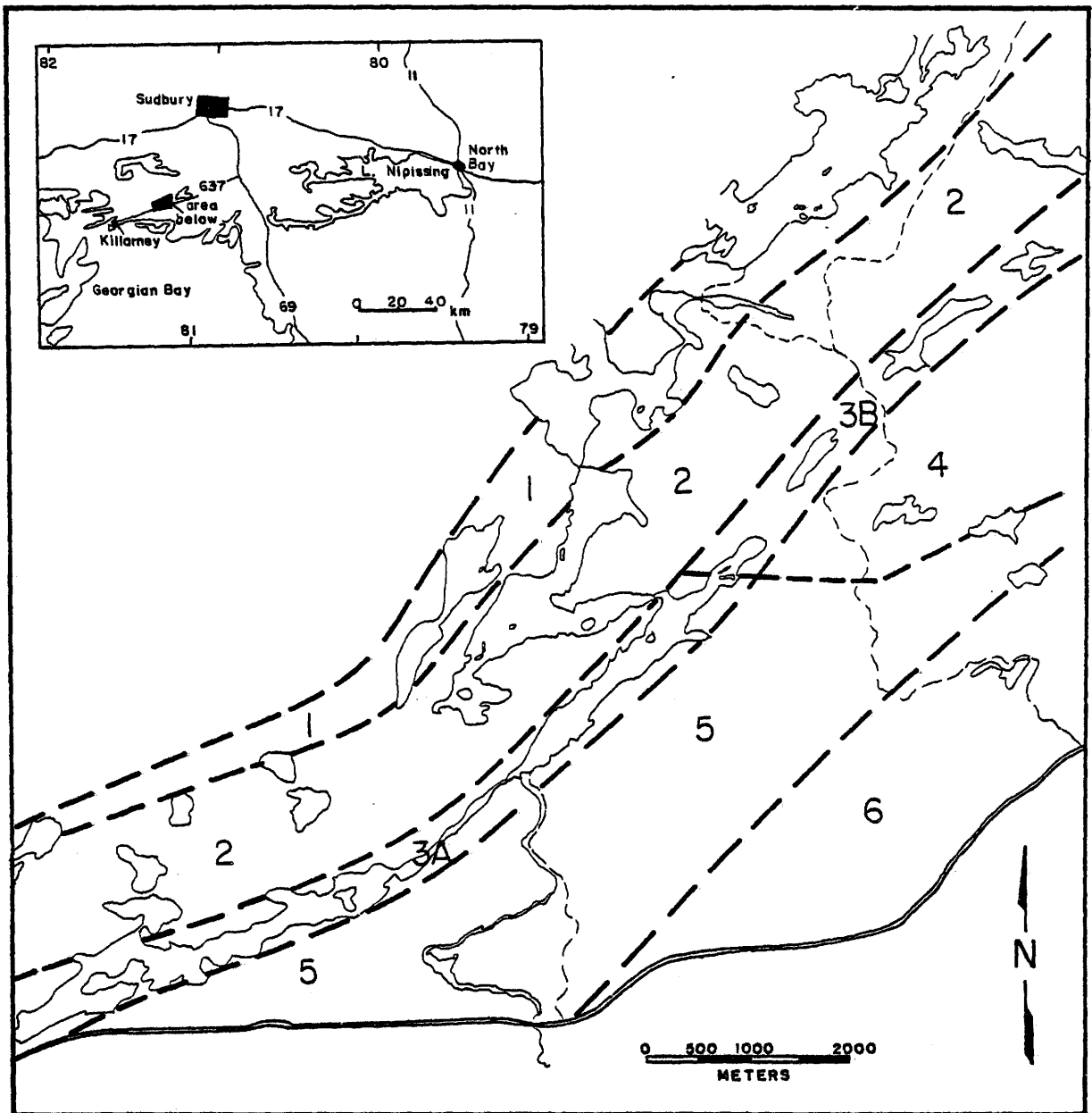


Figure 13. Area map showing the structural divisions discussed in the text.

Along the southwestern half of Bell Lake the Bell Lake Granite is in sharp contact with a fine to medium grained pink to grey quartzofeldspathic unit of unknown origin. This unit appears metasedimentary in some places and granitic in others. No unambiguous evidence has been seen which would allow classification as one or the other.

From the southwestern end of Bell Lake to the northeastern end of Ruth-Roy Lake this contact is faulted. Numerous outcrops of breccia occur containing large blocks of both quartzite and granite porphyry in a matrix of either void filling quartz or crushed rock. Associated with this breccia is the Streaky Biotite Gneiss which continues to the southwest end of Ruth-Roy Lake where it tapers out. At this point the Bell Lake Granite and the quartzite become separated by the Terry Lake Diorite.

The Bell Lake Granite, quartzite and quartzo- feldspathic unit along Bell Lake possess a very well developed foliation. Locally, 5 to 10 centimeter wide, discontinuous mylonite zones are developed within them; these zones have a very strong mineral lineation of quartz rods. The planar elements, in general, have a consistent strike direction which is subparallel to the granite- quartzite contact. Foliation surfaces have dip values which fluctuate by 10 degrees to either side of vertical but the mylonite foliation consistently dips steeply to the southeast.

Where the Streaky Biotite Gneiss and breccia occur, the Bell Lake Granite is less consistently foliated, locally becoming massive. Many microfaults cut the granite, generally with orientations normal or oblique to the foliation; these microfaults are filled with fault gouge or epidote. Rarely, small thin veins of pseudotachylite occur.

Folding occurs in this area within the Streaky Biotite Gneiss. Generally these are tight isoclinal folds. Fold axial surfaces were found to be concordant to the foliation and fold axes that could be measured were found to plunge moderately to the east.

All foliations and lineations have been plotted on equal area (Schmidt) nets in figure 14. These plots have been contoured using a Gaussian distribution weighting function (see Robin and Jowett, 1986) based on the proportion of data points per one percent area. The plots illustrate the general north to east strike and steep southeast to vertical dip of the foliations and the steep southeast plunge of the mineral lineations.

Geometry of Area 2

Area 2 encompasses the main body of the Bell Lake Granite, the Killarney Granite north of Carlyle Lake and the Terry Lake Diorite. All units in this area are generally

massive to weakly foliated. The foliation in these units is defined by a preferential alignment of micas or hornblende which become concentrated into discrete planes. The orientation of this foliation tends to be inconsistent where poorly developed. A second type of foliation also occurs in the Bell Lake Granite which is expressed as a preferential alignment of feldspar phenocrysts. This foliation, which is most likely primary, follows the same trend as the biotite foliation.

Many metasedimentary xenoliths occur within the Bell Lake Granite in area 2. The largest proportion of these are composed of quartzite or quartz-arenite and generally retain their original sedimentary structures, such as bedding and ripple crests. When the bedding of these xenoliths is oriented obliquely to the local foliation, the xenoliths are folded about fold axial surfaces which trend parallel to the local foliation. A large metagreywacke to argillite xenolith also occurs in this area within the Bell Lake Granite. Most of the primary features of this xenolith have been obscured by folding and migmatization.

Locally developed in area 2 are brittle faults, narrow discrete shear zones (possibly brittle-ductile faults) and en echelon tension fractures. Many fault surfaces are coated with a fine grained, commonly micaceous, material or fault gouge often appearing as a shiny black lineated surface;

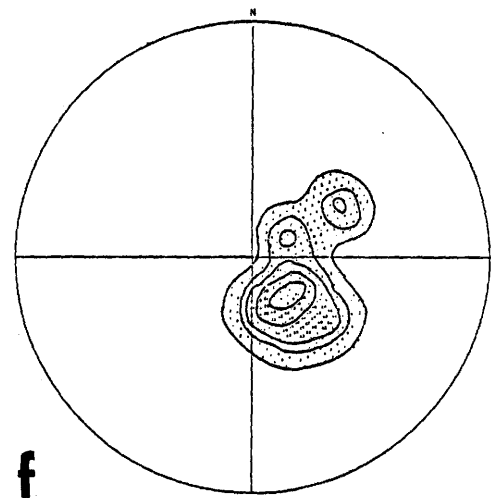
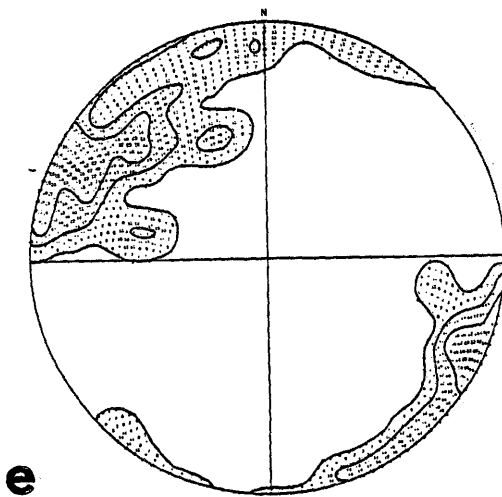
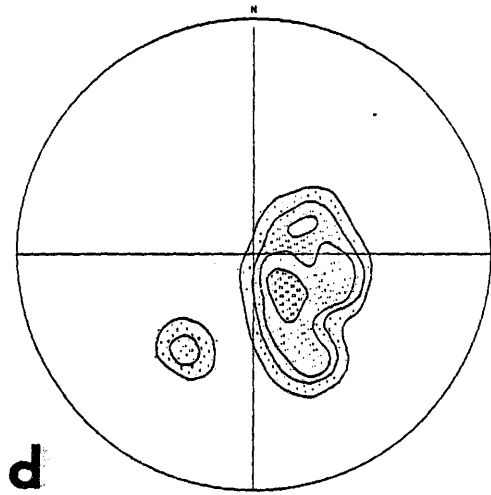
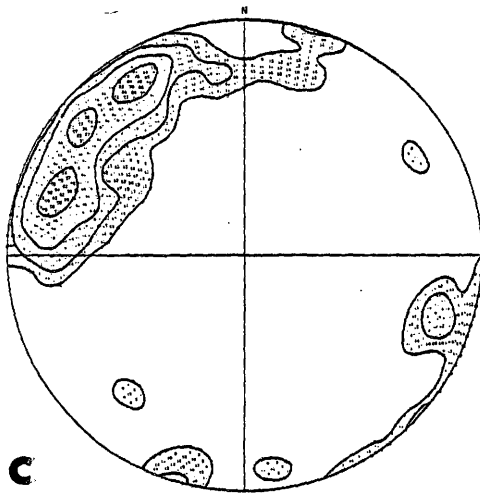
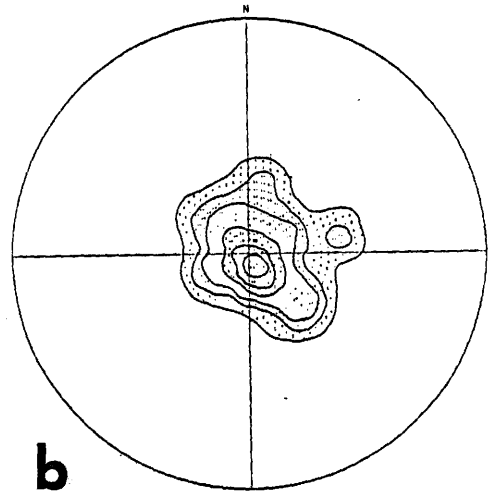
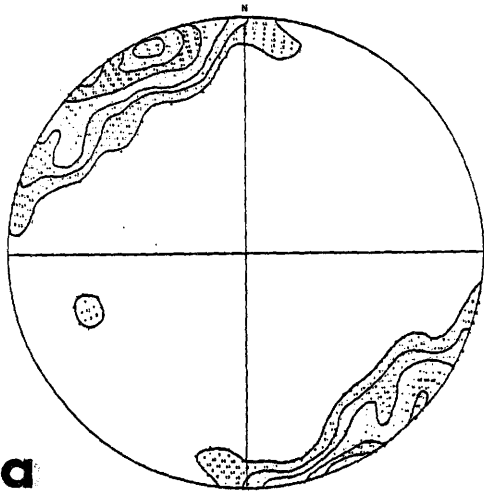
others have brecciated wall rocks.

Foliations and lineations are plotted on contoured equal area nets in figure 15. Again these plots show the statistically significant preferred orientation characteristic of the Grenville Front. Foliations, in general, strike northeasterly and dip moderately to steeply to the southeast with lineations plunging moderately to steeply to the southeast, but the orientations of structural elements in this area show more variability than those in other areas, and evidence for a number of crosscutting features exists.

In all cases, the brittle faults are the youngest feature observed. Where observed these faults cut all rock units, foliations, mylonite zones and dykes. The strike of these faults varies from 75 to 215 degrees with dip values ranging from vertical to 80 degrees to the right of strike. All show some, although minor, movement in the strike-slip direction. Vertical displacements could not be inferred. Another notable variation in planar features is the large number of foliations striking either north or southeast. In many cases, these variable orientations are associated with small shear zones containing mylonites which may or may not crosscut a previously existing foliation. Pegmatites in this area are seen to crosscut and be cut by other fine grained granitic and pegmatite dykes. These dykes are also seen to crosscut and be cut by small mylonite zones.

Figure 14. Contoured stereoplots of poles to foliation surfaces and lineations measured in the field in area 1. a) Poles to foliations, Bell Lake. b) Lineations, Bell Lake. c) Poles to foliations, Johnnie Lake North. d) Lineations, Johnnie Lake North. e) Poles to foliations, Ruth-Roy Lake. f) Lineations, Ruth-Roy Lake.

All plots are contoured based on the number of standard deviations above an even distribution. The first contour represents an even distribution. The second contour represents an even distribution plus two standard deviations. Each subsequent contour represents an increase of four standard deviations. Values for the standard deviation of each plot are given in tables 2 and 3.



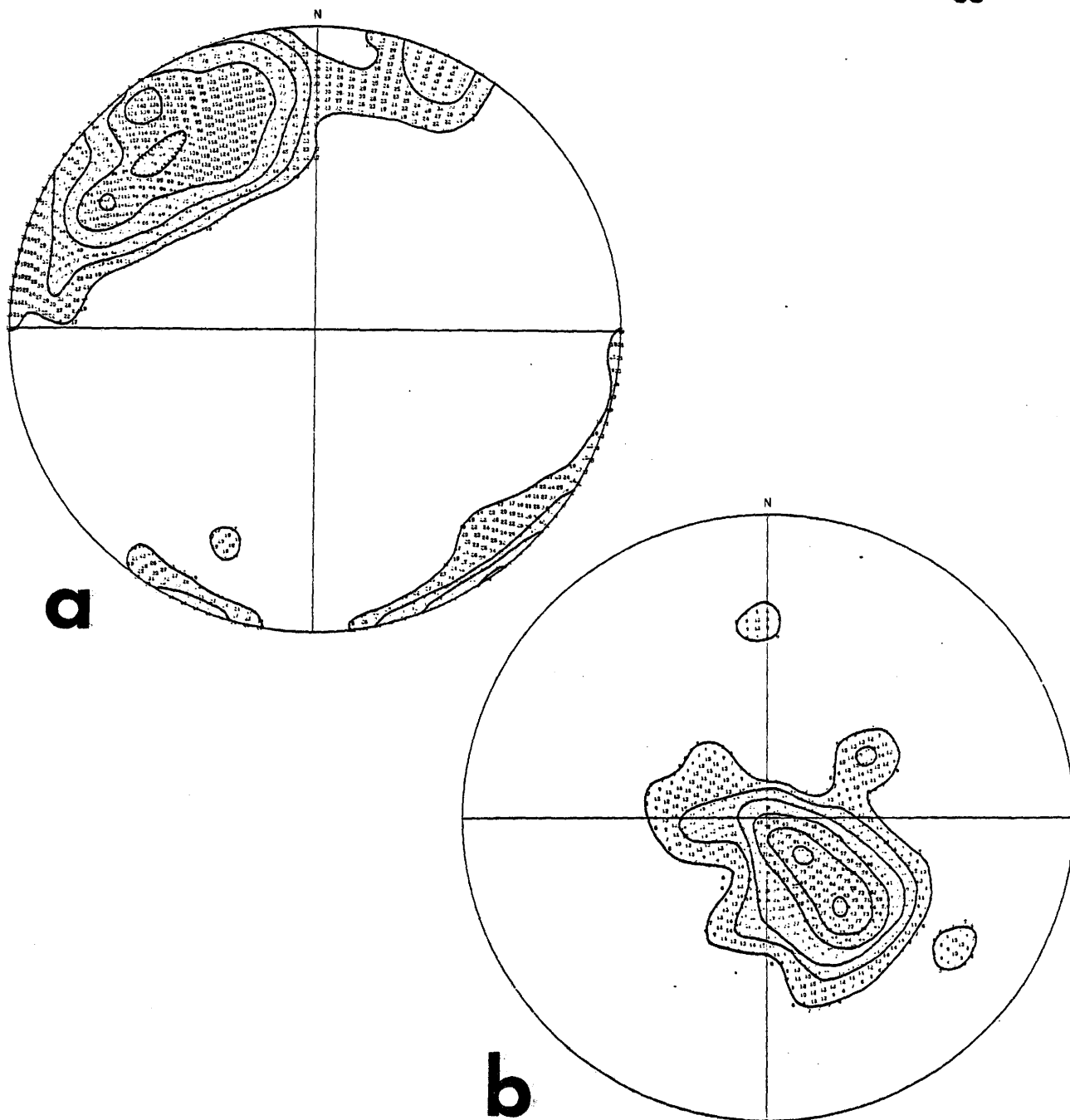


Figure 15. Contoured stereoplots showing a) poles to foliation surfaces measured in area 2 and b) lineations measured in area 2.

Locally developed within the Bell Lake Granite and the Killarney Granite in area 2 is a C & S fabric. The distribution of occurrences of this fabric is patchy, but is generally associated with the occurrence of mylonite zones or faults.

Geometry of Area 3

Area 3 is underlain by a large shear zone which follows the southeastern boundary of the Bell Lake Granite along Carlyle and Johnny Lakes, (the Johnny Lake Shear Zone). Along these lakes this shear zone separates the Bell Lake Granite from granitoid units to the southeast (area 3A). From the eastern end of Johnny Lake through Turbid Lake to the limit of mapping, area 3B follows the contact between the Bell Lake Granite and metasedimentary gneisses.

This area is characterized by rocks which have undergone intense deformation. Through Carlyle and Johnny Lakes (area 3A), mylonite is ubiquitous. The continuation of this zone through Turbid Lake (area 3B) also displays evidence of penetrative deformation but the volume of mylonite is greatly reduced.

Area 3A

Within the Johnny Lake Shear Zone, mylonitized equivalents of Bell Lake Granite, Killarney Granite, Fine

Grained Granite and pegmatite are interlayered forming banded mylonites. The characteristics of each mylonite band depend largely on composition, inherited from the parent rock. Mylonites derived from the leucocratic units, i.e. quartz rich Killarney Granite, Fine Grained Granite and pegmatite, are red and glassy. The more mafic component of the Killarney Granite forms a red and green laminated, glassy mylonite. The foliation developed within these mylonites is very fine compositional banding of alternating lamellae of quartz and feldspar. Plunging down dip on the foliation surfaces is a very strong mineral lineation of quartz and feldspar rods (Figure 16a).

The mylonitized equivalents of the Bell Lake Granite are generally black, less glassy and speckled with small feldspar augen. The foliation is marked by quartz aggregates, biotite and the "tails" of feldspar augen. These minerals also define the lineation seen on the foliation surfaces.

The extent to which these units are mylonitized, recognized in the field by the extent of grain size reduction, tends to fluctuate randomly across each band and from one band to the next, but with an overall increase towards the south. Interlayering of units is most common along the north shore and on the islands of Carlyle Lake (Figure 16b). At the southwestern tip of Carlyle Lake, along the narrows between Carlyle and Johnny Lakes and at the

northeastern tip of the south section of Johnny Lake is seen the widest and highest grade development of mylonite. At these locations, red glassy mylonite occurs continuously across distances of greater than 60 meters.

Along the boundaries of the Johnny Lake Shear Zone the increase in strain is gradational across distances varying from a few meters to a few tens of meters. This increase in strain is seen on surface as an increase in the intensity of both a foliation and a lineation and a decrease in spacing between foliation surfaces which corresponds to a decrease in grain size. When observed in sections parallel to the lineation and normal to the foliation (i.e. $X_f Z_f$) the following systematic progression can generally be seen across the boundary. The units start out initially as massive granular granite. A weak and somewhat inconsistent foliation then develops having a general northeasterly trend in strike and vertical dip. No mineral lineation can be recognized on these foliation surfaces. As the intensity of this foliation increases, its orientation becomes more consistent and a lineation may or may not be developed. At this point, a second foliation develops, having essentially the same trend in strike direction but dipping moderately to steeply to the southeast, i.e. a C & S fabric results. This second foliation, which can be seen to crosscut the first, invariably has a mineral lineation associated with it.

Figure 16a. Powerful mineral lineation of quartz and feldspar rods developed on a foliation surface.

Johnnie Lake.

Figure 16b. Interlayered Bell Lake Granite, fine grained granite and pegmatite. North shore of Carlyle Lake.



Figure 16c. North trending (older) mylonite swings into parallelism with the northeast trending mylonite of the Johnnie Lake Shear Zone (under water). Brunton compass points toward north. Johnnie Lake.



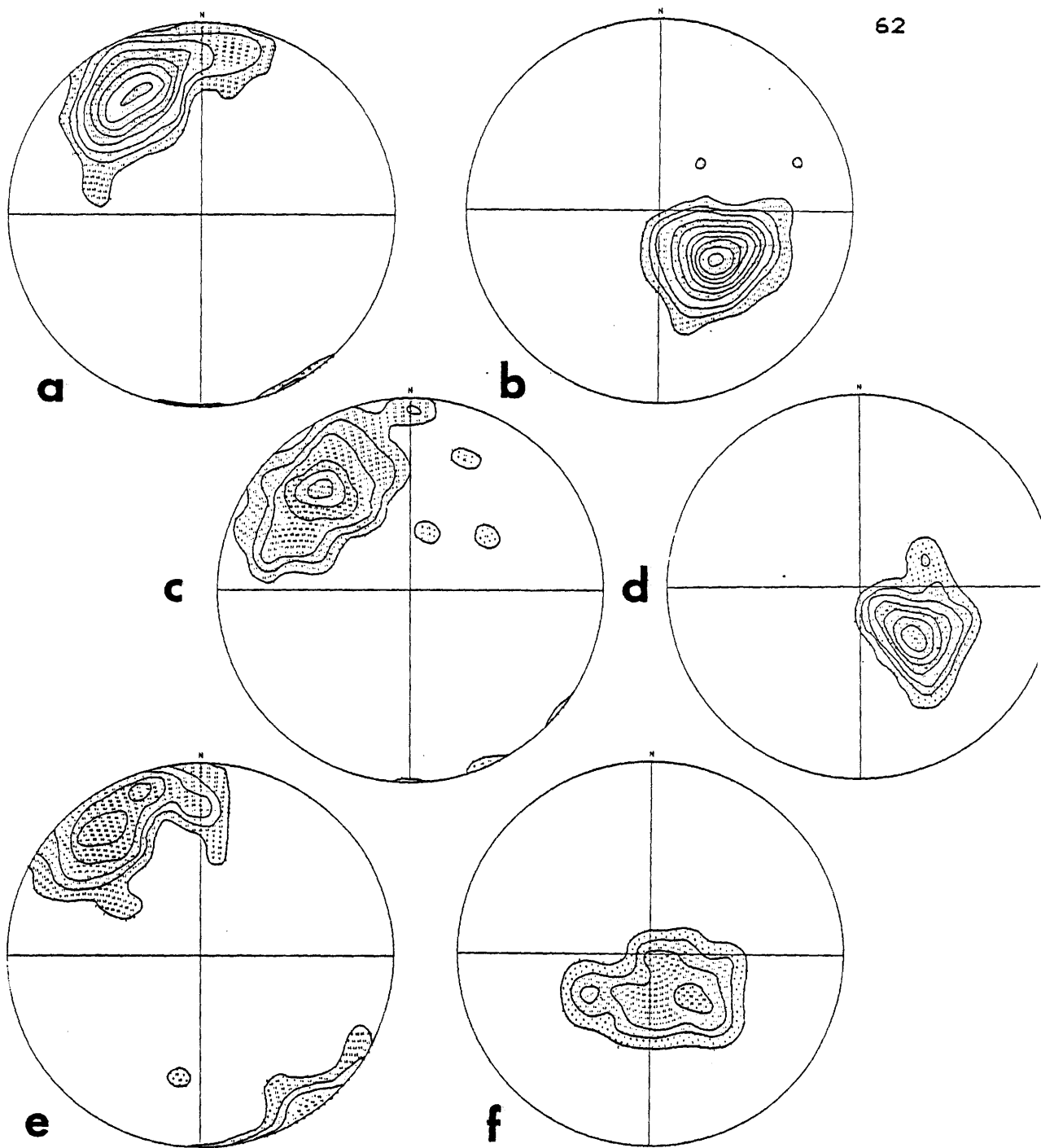


Figure 17. Contoured stereoplots of area 3. a) poles to foliations, Carlyle Lake. b) Lineations, Carlyle Lake. c) Poles to foliations, Johnnie Lake South. d) Lineations, Johnnie Lake South. e) Poles to foliations, Turbid Lake. f) Lineations, Turbid Lake.

Foliation spacing, apparently controlled by feldspar grain size (or vice versa?) then decreases as the grain size decreases until a single strongly lineated foliation exists within a very fine grained rock, i.e. mylonite.

Many of the mylonites seen in outcrop have undulating foliation surfaces. These undulations define very open cylindrical folds with fold axes oriented parallel to the mineral lineation. This folding has resulted in a variation in the strike orientation of foliation surfaces of up to 50 degrees, across distances of 10 to 15 meters, about the general northeasterly trend. Variations in the mineral lineation orientations are minor in comparison.

Several crosscutting features were observed along Carlyle and Johnny Lakes. At the southwestern tip of Carlyle Lake, mylonite with an unusual north to northwest trending foliation has been cut by small well defined faults, with minor offset, which trend northeasterly. Other small faults with minor offset are seen locally within the interlayered units along the shore of Carlyle Lake. At the entrance to the narrows, on the south shore at the east end of Carlyle Lake, the northeasterly trending interlayered units have been crosscut by a fine grained granitoid dyke which in turn has been offset 30 centimeters dextrally by a small fault which trends north. At the southwestern end of Johnny Lake on the south shore, mylonite trending north-south can be seen to

swing eastward into parallelism with the northeasterly trending mylonite which lines the shore (Figure 16c). Minor folds occur in the earlier mylonite.

Foliations and lineations measured along Carlyle and Johnny Lakes are shown in the contoured stereoplots in figure 17(a-d). Although minor local variations exist in the orientation of these elements, the intensity of the preferred orientation of fabric elements is high.

Area 3B

From the northeastern end of Johnny Lake through Turbid Lake, to the eastern limit of mapping, the Bell Lake Granite is in contact with quartzite gneiss. The nature of this contact is equivalent to that seen along the northwestern boundary of the Bell Lake Granite. A penetrative foliation developed within both the granite and the quartzite is defined by flattened and elongated quartz aggregates and phyllosilicates. The Bell Lake Granite locally develops an augen gneissic foliation.

The mylonites which form along this section of the contact are narrow, rarely more than one meter wide. Locally, mylonitized quartzite xenoliths are surrounded by very well foliated granite. A shear band foliation is locally developed within the Bell Lake Granite which trends northeasterly but, on Turbid Lake, dips moderately to the northwest. This foliation is seen to truncate feldspar phenocrysts within the

granite.

Foliations and lineations have been plotted on figure 17(e,f). Foliation surfaces trend northeasterly and generally dip southeasterly but surfaces dipping northwesterly are not uncommon. Mineral lineations are fewer and less concentrated than those along the granite-granite contact to the southwest but the preferred orientation plunging to the southeast can still be identified.

Geometry of Area 4

Area 4, which is located east of Johnny Lake, is underlain by metasedimentary gneisses, pegmatite and granitic dykes. The metasedimentary gneisses include quartzite, feldspathic quartzite, argillite, metagrey-wacke and biotite-muscovite schist. Pegmatite has intruded these units along foliation surfaces, adding to the banded appearance of the gneisses. Foliations measured in this area are shown in figure 18a. These surfaces have an inconsistent orientation and are everywhere tightly and irregularly folded. Surfaces were measured only where they maintained a relatively consistent orientation over a distance of about a meter. In general, planar features preferentially trend eastward and are steeply dipping either north or south. From this point maximum, poles to foliation surfaces define half of a great

circle trending south, the pole to which plunges moderately to the east.

Few mineral lineations could be measured (Figure 18b). Those that were measured were found to plunge moderately to the east or southeast.

Pegmatite and granitic dykes in area 4 are generally undeformed, although a few foliated or mylonitized dykes were seen.

Geometry of Area 5

Area 5 is located south of the Johnny Lake Shear Zone and is bounded to the southeast by the augen gneiss. The area is underlain by fine to coarse grained granite and fine grained tonalite. The rocks in area 5 are characterized by a persistent and consistent foliation and a large number of pegmatite dykes.

The intensity of the foliation is variable and ranges from poorly developed to mylonitic, commonly within a single outcrop. Generally, pods of weakly to moderately foliated rocks ranging in size from a few meters to a few hundreds of meters, are surrounded by rocks which have suffered much higher strains. The intensity of the foliation, which has a patchy distribution in the northwest part of the area, tends to increase toward the southeast. Commonly a C & S fabric is

developed in the coarser grained units where the intensity of the foliation is high.

The foliations and lineations measured in the area are shown in figure 19. These diagrams illustrate the very strong preferential orientation of fabric elements which is characteristic of the Grenville Front Tectonic Zone.

The pegmatites occurring in area 5 display a wide variability in orientation, form and level of deformation. Pegmatite sheets, which range in width from a few centimeters to a few meters, may occur in positions which conform to the foliation or they may trend obliquely. Where the foliation intensity in the host rock is high, obliquely oriented pegmatites are folded about the foliation and all pegmatites show evidence of strain. Strain evidence in pegmatites includes the development of a foliation and lineation, recrystallized or fine grained quartz, fractured, broken or rotated feldspars and a reduction in bulk grain size producing mylonite. Pegmatite material may also occur in irregular masses of migmatite which have gradational boundaries with the country rock. These masses commonly interfinger along foliation surfaces of the host rock. Inclusions of foliated country rock occur within these migmatites, which themselves may or may not display a foliation.

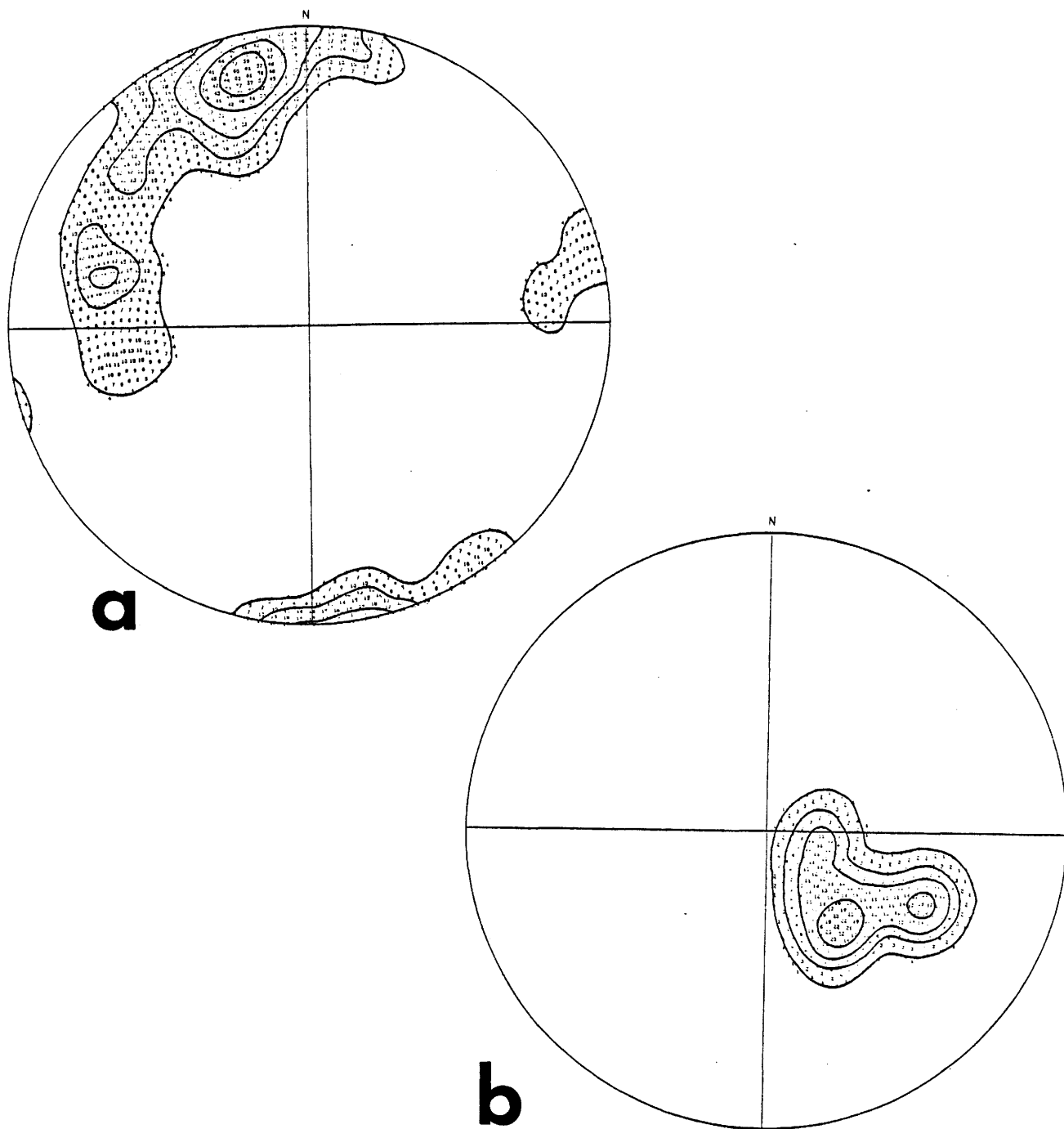


Figure 18. Contoured stereoplots of a) poles to foliations and b) lineations measured in area 4.

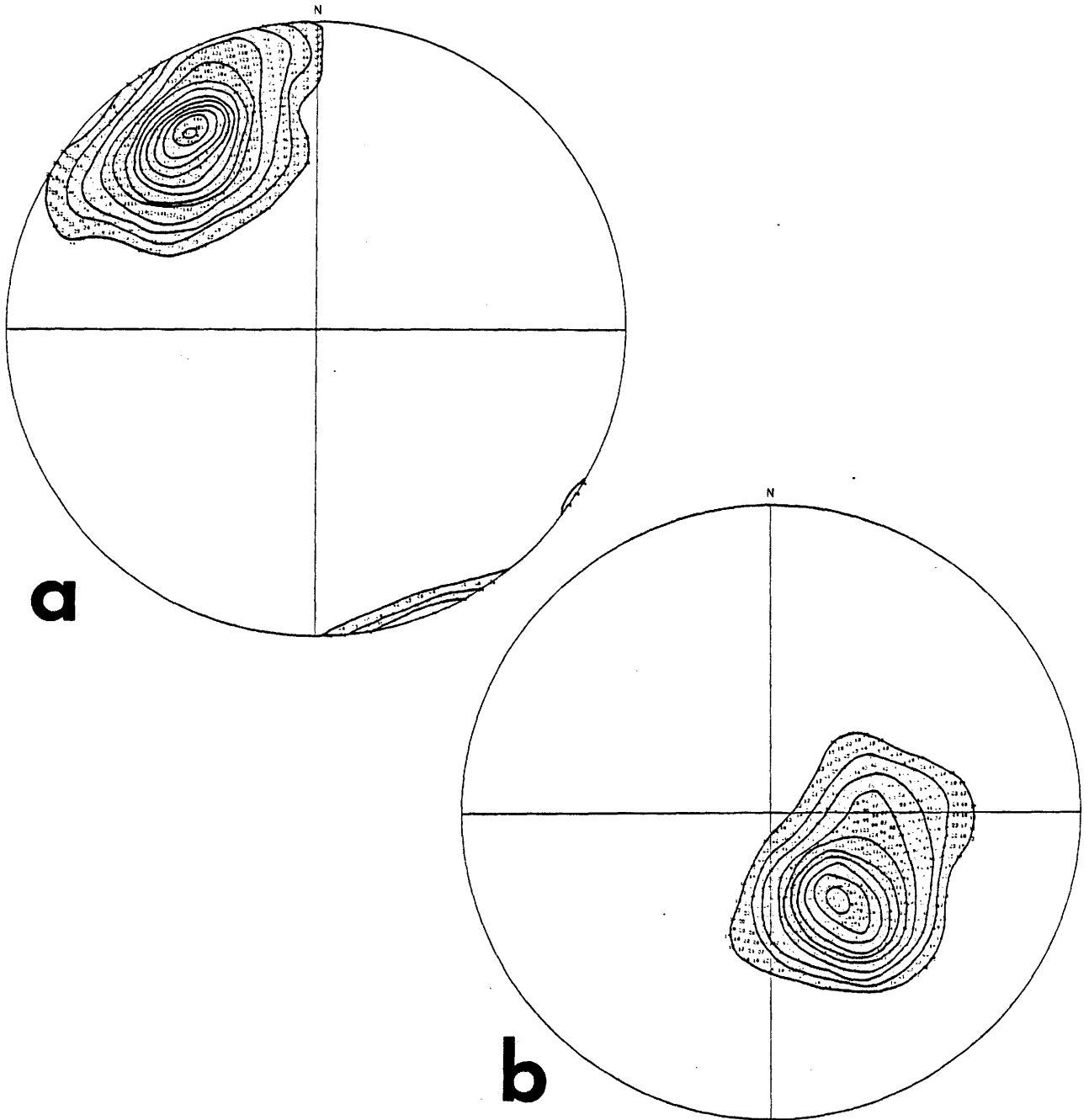


Figure 19. Contoured stereoplots of a) poles to foliations and b) lineations measured in area 5.

Several folds are seen in the rocks in Area 5. These are most commonly sharp nosed Z-folds with amplitudes of a meter or less developed in the foliation. Pegmatite and diabase dykes are concordantly folded. The trend of axial surfaces of these folds ranges from 25 to 50 degrees. Fold limbs trend north to northeast and dip moderately to steeply east to southeast.

The mylonites developed in area 5 tend to be restricted to narrow zones which range in width from a few centimeters to a few meters. These mylonites are extremely fine grained and strongly foliated and lineated. They are generally white, pink and black banded and may contain feldspar augen as large as 5 centimeters. More commonly, feldspar porphyroclasts in the mylonites, which are apparently derived from pegmatites, are one centimeter or less in diameter. In many places mylonite is seen to form in pegmatite dykes oriented parallel to the foliation while the host rock adjacent to these pegmatites shows a much lower level of deformation. In a very few outcrops, brittle microfaults are seen to offset dykes and veins in this area by a few centimeters.

Geometry of Area 6

Area 6, located in the southeast corner of the study area, is underlain predominantly by red and black augen gneiss. Foliations are well developed everywhere in this area and commonly define a C & S fabric. Foliation spacing ranges from a centimeter to less than a millimeter where mylonite is developed. Mylonite zones gently anastomose around pods of less deformed rock. A mineral lineation is also strongly developed in this area on foliation surfaces and is defined by quartz and feldspar rods. All dykes occurring in this area have undergone some deformation. Dykes oriented parallel to the foliation are generally mylonitized and those in oblique orientation are folded and may also be mylonitized.

Planar and linear elements are plotted on contoured equal area nets in figure 20. Fabric elements in this area are not only more abundant than in any of the other areas, but also show the strongest preferred orientation. Foliations strike consistently to the northeast and dip moderately to the southeast. Lineations plunge southeast and essentially follow the true dip direction of the foliation surfaces.

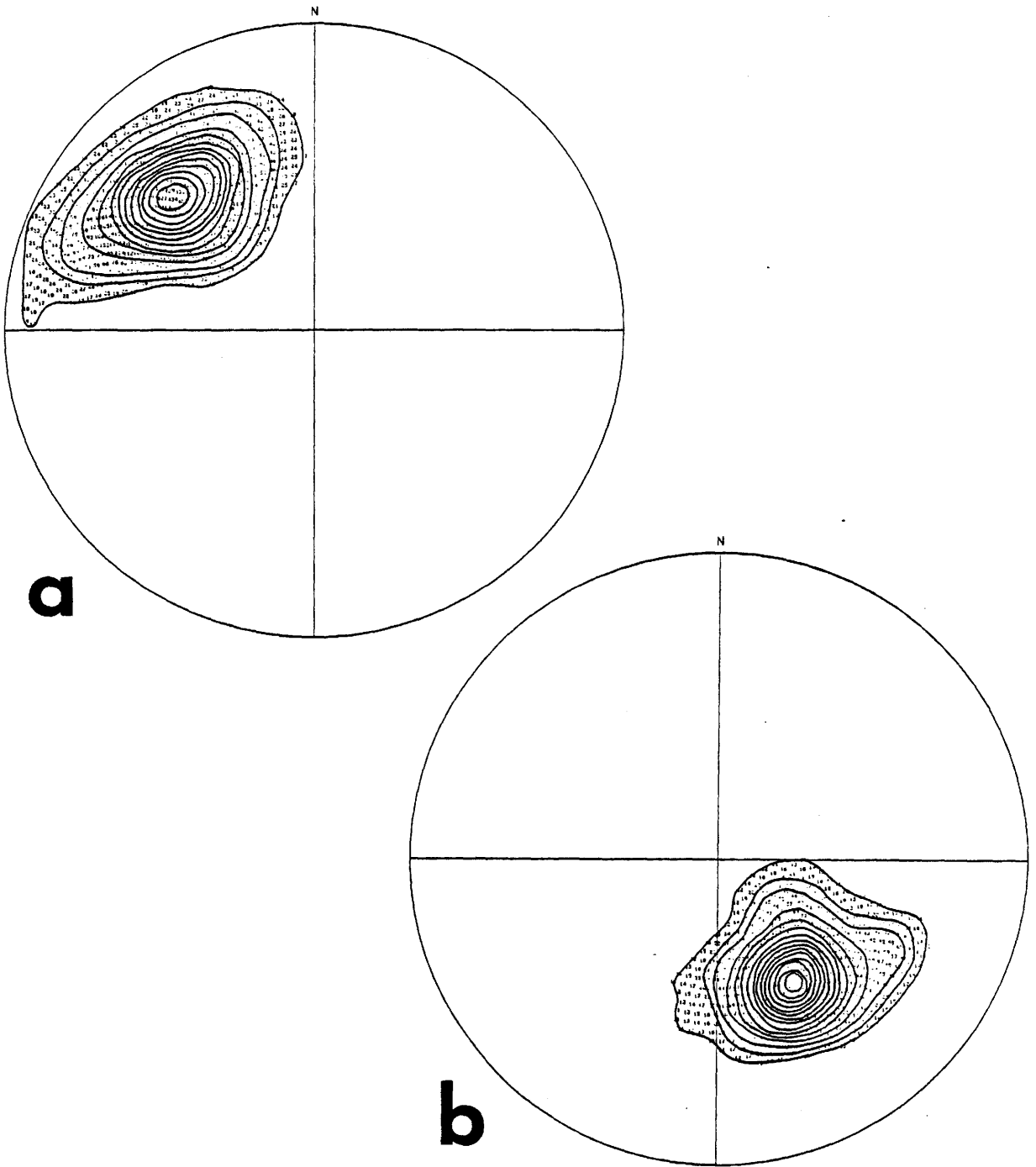


Figure 20. Contoured stereoplots of a) poles to foliations and b) lineations measured in area 6.

Regional Shear Zone Geometry

Introduction

The Grenville Front has been well documented as a major zone of north to northward reverse fault movement (eg. Davidson, 1986). Evidence for such movement can be seen at all scales from regional to microscopic.

Ramsay (1980) has outlined the general geometry and some associated features which can be applied to most large scale shear zones. Many of these features can also be applied to smaller scale structures, which will be discussed later. Those features discussed by Ramsay (1980) which pertain to the Grenville Front Tectonic Zone in Carlyle Township are outlined below.

Shear zones can be defined as areas in which intense deformation is localized into narrow subparallel sided zones. These zones can be divided into three major types; brittle, brittle-ductile and ductile.

- 1) A brittle shear zone (Figure 21a), more commonly called a fault, is characterized by the existence of a clear discontinuity which exists between the two sides of the zone. The walls of the fault may be either totally unstrained or they may be brecciated. All features seen in brittle faults can be attributed to brittle failure which is controlled by

the elastic properties of the rocks involved.

2) A brittle-ductile shear zone may occur in one of two forms. The first and most commonly recognized, is that in which a fault clearly exists, seen as a discontinuity between the two sides, but the walls of the fault show permanent strain (Figure 21b). The extent of the strain and the distance to which it penetrates the wall rock depends on such things as strain rate, temperature and confining pressure. This feature is sometimes called a "drag fold" implying that the folding is a result of frictional drag effects but the permanent deformation may, in fact, predate the actual movement along the fault. In this type of brittle-ductile shear zone the conditions existing during deformation are such that the rock behaves ductilely at the onset of deformation but reaches the point at which straining has "hardened" the rock and continued stress causes the rock to fail brittlely. (The mechanism involved in strain hardening will be discussed in a later chapter).

The second type of brittle-ductile shear zone is that which is known as extension failure or extension opening. In this type of shear zone the bulk of the rock shows a coherent permanent deformation similar to that of a ductile shear zone. During continued deformation extension fractures or gaps form which crosscut the shear zone fabric, making an angle of 30 degrees or more with the shear zone boundary

(Figure 21c). If the shear zone boundary cannot be identified, these fractures appear as an en echelon set in which the tips of the fractures define the boundary. These gaps may be filled with fibrous crystalline material such as quartz or calcite. As in the previous case, these fractures develop after the limit of coherent flow in the rock has been reached but failure in this case is a result of tensile rather than shear stress.

3) In a ductile shear zone all deformation and differential displacement has been accomplished by ductile flow (Figure 21d). This commonly occurs in crystalline basement rocks since it is the dominant deformation mode which allows large volumes of homogeneous rock to change shape. Ductile shear zones can form under metamorphic conditions of greenschist and above.

Regional Development of Shear Zones: Relationships Between Deep Level Ductile and High Level Brittle

In an area where regional scale thrusting has occurred, the general sequence includes crystalline basement with a sedimentary cover. In such a situation the crystalline basement will contain ductile shear zones. Such a shortening of basement rocks produces uplift in the core of the zone resulting from crustal thickening. Assuming the sedimentary

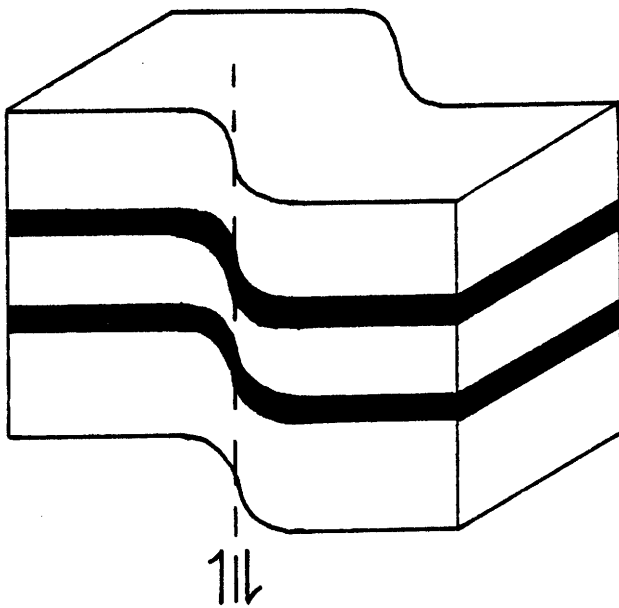
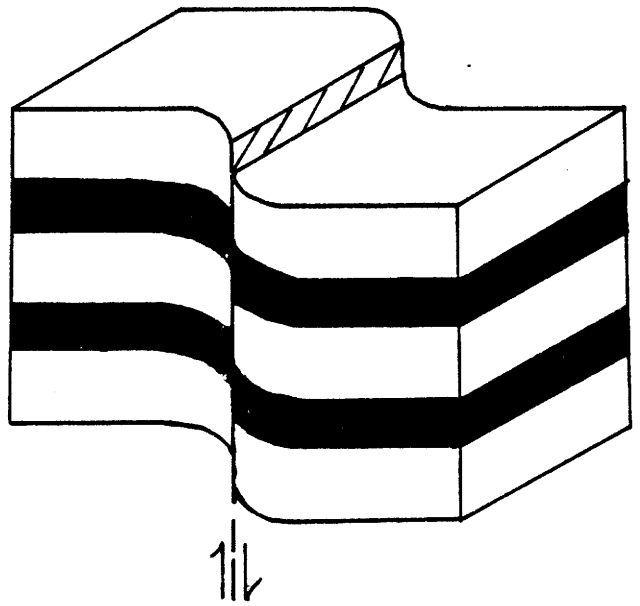
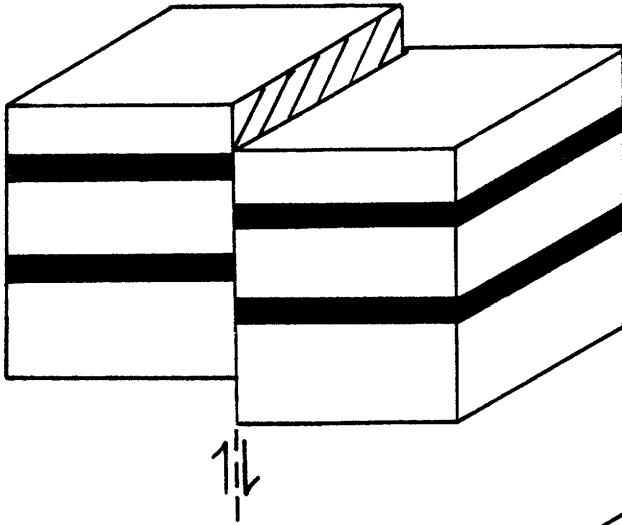
sequence is thick enough, the ductile shear zone will pass through the basement unconformity into the overlying sediments. As the shear zone continues to higher crustal levels, the ductile nature will change to brittle-ductile as the confining pressure is progressively relaxed. The exact level at which this occurs will vary depending on the mechanical properties of the rocks through which it passes. As the zone approaches the surface, the internal deformation of cover rocks becomes less important. The continuation of the thrust through the upper sequence occurs at low angles through the less competent layers while cutting through the competent layers at a high angle as a purely brittle fault.

During thrusting, movement of the upper side of the zone brings material from lower more ductile levels adjacent to that which has been deformed under less ductile conditions. When such an event is followed by a long inactive period, subsequent erosion can expose evidence showing all levels of deformation from brittle through ductile.

Figure 21a. Brittle fault geometry.

Figure 21b. Brittle-ductile fault geometry.

Figure 21d. Ductile fault geometry.



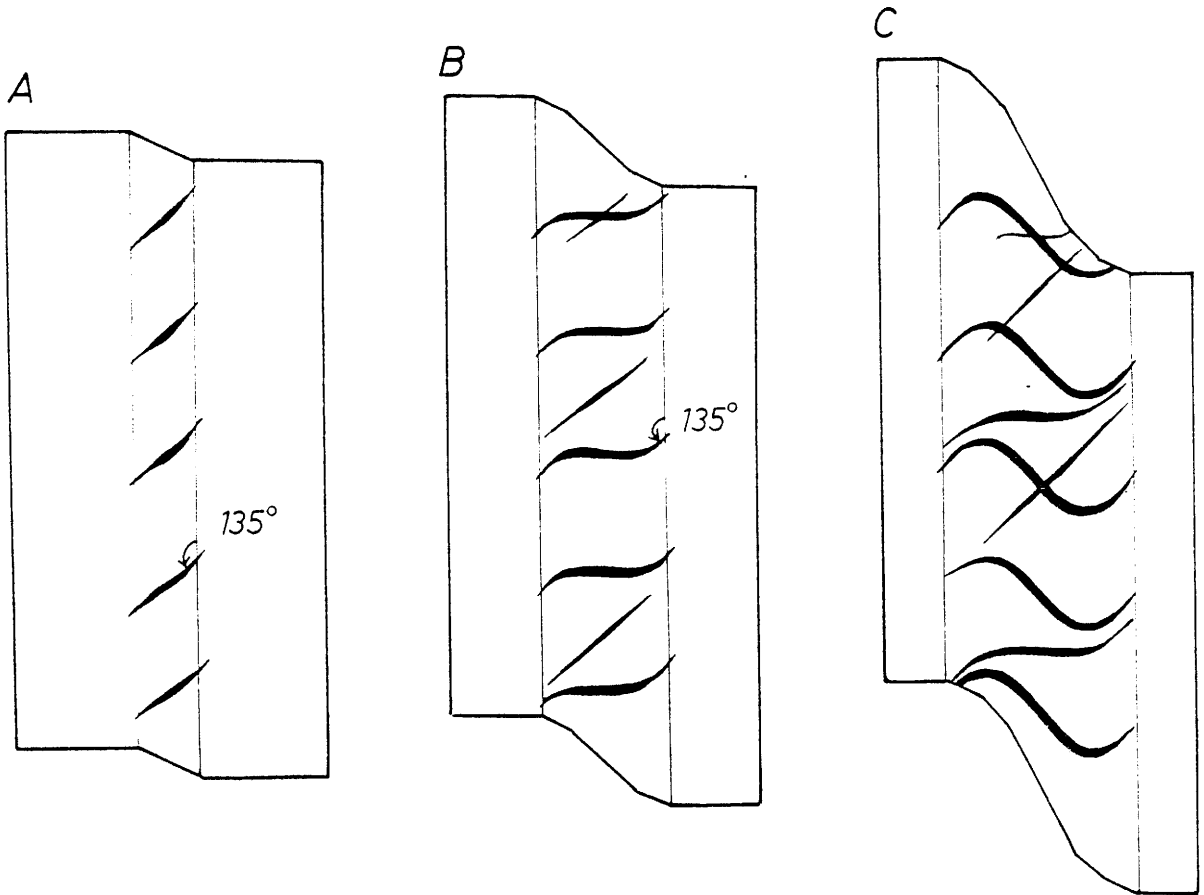


Figure 21c. Ductile-brittle fault geometry showing extension opening. (From Ramsay and Huber, 1985).

Distribution of Brittle/Ductile Strain

Based on field observations of macroscopic geometry, a general transition in deformational style from brittle to ductile can be recognized across the study area.

Area 1, which follows the northwestern limit of mapping, is characterized by a style of deformation attributable largely to brittle processes. The large volume of cataclastic breccia which contains large and angular fragments along with the occurrence of void-filling quartz crystals is indicative of a high level brittle fault. The Streaky Biotite Gneiss which is associated with this fault is a less competent unit than either the quartzite or the granite and could therefore deform more ductilely by slipping on the phyllosilicate rich layers. The existence of microfaults containing microbreccia which penetrate the granite in this vicinity, as well as the occurrence of pseudotachylite, also attest to the brittle nature of this deformation.

The location of the fault, along the granite-quartzite contact does not appear to be coincidental. Intrusion of the granite along the bedding planes of the quartzite and the mixing of these components to form the Streaky Biotite Gneiss, produced a boundary zone which was weaker than either unit involved. A large part of this weakness resulted from the heterogeneity or banding produced as a result of the

intrusion. The strain that resulted from the imposed stress on the system would tend to concentrate along this heterogeneity, especially if the heterogeneity was planar and suitably oriented for slip.

It is not clear whether the vertical orientation of the bedding in the quartzite and the banding in the contact was imposed prior to the onset of the deformation which produced the brittle fault. Rotation of planar elements in the early to mid stages of deformation followed by late faulting is also possible.

Areas 2 and 3 are dominated by deformation styles characteristic of the brittle-ductile regime. In area 2, the areal distribution of fabric development is inconsistent and the preferred orientation of this fabric is weak relative to areas to the south. This variability in orientation, although partially due to a pre-existing fabric, is largely due to the low ductile strain levels that existed in this area during their formation. Although a penetrative fabric is widely developed in area 3, many of the surfaces show dislocation (Figure 22a) indicating brittle-ductile strain. In the outcrop of tonalite which occurs on the south shore of Johnny Lake, a series of en echelon tension fractures are developed (Figure 22b), also indicative of brittle-ductile deformation. The large number of crosscutting features in these areas, which involve both the foliation and small shear zones

Figure 22a. Foliation surface in Bell Lake Granite showing dislocation, offsetting a thin folded granitic dyke. Movement on the surface was largely in a dip-slip direction. Johnnie Lake.

Figure 22b. A series of en echelon tension fractures in tonalite. Colour banding is a result of water alteration. Hammer handle points north. Johnnie Lake.



indicate that the ductile deformation may be the result of more than one deformational event. The mylonites developed at "non-Grenvillian" orientations which have been crosscut by mylonites in a "Grenvillian" orientation or by late brittle microfaults require at least two separate deformational events. The fact that the brittle faults are seen everywhere to crosscut all other features, indicates that the last stages of deformation in the area occurred under high level (brittle) conditions while the latest developed mylonites required brittle-ductile or ductile conditions. In area 2, deformation appears to have been restricted to the brittle-ductile regime at all times while, in area 3, deformation which began under ductile conditions was later succeeded by brittle deformation resulting from uplift during thrusting.

South of the Johnny Lake Shear Zone, in areas 4,5 and 6, deformation is generally restricted to that of a ductile nature. A penetrative fabric is developed which increases in intensity toward the southeast. The mylonites in these areas are less glassy in appearance than those occurring in area 3 and the frequency of late crosscutting microfaults drops to zero. The increase in fabric intensity and its associated ductility also corresponds to an increase in the volume of pegmatite and migmatite. The occurrence of little to non-deformed pegmatites in areas 4 and 5, which is not seen

in area 6, suggests that pegmatite generation occurred during deformation, but that this deformation continued in area 6 after that in other areas had begun to subside.

The distribution of structural styles and macroscopic fabric development in the study area corresponds to the transition from brittle to ductile deformation which is characteristic of regional reverse fault systems (Ramsay, 1980). This evidence therefore supports the theory that the Grenville Front has been the locus of reverse fault movement at some time in the past. Although deformation has not been restricted to a single event, the event responsible for the brittle ductile deformation (i.e. the reverse fault movement) overprints all earlier deformation and was therefore the last major event to have affected this area. Other evidence for reverse displacement will be discussed under kinematic analysis.

Regional Trends in Fabric

Foliations measured in the field are shown in figure 23, (pocket). A similar map of lineations is shown in figure 24, (pocket). The general trend of both foliations and lineations appears to be relatively constant throughout but the density of measurements in the north and northwestern parts of the area is low.

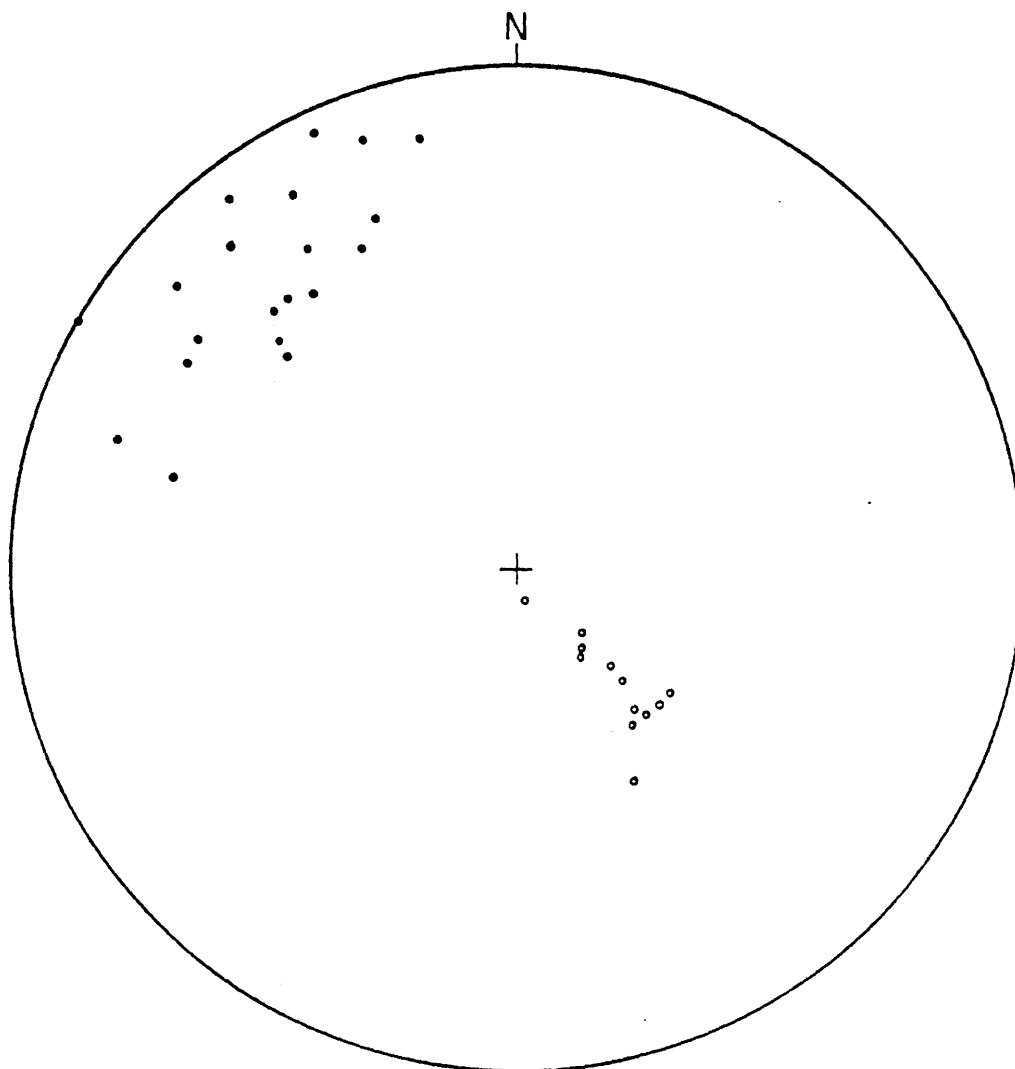


Figure 25. Stereoplot of the modes for the poles to foliations (•) and lineations (◦) given in tables 2 and 3.

TABLE 2
FOLIATIONS

Location	Average		Mode 1		Mode 2		Mode 3		N	σ
	S	D	S	D	S	D	S	D		
Ruth-Roy Lake	48	48	30	90					39	.44
Bell Lake	60	68	65	85					58	.53
Johnny Lake N	41	66	59	75	18	72	40	77	62	.55
Area 2	58	67	52	82	32	66			170	.91
Turbid Lake	59	67	49	75	70	80			66	.57
Area 4	67	65	77	77	15	60			33	.40
Johnny Lake S	50	59	47	60					60	.54
Carlyle Lake	63	61	64	60					143	.84
Area 5	56	64	57	65					210	1.01
Area 6	44	54	43	52					167	.90
Bell Lake Granite	52	64	36	67	54	58			195	.98
All Foliations	53	62	50	60					735	1.90
Mylonite Foliations	52	59	44	55	68	64			120	.77

S=Strike;D=Dip; N=# of data points; σ =standard deviation.

TABLE 3
LINEATIONS

Location	Average		Mode		N	σ
	S	D	S	D		
Ruth-Roy Lake	125	71	139	73	9	.21
Bell Lake	100	86	166	85	21	.32
Johnny Lake N	135	69	139	73	15	.27
Area 2	140	70	133	75	53	.51
Turbid Lake	159	71	136	65	19	.31
Area 4	126	58	143	58	7	.19
Johnny Lake S	128	59	134	58	28	.37
Carlyle Lake	128	58	129	58	91	.67
Area 5	132	60	140	60	127	.79
Area 6	146	51	151	50	106	.72
Bell Lake Granite	134	64	135	68	64	.56
Mylonite Lineations	132	59	138	58	67	.57

A=Azimuth; P=Plunge; N=# of data points; σ =standard deviation.

Although the structural signature of the Grenville Orogeny has largely overprinted any possible evidence of earlier events in areas 1,2,3B and 4, the fabric diagrams (Figures 14, 15, 17c, and 18) are diffuse when compared to the areas to the south. This indicates that the imposed structural fabric is less intense in these areas than in areas 3A,5 and 6, which have a strongly concentrated fabric (Figures 17a-d, 19 and 20) typical of the Grenville Front Tectonic Zone. Any evidence that a pre-Grenvillian deformational event occurred along this section of the Grenville Front is most likely to be preserved in areas 1,2,3B and 4 since the tectonic overprint has not been strong enough in these areas to completely destroy previous fabrics. The east-west trend in fabric in area 4 corresponds to a fabric which is typical of Huronian rocks resulting from the Penokean Orogeny. This supports the conclusions of Frarey (1985) that these paragneisses are Huronian equivalents. Also area 4 is located in a position which corresponds to the extension of the McGregor Anticline.

Values for the average and the mode of the foliation distribution are shown in Table 2. These values were calculated during the computer plotting of the contoured fabric diagrams. In cases where more than one mode occurs, the values are listed in order of importance. The order in which the locations are listed essentially corresponds to

their occurrence from north to south. Area 4 has been listed above the Johnny Lake Shear Zone due to the diffuse nature of the fabric.

It can be seen from the data in table 2 that the strike values do not follow any sort of regional trend other than their being northeasterly. Although the range in strike values varies by as much as 60 degrees (eg. area 4), this variation appears random both from northwest to southeast and from northeast to southwest. This variation in strike values can be attributed, not only to remnant fabrics from earlier events, but also to the undulatory nature of the mylonite surfaces as they are traversed along strike. The same undulation is seen on the outcrop scale with the same or larger variations in strike. Since all of the movement on these surfaces was restricted to essentially dip slip, undulations along strike would not present a mechanical problem. It is, in fact, to be expected in mylonitic terrains (Bell and Hammond, 1984).

The dip values for the mode of each area do follow a definite trend. These values show a strong tendency to decrease across the area from the northwest at the granite-metasediment contact to the southeast in the augen gneissic terrain. Another noteworthy feature of these data is the decrease in the amount of variation in measurements which is displayed by the difference between the average and the

mode. The increased concentration in attitudes follows the same trend as the decrease in dip values and the transition from brittle to ductile behavior.

The average and the mode of the lineation distribution in each area are listed in Table 3. The variation in azimuth is generally less than 20 degrees which is much smaller than that of the corresponding foliations. Plunge values, on the other hand, appear to follow the same trend as the foliation dip values. Although the foliation surfaces on which these lineations occur fluctuate in strike direction, the lineations maintain a consistent orientation. To illustrate this, the poles to foliation modes from table 2 have been plotted with the lineation modes from table 3 on the stereonet in figure 25. This geometry corresponds reasonably well to that which would result from sliding on a corrugated surface. The consistency in attitude of mineral lineations and the increase in abundance of lineations toward the southeast indicates that this feature has resulted from a single deformational event.

CHAPTER 4

MICROSTRUCTURES

Introduction

This chapter will deal with deformational features which are observable in thin section. Many of these features are expressed in hand sample, i.e. mylonites, C & S fabrics, but the development of these fabrics occurs at a grain or subgrain scale and therefore can only be characterized in thin section.

Mylonites

During deformation within a shear zone, dynamic recrystallization is common and leads to the formation of mylonite. The term mylonite was first introduced by Lapworth in 1885. It is derived from the Greek word "mylon" meaning mill, and was used to describe rocks of the Moine Thrust Zone in Scotland which had apparently been crushed during thrust movement. Since that time, the mechanisms involved in the formation of mylonites, as well as the definition of the word itself, has been the subject of repeated controversy. When first introduced, the term mylonite was meant to imply brittle deformational processes and was used as such by later authors (eg. Christie, 1963; Higgins, 1971). More recently, the importance of ductile processes in mylonite formation has been recognized (eg. Bell & Etheridge, 1973) such that the term "mylonite" is now used as a field term and must be accompanied by a complete description of the nature of the deformation.

At the annual meeting of the Canadian Tectonics Group in 1984, each of the members was asked to submit a definition of the word "mylonite". The results of this survey led to the following definition:

"Mylonite occurs in shear zones, that is, zones across which one block of rock is displaced with respect to another, and which show no evidence of major loss of material continuity. They develop primarily by ductile deformation processes. They are well foliated and commonly well lineated, and show an overall reduction in grain size when compared to their hosts. Mylonites commonly contain a suite of diagnostic asymmetric structures, such as rotated porphyroclasts/blasts and S-C textures. Mylonite zones can develop at any scale, in rocks of any composition and fabric."(Mawer, 1986)

The microstructural development of mylonites has been paid a great deal of attention in the past decade. Much of this research has been confined to the study of quartz fabric development (eg. Ransom,1971; Shelly,1972; White, 1976,1977; Bouchez, 1977; Carreras et al.,1977; Christie & Ord,1980; Gapais & White,1982; Culshaw & Fyson,1984; Evans & White, 1984; Burg,1986), while others deal with the overall fabric development of quartzo-feldspathic rocks (eg. Bell & Etheridge,1973; Burg & Laurent,1978; Lister & Price,1978; White et al.,1982).

At present the processes and mechanisms involved in the formation of mylonite in quartzites are fairly well understood. Research is now tending toward the more heterogeneous (and more common) rock types such as granites. Because the various minerals within granitic rocks behave

differently under the same metamorphic conditions, mylonite formation must be studied in rocks deformed under different metamorphic grades. An area which has undergone regional thrust faulting is ideally suited for this type of study. Such an area contains not only an abundance of mylonite, but it also provides access to a series of mylonites produced under increasing metamorphic conditions.

Thin sections cut from samples of granitic rock, collected across the study area, have been examined in order to characterize the the nature of the deformation in quartz and feldspar during mylonite formation. The level of deformation within these samples ranges from relatively undeformed to mylonitized and samples span a wide range in metamorphic conditions. All sections have been cut parallel to the lineation and perpendicular to the foliation (i.e. $X_f Y_f$) unless stated otherwise.

QUARTZ MICROSTRUCTURES

Progressive Development of Microstructural Strain Features

One series of samples was collected midway across the study area in area 5 (see Figure 13) and shows the transition from not visibly deformed in hand specimen to mylonitized. This series consists of three samples collected approximately one meter apart at location P35 (see Figure 2) with the average composition being that of a granodiorite (Table 1).

In the sample not visibly deformed (P35-1), the quartz occurs as aggregates filling the interstices between feldspar crystals. The grain size within these aggregates ranges from 1mm to 0.05mm. Grain shapes are irregular. Strain features observed include undulatory extinction and deformation bands. The deformation bands (Figure 26a) are broad and may have either faint or sharp boundaries, often within a single grain.

The second sample examined (P35) was collected approximately one meter away from that described above. This sample possesses a penetrative C & S fabric and in thin section displays a much larger number of strain features. Quartz occurs in two forms which can be directly associated with location relative to large feldspar grains. Quartz occurring in protected areas such as pressure shadows beside feldspar augen, displays the same strain features described

for the first sample, i.e. undulatory extinction and deformation bands, as well as deformation lamellae and subgrains (Figure 26b). Deformation lamellae differ from deformation bands in that they are much thinner. The spacing of deformation lamellae in Figure 26b is 0.015mm. Quartz in this sample also occurs in the form of ribbons (Figure 26c) which define the foliation. The ribbons are composed of aggregates of quartz and contain both subgrains and recrystallized grains which are elongated. The long axes of these grains are oriented at 30 degrees to the ribbon boundary. These ribbons are similar to those described by Boullier and Bouchez (1978) as "Type 4 polycrystalline ribbons". Ribbons vary in width from 0.2 to 0.5mm and are generally one grain wide. The length of ribbons is highly variable, being two orders of magnitude or larger than the width. The overall quartz grain size in this sample ranges from 0.5 to 0.05mm with the larger grains occurring in the protected areas. Grain boundaries are irregular and serrated. The boundaries of the quartz ribbon aggregates are generally smooth.

The third sample in the series (P35a), collected approximately one meter away from the second, is a quartz-feldspar augen mylonite of granodioritic composition. In hand sample, the rock contains large pink feldspar augen (average size ~1cm) surrounded by an extremely fine grained

black matrix. This rock possesses a very powerful mineral lineation which can be seen on submillimeter spaced foliation surfaces. All quartz in this sample is confined to the matrix and occurs in one of two forms; 1) as ribbons or 2) as small, preferentially oriented, inequant grains which together with fine grained feldspar and mica, compose the bulk of the matrix (Figure 26d).

The quartz ribbons are narrow, 0.2mm wide aggregates of recrystallized grains and subgrains. The ribbons are generally straight sided but in the vicinity of large feldspar augen they become curved. Ribbon boundaries appear sutured as they grade rapidly into the finer grained matrix. The subgrains and recrystallized grains within the ribbons are elongated with long axes oriented again at 30 degrees to the ribbon walls. Subgrain and recrystallized grain boundaries within ribbons are irregular and serrated.

The majority of quartz occurs as 0.05mm inequant grains (average aspect ratio of 2) which are combined with grains of feldspar and mica of similar size to form the bulk of the matrix. The long axes of these quartz grains have a strongly preferred orientation parallel to the foliation direction. Grain shapes vary from square or rectangular to elliptical, grain boundaries are irregular and may be serrated. Undulatory extinction is common in both matrix and especially ribbon quartz.

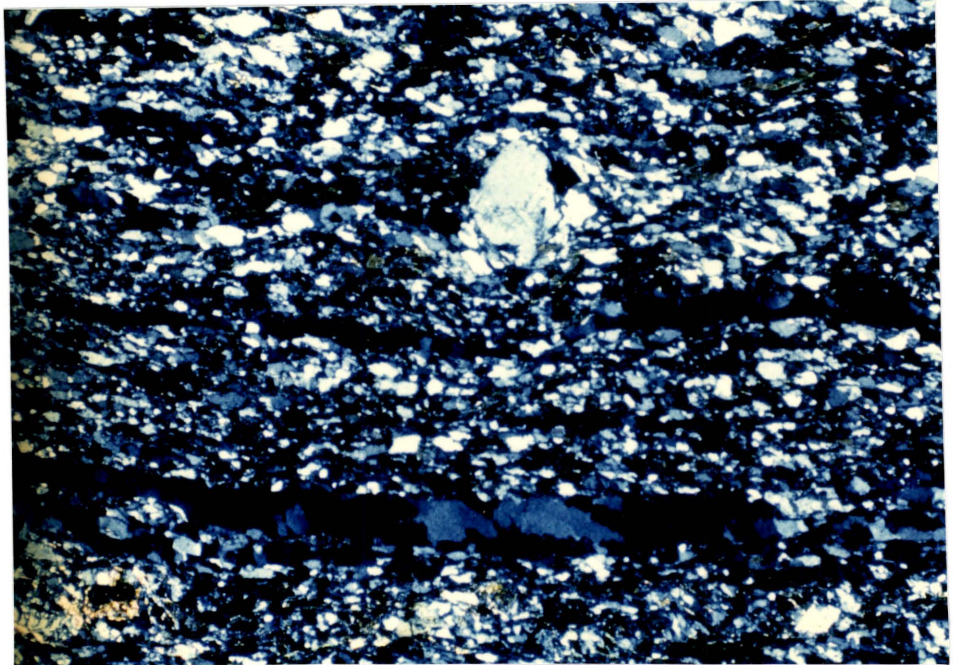
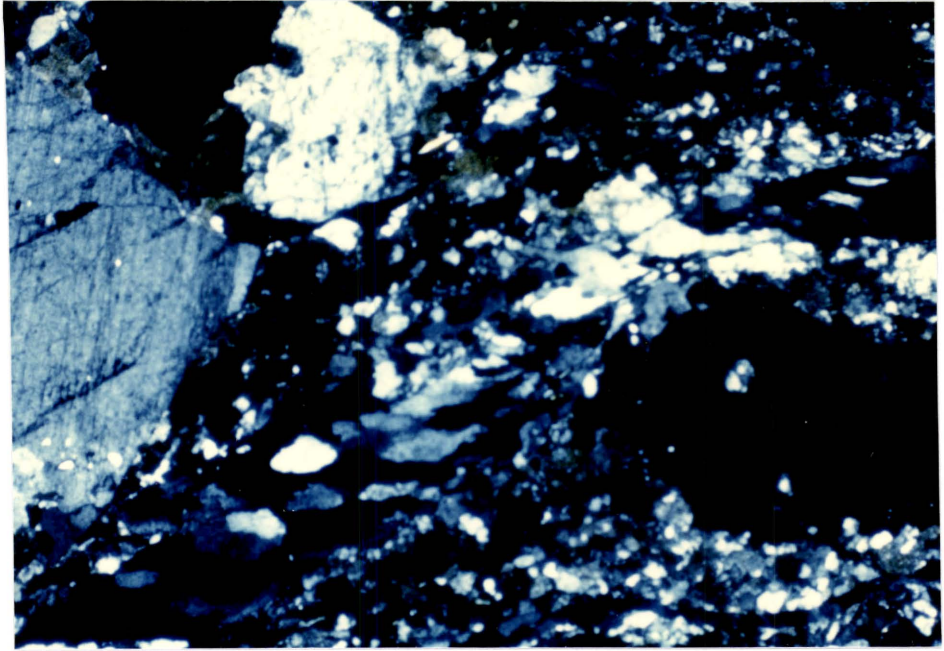
Figure 26a. Deformation bands in quartz occurring in a quartz-monzonite which appears undeformed in hand specimen. Field of view 3.25mm. P35-1.

Figure 26b. Strain features in quartz occurring in a deformed granodiorite which possesses a C & S Fabric. Features include deformation lamellae (l), undulatory extinction (u) and subgrains (sg). Field of view 1.3mm. P35.



Figure 26c. Quartz ribbon aggregate in a deformed granodiorite. Subgrains and recrystallized grains are elongated at an angle of 30 degrees to the ribbon boundary. Field of view 3.25mm. P35a.

Figure 26d. Quartz-feldspar mylonite of granodioritic composition. Average grain size is 0.05mm. Subgrains within the larger, 0.2mm wide quartz ribbon are elongated and oriented obliquely to the ribbon wall. Field of view 3.25mm. P35a.



Variations in Microscopic Strain Features

A number of samples of deformed rock, collected throughout the study area, have been examined in thin section to determine the variation, if any, in microstructural strain features in quartz from northwest to southeast. Although some of the variations observed may be in part the result of differences in host rock composition, all samples studied are quartzo-feldspathic rocks believed to be of plutonic origin, the mean composition of which is granodiorite.

Along the northwestern boundary of the study area (area 1, Figure 13), within the Bell Lake Granite, ductile strain features are restricted largely to undulatory extinction and deformation bands. Some grains have serrated boundaries and rarely very small (~5 micron) recrystallized grains are seen along these boundaries. The most pervasive type of deformation, seen in all crystals, is brecciation (Figure 27). The microfaults which cut through the granite contain angular fragments of quartz and feldspar surrounded by rock flour (or gouge).

Within area 2, a much larger number of ductile strain features can be observed in quartz. Subgrain formation and dynamic recrystallization have led to the formation of quartz grain aggregates which occur in a number of different forms. The simplest form is that in which an original quartz grain

has undergone incomplete recrystallization to form a quartz aggregate that still retains the outline of the original grain (Figure 28a). Within the aggregate, subgrains (diffuse boundaries) and recrystallized grains (sharp boundaries) display undulatory extinction, deformation bands and deformation lamellae. Grain boundaries are highly irregular and serrate. Grain shapes are also irregular and grain sizes range widely from 3mm to less than 0.01mm. Flattening of this type of aggregate by either pure or simple shear, leads to a quartz ribbon aggregate such as that shown in Figure 28b. Highly elongated subgrains, which again show undulatory extinction and deformation bands, are preferentially oriented along the foliation direction. Grain shapes, although largely elongated, remain irregular and grain boundaries serrate.

A second type of quartz aggregate which commonly occurs in area 2, is that which has been described by White (1976) as a core and mantle structure (Figure 28c). During deformation under conditions of high differential stress, the strain gradient can become extremely high along grain boundaries. This strain concentration leads to the formation of dynamically recrystallized grains along the grain boundary, leaving a relatively undeformed core. If the stress level is maintained, this process can continue until the recrystallizing mantle totally consumes the core leaving a quartz aggregate composed entirely of very fine grained

recrystallized quartz. The cores of these structures may show undulatory extinction, deformation bands or deformation lamellae, or may themselves be subgrained but the surrounding mantle is always finer grained. In the core and mantle structure shown in Figure 28c, the recrystallized grain size in the mantle is less than 0.01mm. The core shows undulatory extinction as well as a faint deformation band. A core and mantle structure is not restricted to equant grains. Many highly inequant grains are also seen to have this structure but flattening through either pure or simple shear, may have occurred before, during or after mantle formation. Figure 28d illustrates an example of this feature. The remnant host grain shows evidence of having undergone a large amount of strain, i.e. deformation bands and kink bands. Recrystallized grains in the mantle are generally equant and extend from the host farther at the tips than in the center.

In the northeast section of area 2, quartz ribbons are similar to those occurring in the central section of area 5, which have already been described under progressive development of strain features. In this area however, the ribbon morphology is not as well developed. Aggregates tend to be more tear drop shaped but the configuration of elongated subgrains and recrystallized grain oriented obliquely to the long axis of the aggregate is the same as that described previously.

Figure 27. Fault gouge in a microfault within the Bell Lake Granite. The fault gouge consists of angular fragments of quartz and feldspar in a rock flour matrix. Deformation bands can be seen in the quartz grain at the right hand side of the photo. Field of view 6.5mm. P204.

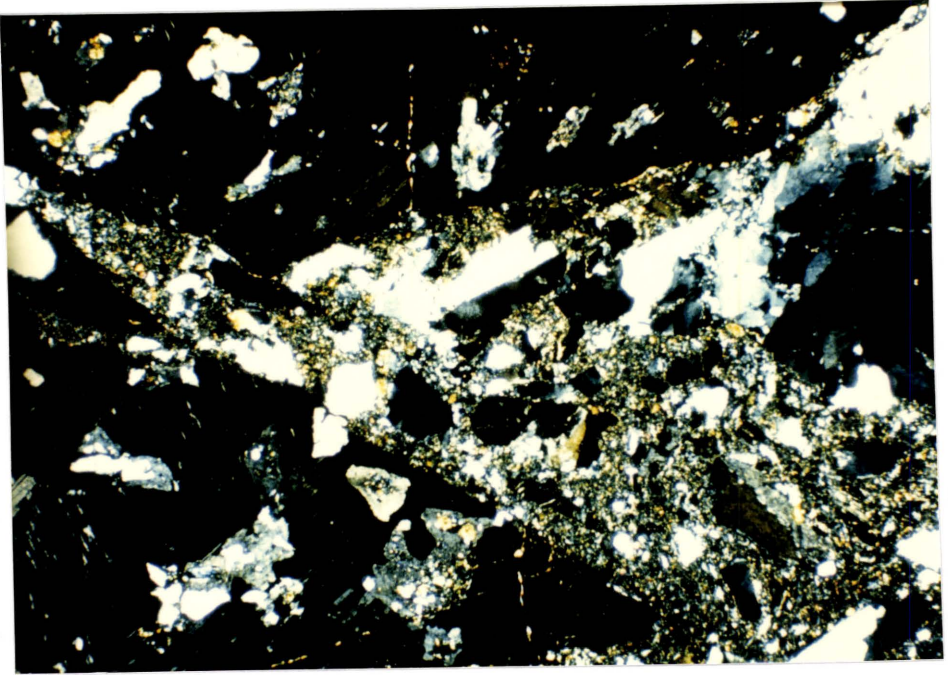


Figure 28a. Recrystallization of a quartz grain to form a quartz aggregate. Note irregular grain shapes, highly sutured boundaries and undulatory extinction. Aggregate is crosscut by late brittle fracture. Field of view 6.5mm. P121.

Figure 28b. Quartz ribbons in deformed Bell Lake Granite. Ribbons are composed of elongated and irregularly shaped subgrains which show undulatory extinction. Ribbons also contain small recrystallized grains. Grain boundaries are serrated. Field of view 3.25mm. P347.

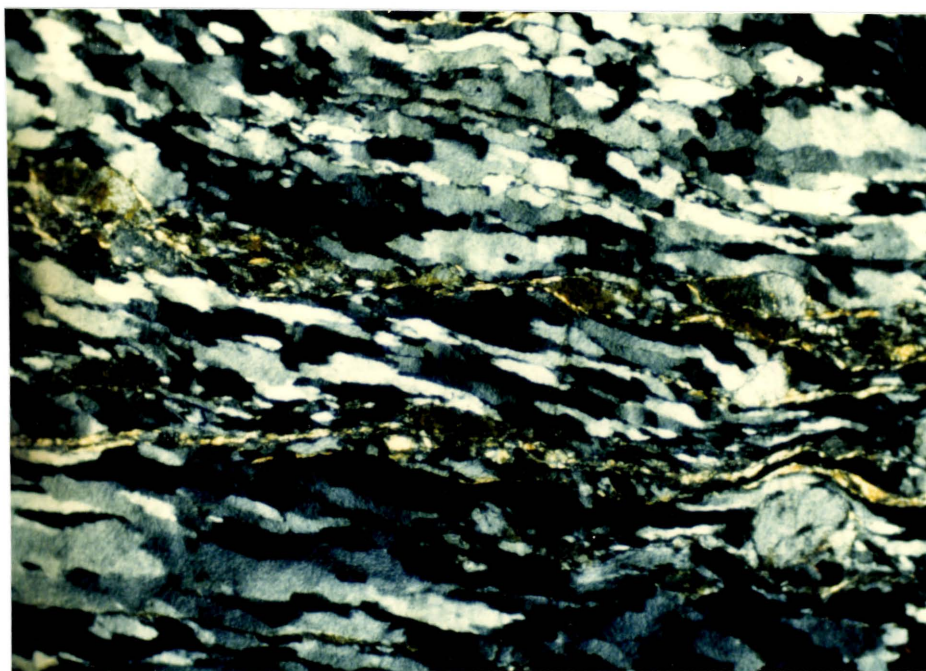
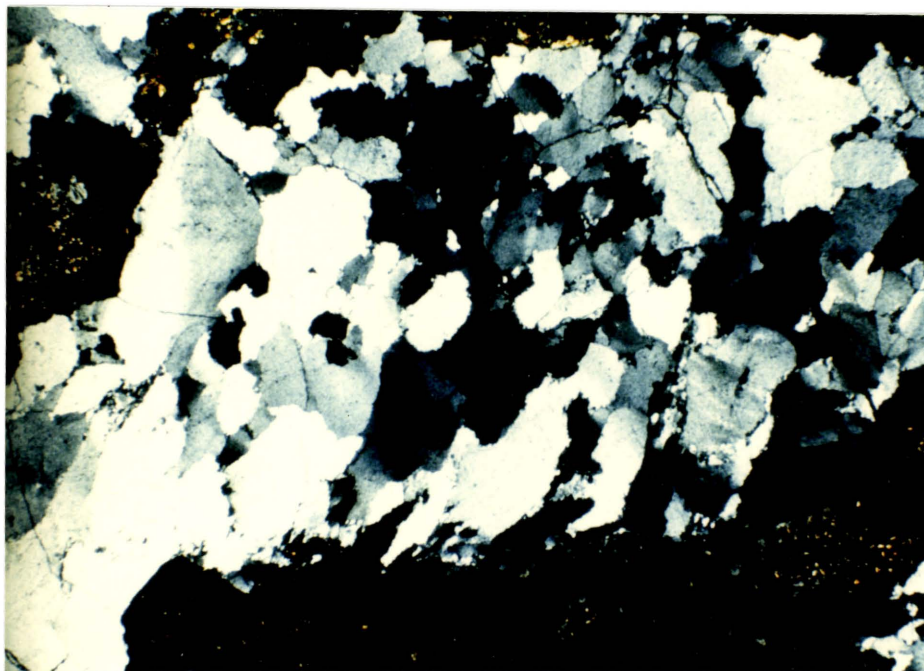
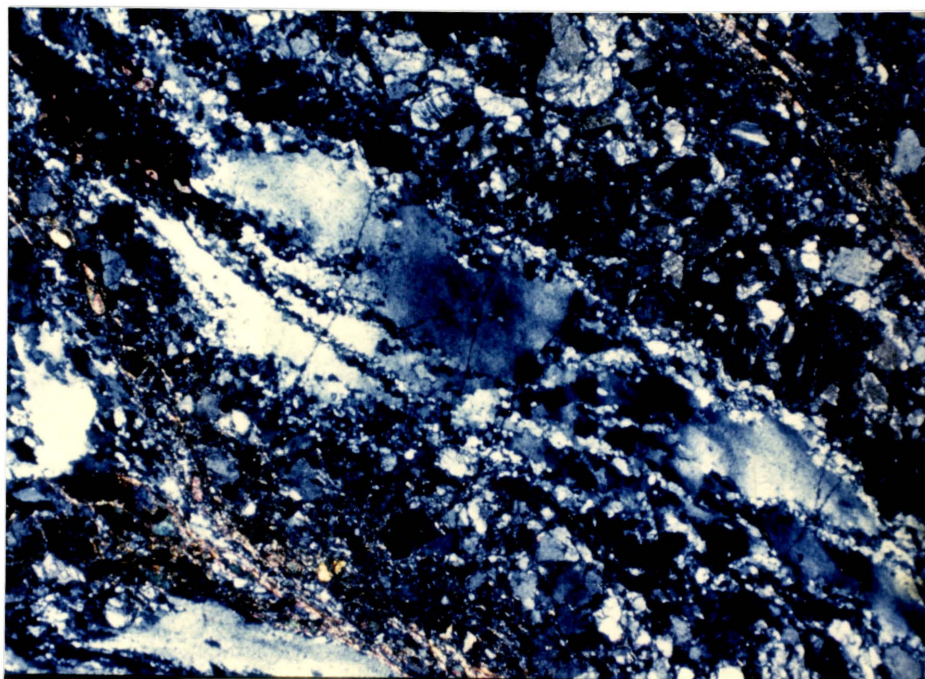
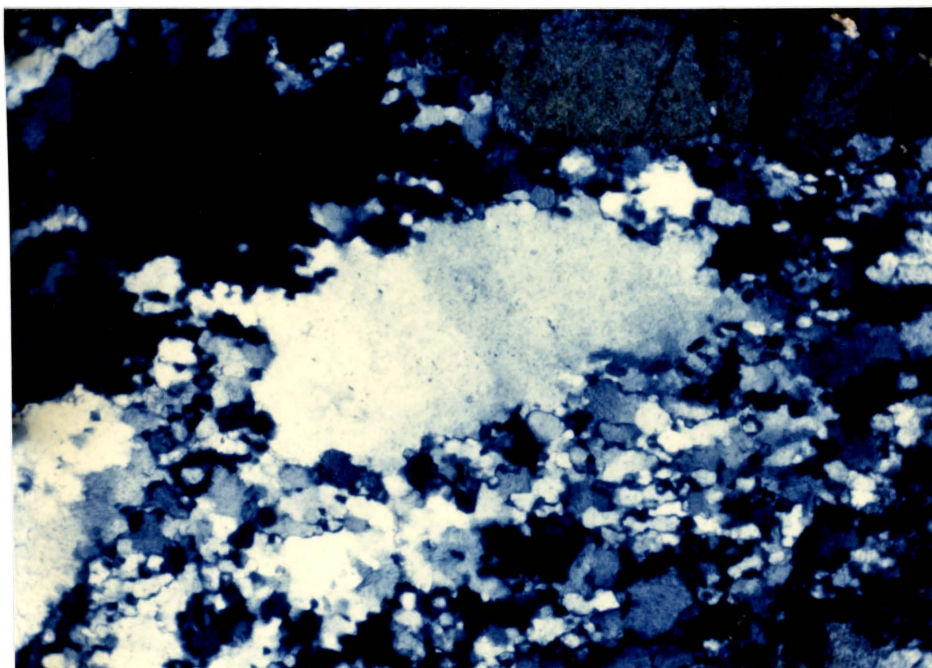


Figure 28c. Core and mantle structure in quartz. The unrecrystallized core shows undulatory extinction and deformation bands. Note highly sutured grain boundary as the core grades into mantle. Field of view 1.3mm. P115.

Figure 28d. Core and mantle structure in quartz. Host remnant is elongated and shows strong undulatory extinction. Initiation of quartz ribbon structure. Field of view 3.25mm. P115.



All quartz observed in samples from area 3 occurs in the form of ribbons. Along the northwestern boundary of the mylonite zone in area 3A these ribbons consist of highly elongated continuous quartz grains that can be up to two orders of magnitude longer than they are wide (figure 29). Grain widths in ribbons range from 0.3 to 0.05mm. Along their length quartz ribbons display undulatory extinction, deformation bands, kink bands and subgrain boundaries. The boundaries between ribbon grains are generally serrated and lined with very fine (<0.01mm) recrystallized quartz grains. The long axes of ribbon grains define the foliation which anastomoses around large feldspar augen with no discrete breaks in crystal continuity. These quartz ribbons correspond to Type 1 polycrystalline quartz ribbons of Boullier and Bouchez (1978).

Within the mylonites of the Johnnie Lake Shear Zone of area 3A, quartz ribbons consist of very fine, 0.02mm polygonal subgrains and recrystallized grains. Remnant host grains are rare and occur only in pressure shadowed areas adjacent to feldspar porphyroclasts. Host remnants are highly elongated parallel to the ribbon boundaries which define the mylonite foliation (Figure 30). The extinction pattern of recrystallized grains within the ribbon also trends parallel to the ribbon boundary. It is likely that segments of the quartz ribbon containing similarly oriented grains and

sugrains, indicated by similar extinction angles, originated from a single host grain (Ransom, 1971). Very fine grained recrystallized quartz ribbons such as these correspond generally to Type 2 polycrystalline quartz ribbons of Boullier and Bouchez (1978).

Quartz ribbons in area 5 occur in three distinctly different morphologies. Those examined from the northern part of area 5 are equivalent to that just described, i.e. quartz ribbon aggregates of very fine polygonal grains. Within the central section of area 5, quartz ribbons with well defined boundaries are composed of elongated recrystallized grains and subgrains which are oriented obliquely to the ribbon boundary (Figure 26c,d). Individual grains may be irregular in shape and have serrated boundaries.

In the southern part of area 5 and in area 6, quartz occurs most commonly as ribbons similar to Type 3 ribbons of Boullier and Bouchez (1978). This type of quartz ribbon has also been described by Culshaw and Fyson (1984) in rocks from the Central Gneiss Belt of the Grenville Province in Ontario. These ribbons consist of elongated quartz aggregates which normally have the width of a single grain and may be several grains long. Individual grain boundaries within these ribbons are smooth or serrated and tend to be oriented at a high angle to the ribbon boundary. Grain shapes vary from equant to highly inequant along the length of the ribbon and may be

irregular to square or rectangular in outline (Figure 31a,b). All of the quartz microstructures described previous to this can be attributed largely to deformation and recrystallization in a dynamic regime. This type of quartz ribbon requires initial dynamic recrystallization to produce the ribbon itself which must then be followed by an episode of static grain growth (Boullier & Bouchez, 1978). Late annealing is necessary to allow grain boundaries to become smooth. Static grain growth occurs through the migration of grain boundaries along the length of the ribbon such that favorably oriented grains grow at the expense of those not favorably oriented. Grain growth in a direction normal to the ribbon length is constrained by minerals of a non-quartz composition along the ribbon walls. In the quartz ribbons described here other strain features are also apparent. Undulatory extinction and deformation bands are common and sutured contacts between grains are seen. These other strain features become less evident toward the southeast boundary of the study area. Since the morphology of these quartz ribbons generally conforms to descriptions given by other authors, the deformational history must involve the process mentioned above. In addition to this, a dynamic episode following the static growth period is necessary to account for the other strain features. An alternative to this would be that during metamorphism, temperatures were high enough that dynamic

recrystallization and static grain growth were competing processes. In a regional thrust fault system such as this, which involves uplift of material from deep crustal levels, either scenario would be possible.

Discussion of Quartz Microstructures

The progressive development of microstructural strain features in quartz has been documented by many authors (eg. Bell & Etheridge, 1973; White, 1976, 1977; Carreras et al., 1977; Bouchez, 1977; Burg & Laurent, 1978; Poirier, 1980; White et al., 1980; Burg, 1986) and corresponds well with the sequence which has been described for this area. It is now agreed that quartz microstructures which develop in mylonites are the result of different glide or creep processes which act at the lattice level.

When a crystal is subjected to differential stress, the crystal responds through the formation of dislocations in the lattice, thus increasing the internal energy of the crystal in an attempt to attain thermodynamic equilibrium with the surroundings. The higher the differential stress, the more dislocations are necessary for equilibrium to be maintained. Once formed, dislocations tend to migrate through the crystal until they reach a stable configuration such as a dislocation wall. Should these dislocations become pinned or tangled, eg.

due to an impurity in the crystal, so that dislocations can no longer move through the crystal, strain hardening results and further deformation can only be accommodated through brittle processes. At temperatures greater than 0.4 to 0.5 of melting, hot creep conditions exist which allow dislocations to move around obstacles and continue migration until a stable configuration is reached. (For more information on dislocation theory see Hobbs, Means & Williams, 1976; Nicolaes & Poirier, 1976).

At the onset of deformation the first optical strain feature to occur is undulatory extinction. This strain feature can result from one or more of three possible substructures (White, 1976):

- 1) A large density of individual dislocations,
- 2) The formation of closely spaced dislocation walls,
- 3) The presence of lattice rotations.

Of these 2) is most commonly responsible for undulatory extinction in quartz. Dislocation walls are generally oriented along prism planes and all have a similar sense of tilt.

The next optical strain features which develop in quartz are deformation bands and deformation lamellae; these constitute the next level of strain following the formation of dislocation walls. Small segments of dislocation walls form parallel to a rhomb plane such that the final product is

the concentration of elongated subgrains into bands which lie parallel to prism planes. Deformation bands may form either parallel or perpendicular to the most active slip plane in the crystal. Deformation lamellae are similar to deformation bands in their make-up but tend to be much thinner and more intense. In deformation lamellae, narrow zones of subgrains form subparallel to a basal plane.

With increasing strain, elongate and equidimensional subgrains will form. Before the development of discrete subgrains, the host grain may appear polygonized (lattice misorientations of ~ 1 degree). As the amount of misorientation between the subgrain and the host grain increases, the walls become better defined. After a misorientation of between 7 and 10 degrees has been reached, a strain free new grain is formed.

In a rock adjacent to a shear zone, which appears undeformed in hand sample, all of the above features can be seen in thin section. The location of each feature within the grain indicates the strain distribution. As the level of strain increases, undulatory extinction and deformation bands and lamellae are most often seen in quartz located in "protected" areas which include grain cores (White, 1976; White et al., 1980), inclusions in feldspar grains (Bell & Etheridge, 1976) and adjacent to the sides of large feldspar porphyroclasts which are oriented normal to the foliation

(Lister & Price, 1978). Figure 32 illustrates another example of quartz which has suffered lower strain through the protection of a large feldspar grain. Subgrains and dynamically recrystallized grains may be restricted to grain boundaries where the strain gradient is highest (Figures 28c,d) while other quartz grains may be completely converted to aggregates (Figures 28a,b). The shape of quartz grains and quartz aggregates indicates the amount of strain the crystal has undergone.

Once the deformation becomes highly visible in hand specimen, the majority of original quartz grains will have been converted to polycrystalline aggregates which are elongated parallel to the main stretching direction, i.e. ribbons. The size of the recrystallized grains is mainly controlled by the differential stress although strain rate and temperature may have some influence. Mylonites produced in high grade environments tend to have a larger recrystallized grain size than those from lower grade environments. Because of this dependence, the stress gradient across a shear zone may be seen as a change in recrystallized grain size. This point will be discussed in more detail in a later section on stress estimates.

During mylonite formation, the percentage of grains which have been recrystallized continuously increases until the rock acquires a steady state microstructure. In quartzites

this occurs at a shear strain of 5 (White et al., 1980). Once a steady state has been reached, any further straining has very little effect on the microstructural appearance. On a substructure scale, steady state corresponds to that in which the strain hardening rate, i.e. the dislocation density and dislocation entanglement, is balanced by the recovery rate, i.e. subgrain formation (White, 1976). In quartzo-feldspathic rocks, large, strong feldspar porphyroclasts have a major influence on the strain distribution within the rock (Lister & Price, 1978). Much higher strain is required before a steady state can be reached (if at all). In this type of rock, a steady state microstructure may develop in the matrix where it is removed from the influence of the porphyroclasts. An overall steady state fabric will only occur after all porphyroclasts have been reduced and incorporated into the matrix.

Figure 29. Quartz ribbon texture. Ribbons may extend for up to 3mm as a single grain. Large ribbon grains have subgrained boundaries. Undulatory extinction is ubiquitous in large grains. Field of view 1.3mm. P268.

Figure 30. Dynamically recrystallized quartz ribbon aggregate with small elongate remnant of host grain. Host remnant is flattened in the plane of the foliation which follows the extinction pattern in the ribbon. Field of view 3.25mm. P268.

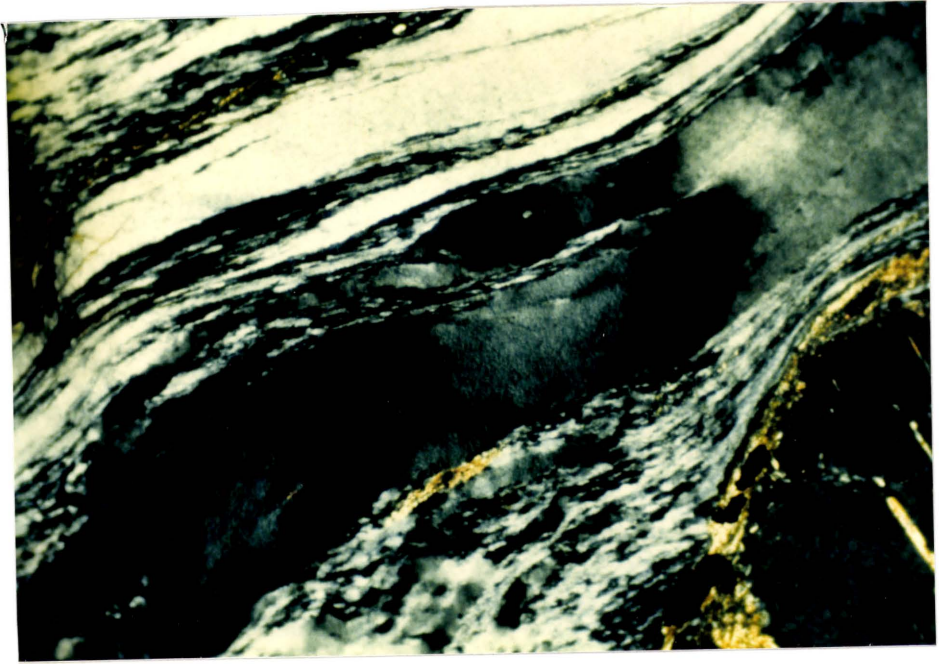


Figure 31a. Quartz ribbon aggregates in a deformed granite. Ribbons are generally one grain wide and several grains long. Grain boundaries within the ribbon are generally normal to ribbon walls. Field of view 3.25mm. P54.

Figure 31b. Deformation textures in a granite. Recrystallized quartz grains form irregular or ribbon shaped aggregates which wrap around large feldspar porphyroclasts. The very fine grained material contains dynamically recrystallized grains of K-feldspar, plagioclase and minor hornblende. Field of view 6.5mm. P244.

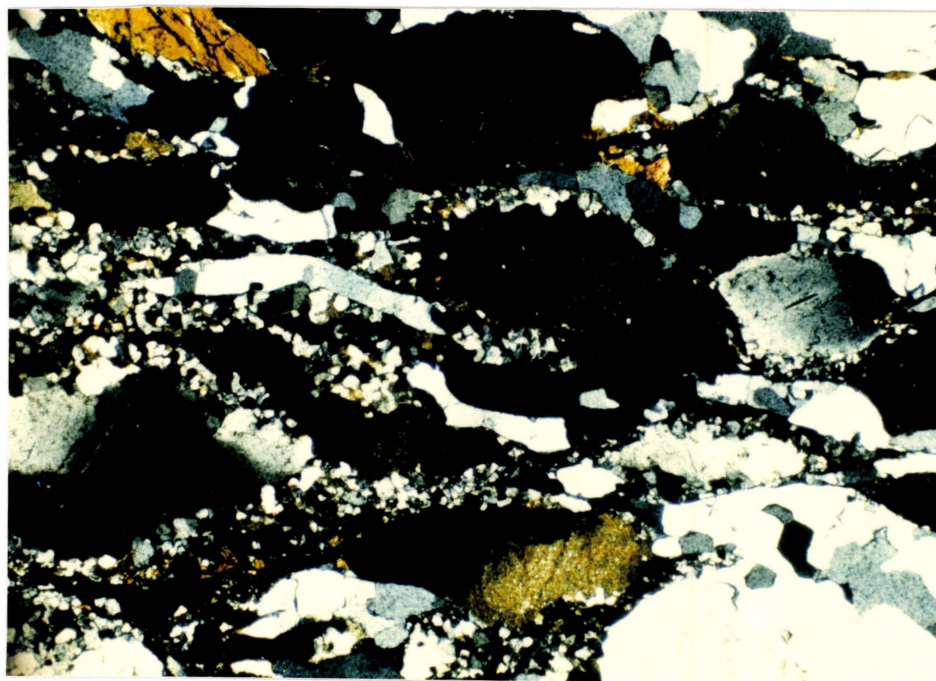
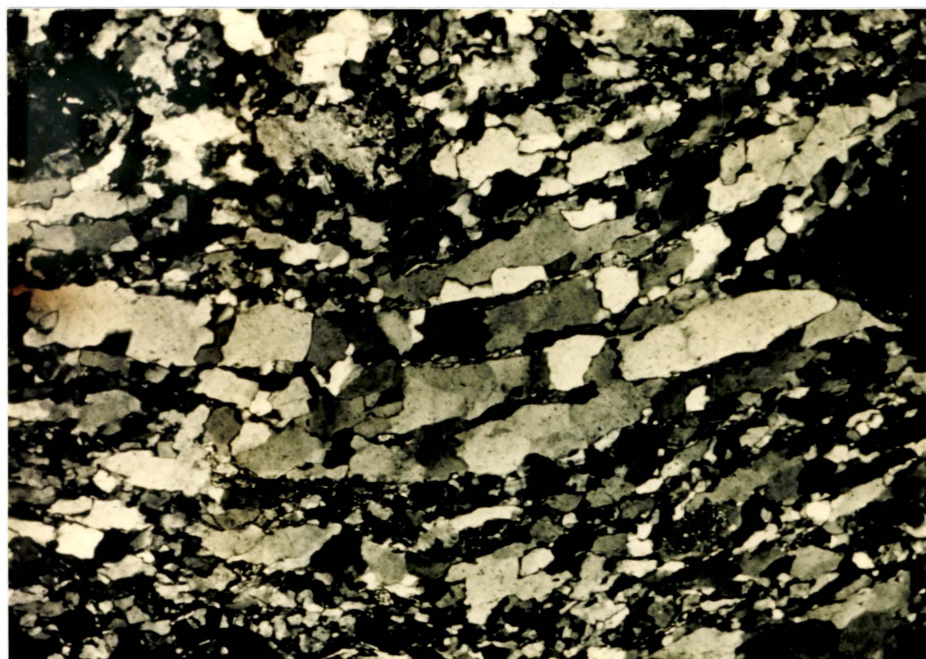
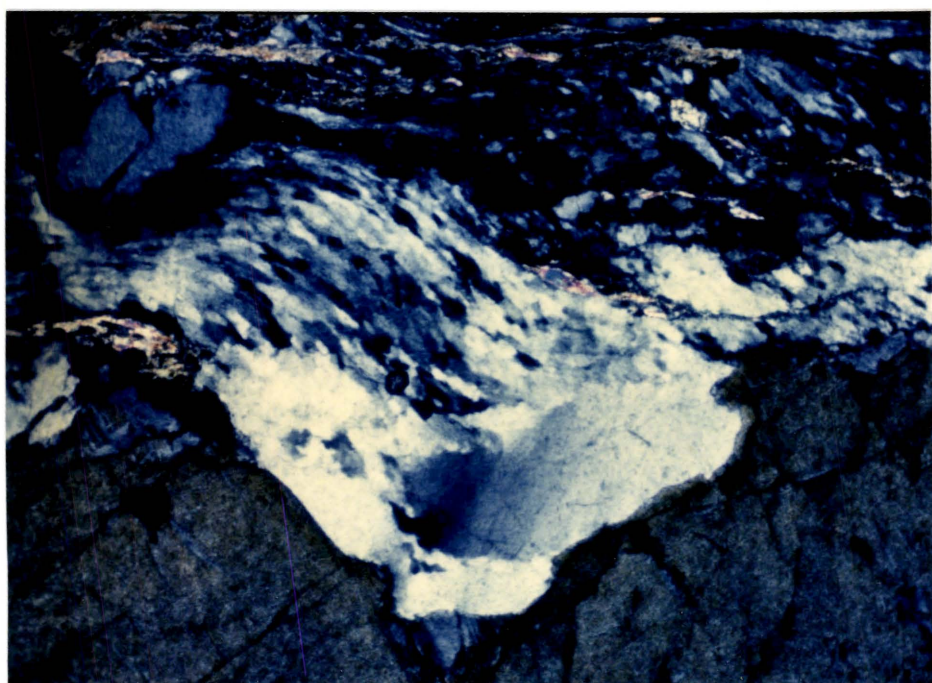


Figure 32. Deformed quartz grain in a quartz-feldspar mylonite which illustrates the difference in strain between "protected" and "unprotected" regions. The portion of the quartz grain located in the "V" of the feldspar grain has been protected from the high level of strain which has affected the rest of the grain. Field of view 1.3mm. P139.



FELDSPAR MICROSTRUCTURES

Progressive Development of Microstructural Strain Features

The same series of three samples used to define the progressive development of quartz fabrics during mylonite formation have been used to describe feldspar fabric development. Due to the widely varying behavior of feldspars under different metamorphic conditions, these samples do not necessarily represent the most common behavior of feldspars in deformed granites. Because these samples were collected approximately half way between the northwest and southeast boundaries of the study area, they are taken to be representative of the average behavior of feldspar for the purposes of this study. All slides have been stained for K-feldspar (Deer et al., 1966; p.311).

In the sample not visibly deformed (P35-1), plagioclase occurs most commonly as equant grains with irregular boundaries. The average size of these grains is 2.5mm. Fracturing is common in these grains and may be short and discontinuous or may be throughgoing. Approximately one half of the fractures observed occurred along crystallographic cleavage directions. The rest are crosscutting. Small fractures may occur at the boundary or isolated within a crystal. These fractures, long and short, show no offset but

may be filled with quartz, biotite or epidote. Twinning occurs in some plagioclase but the distribution of twins within a grain may be highly irregular. Commonly, twins are very thin and taper to a point or end abruptly within a grain (Figure 33a) indicating that these are deformation twins (White, 1975). Bent twins are seldom seen, although undulatory extinction does occur. Aggregates of very fine grained (0.05mm) feldspar, both plagioclase and K-feldspar, also occur giving both feldspar types a bimodal distribution.

Alkali feldspar occurs in this sample in very irregular shapes, filling interstices between plagioclase grains. The range in grain size and bimodal distribution is similar to that of plagioclase but because of the highly irregular grain shapes, this feature is less obvious. Small zones of undulatory extinction can be seen in some of the large K-feldspar grains. Fracturing occurs as in plagioclase. Myrmekite is commonly seen associated with or grown into K-feldspar.

In the sample displaying a C & S fabric, fracturing is the same as that described in the previous sample. Deformation twins are the only twins seen in plagioclase. Bent twins and undulatory extinction are common. Kink bands, not seen in the previous sample, occur in two different forms. The most obvious kink bands have narrow diffuse boundaries and traverse the entire grain. Twins can be seen

to bend into and out of the band which has a different extinction angle than the rest of the grain (Figure 33b). The kink bands in this sample invariably occur at an angle of 25 to 30 degrees to the quartz ribbon boundaries (i.e the shear foliation direction) but in the opposite sense to that seen for elongated quartz subgrains. As well as this, kink band boundaries are invariably oriented at a high angle (subnormal) to the twin lamellae. From this it appears that these kink bands do not form in feldspar grains unless they have a specific crystallographic orientation with respect to the shear foliation. Other kink bands, which are rare in this sample, are discontinuous, ending abruptly at microfractures within the grain. A large number of these kinks can occur within a single grain resulting in a very distinctive "krinkled" extinction pattern.

Plagioclase grains vary from equant to slightly inequant and are generally subrounded in outline. Inequant grains are oriented with their long axes subparallel to the quartz ribbon elongation direction. The bimodal distribution in grain size still exists but the number of finer grains is greater. Large grains are on the average 1.5mm in diameter. Grains larger than 2.0mm are generally aggregates. The fine grains are 0.05mm in diameter. The boundaries of the large plagioclase grains are serrated where they are in contact with other feldspar grains and smooth where they are in

contact with biotite or quartz. Small recrystallized grains can be seen along the serrated grain boundaries in a core and mantle configuration.

Features observed in K-feldspar are generally the same as that seen in plagioclase with two exceptions; no kink bands were observed and the twinning is that of microcline. Large K-feldspar grains are less abundant than that of plagioclase. Myrmekite, which is not common in this sample, is associated with K-feldspar and appears more pristine than that in the previous sample. These well developed vermicular intergrowths are found only along the sides of K-feldspar grains that face the finite flattening direction.

In the mylonite, feldspars occur as porphyroclasts widely dispersed throughout a fine grained quartz + feldspar foliated matrix. The great majority of porphyroclasts are plagioclase; K-feldspar porphyroclasts are rare but some very large ones do occur. Porphyroclasts vary from largely equant to inequant; the orientation of long axes of inequant grains relative to the foliation direction is variable (Figure 33c; see Ghosh & Ramberg, 1976, for rigid body rotation in a ductile matrix). Many porphyroclasts have well rounded outlines while others display a well developed core and mantle structure (Figure 33d). This difference in behavior may reflect a difference in plagioclase composition. The progressive decrease in grain size from core to outer mantle

is well illustrated in Figure 33d. In these grains the fine grained outer mantle appears to be spalling off to become incorporated into the matrix. It is these grains which are seen as the tails of feldspar augen. This process of grain size reduction is responsible for the high proportion of fine grained plagioclase in the matrix. The well rounded porphyroclasts, as well as the cores of mantled augen, show very little evidence of internal deformation other than minor fracturing. This indicates that much of the stress imposed by neighbouring feldspar grains is relaxed as the proportion of matrix, which can accommodate high strain, increases.

Variations in Strain Features in Feldspar

The feldspars in area 1 (Figure 13) have undergone deformation by fracturing and brecciation. Fractures within grains are randomly oriented and may be filled with micas, epidote or gouge. Microfaults which crosscut all grains are common and contain angular fragments of quartz and feldspar in a gouge matrix (Figure 27). Plagioclase is almost completely replaced by epidote +/- chlorite, muscovite and quartz resulting in aggregates of these minerals in the form of pseudomorphs.

Figure 33a. Plagioclase grain in a quartz-monzonite which appears undeformed in hand specimen. Within the grain, very thin deformation twins taper out or end abruptly at dislocation walls. Field of view 1.3mm. P35-1.

Figure 33b. Plagioclase grain from a deformed granodiorite which possesses a C & S fabric. Developed within the crystal are deformation twins and a well developed kink band. Field of view 1.3mm. P35.

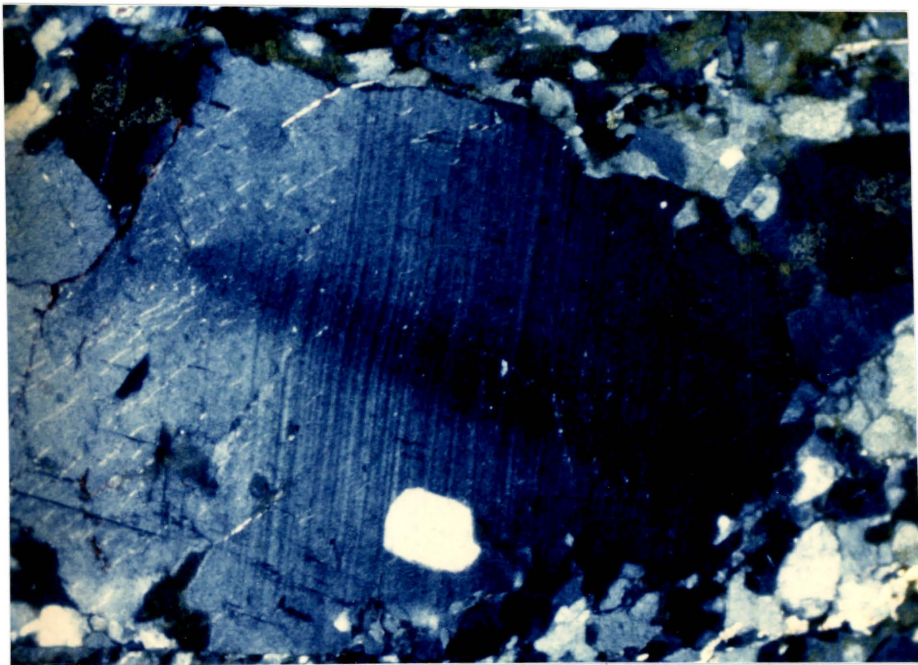
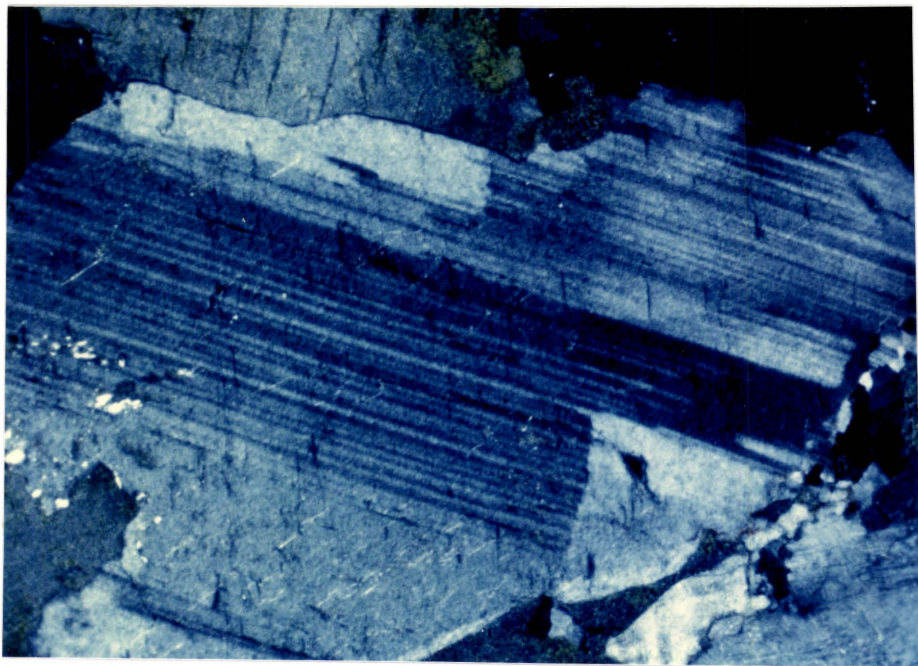
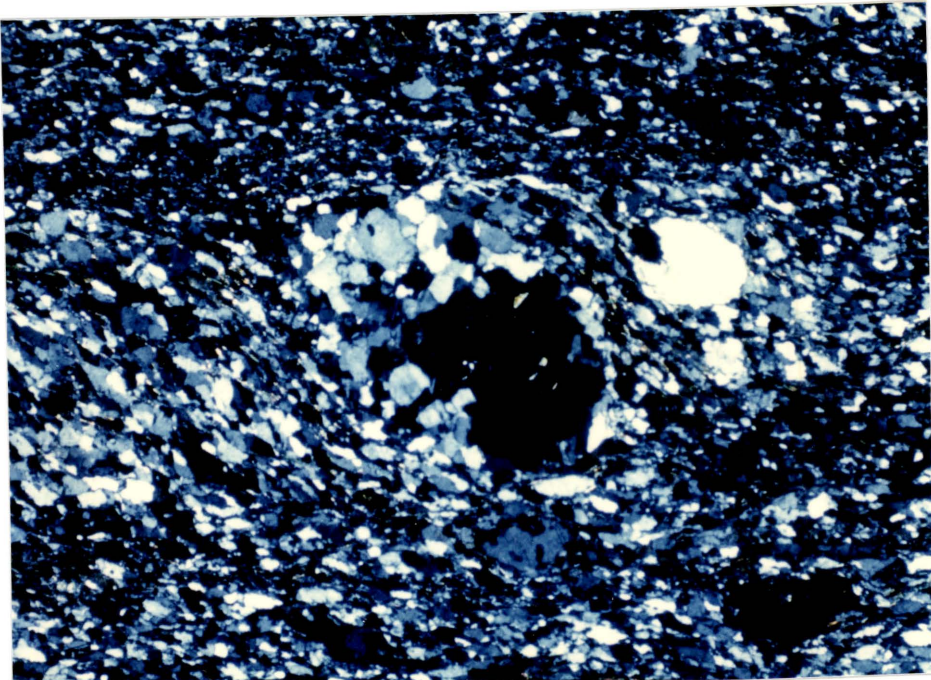
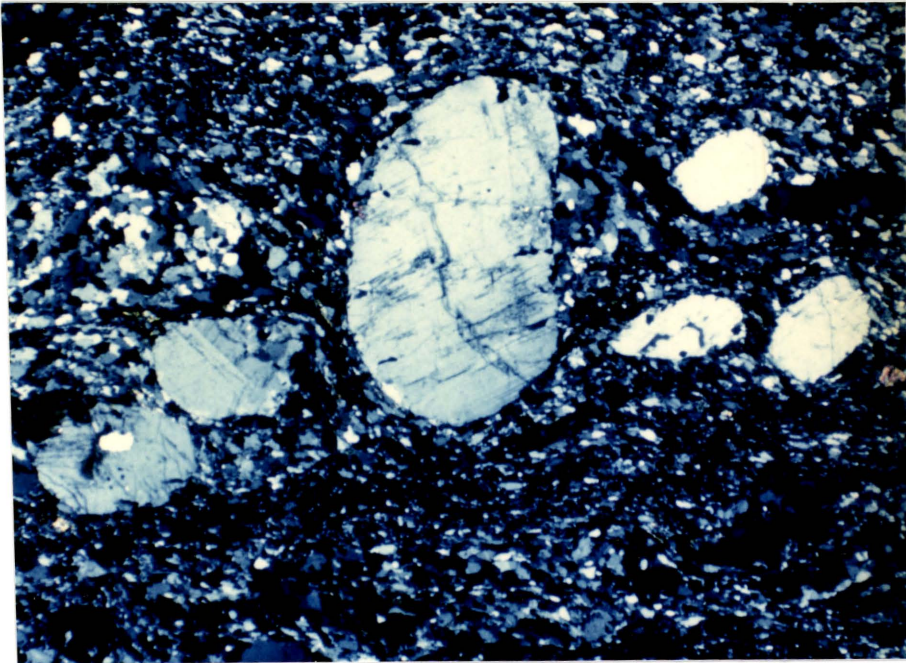


Figure 33c. Well rounded plagioclase porphyroclasts from an augen ultramylonite of granodioritic composition. Field of view 6.5mm. P35a.

Figure 33d. Core and mantle structure in a feldspar porphyroclast from the same sample as above. Recrystallized grains in the mantle are "spalling off" to become incorporated into the fine grained quartz and feldspar matrix. Field of view 3.25mm. P35a



In area 2 a large number of strain features can be observed in feldspar. Alteration to hydrous minerals has been restricted to the plagioclase feldspars although the extent to which this has occurred is much less than that of area 1. As in area 1, the most obvious strain feature is fracturing. Between area 1 and the center of area 2, the fractures change from being randomly oriented to having a preferred orientation normal to the foliation. These fractures show no apparent offset and are interpreted as being tensile fractures. Midway through area 2, conjugate shear fractures become the dominant form. The number of fractures which are antithetic to the deduced sense of movement on the shear foliation are more than twice as frequent as the number of sympathetic fractures. In plagioclase, these fractures are generally filled with fine grained quartz, plagioclase or phyllosilicates (Figure 34a). In K-feldspar, fractures may contain very small abraded fragments or recrystallized grains of the host feldspar (Figure 34b). Many feldspar grains are largely broken down into angular fragments. Plagioclase fragments are more angular than those of K-feldspar.

Several more ductile strain features are also seen in the feldspars of area 2. The abundance of these features tends to increase from the southwest to the northeast of the area. The most common of these features is deformation twinning. Twins occurring in plagioclase are commonly much thinner than those

formed in K-feldspar. Twins appear to both pre- and postdate the shear fractures, the latter ending abruptly at the fracture boundary. Deformation twins which predate fractures are offset across the fracture and may be bent along fracture boundaries (Figure 34a). Undulatory extinction, deformation bands and kink bands are common within plagioclase.

In the northeastern half of area 2 feldspar grains may be incompletely fractured. Shearing along these fractures leads to the formation of feldspar "dominoes" (Figure 35; Tullis, 1978). In the central section of area 2, deformation perthite and myrmekite begin to appear, becoming more common toward the northeast. The deformation perthite (Figure 36) which occurs in K-feldspar, consists of flames of plagioclase which originate at grain boundaries generally oriented along the foliation direction. The flames themselves trend perpendicular to the boundaries and therefore the flattening plane. The width of these flames is generally the greatest at the grain boundary, tapering to a point within the grain. Flames are frequently sigmoidal in shape. Myrmekite also occurs along these boundaries in K-feldspar grains. Both features may occur within a single grain.

Along the northern boundary of area 3A, feldspars show grain size reduction through continued fracturing and separation along the foliation. Fractured fragments which are still in contact with one another are angular; those which

have been separated are rounded. A wide range of grain sizes, from 8mm to 0.008mm, is represented in all samples observed. Generally grains larger than 0.7 or 0.8mm are fractured, usually along cleavage planes, into rectangular fragments. Grains less than this size are rounded and display very little fracturing (Figure 37). The dominant fractures are shear fractures. The even representation of all grain sizes is evidence that grain size reduction has occurred through fracturing rather than recrystallization.

In the mylonites, strings of feldspar augen are connected along the foliation by a thin band of very fine grained (8 micron) feldspar (Figure 37). Individual strings are generally restricted to a single feldspar composition and are separated from one another by quartz ribbons. This compositional banding indicates that all grains along a single string have probably been derived from the same parent grain.

Other more ductile strain features are also observed. Deformation twinning (Figure 38a), kink bands (Figure 38b) and bent twins are ubiquitous. Deformation perthite is developed to such an extent that the grains are commonly composed of half plagioclase and half K-feldspar in a zebra pattern. Myrmekite is not seen.

Well within the mylonites of area 3A and in area 3B feldspars begin to behave in a truly ductile fashion.

Fracturing of grains is much less common. The fractures which do occur are minute and show no offset. Feldspar grain sizes in the rocks of these areas show a bimodal distribution, the difference in size between grain populations being one to two orders of magnitude. One grain population consists of feldspar augen which can vary in size from 12mm to 0.1mm. Plagioclase augen are generally equant and rounded. K-feldspar augen may be equant or elongated; the size of equant grains is normally greater than that of inequant grains.

The most common deformation feature in feldspar is recrystallization at grain boundaries producing a core and mantle structure (Figure 39a). This process of recrystallization has produced the second grain size population. The recrystallized grain size shows little variation within a sample but may vary from one location to the next. Fine grain sizes range from 0.07 to 0.01mm. The width of recrystallized mantles may be small where recrystallized grains have moved away from the host grain through grain boundary sliding to form tails on the feldspar augen. All feldspar augen, with or without a well developed mantle, have highly serrated boundaries which indicates that grain size reduction is occurring through the process of recrystallization.

Recrystallization is not restricted to grain boundaries.

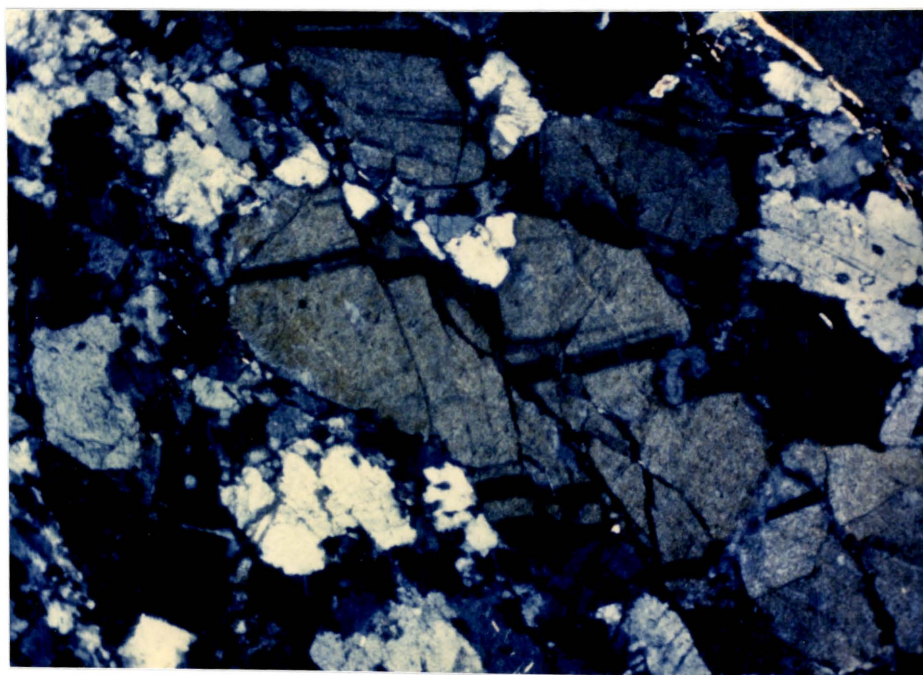
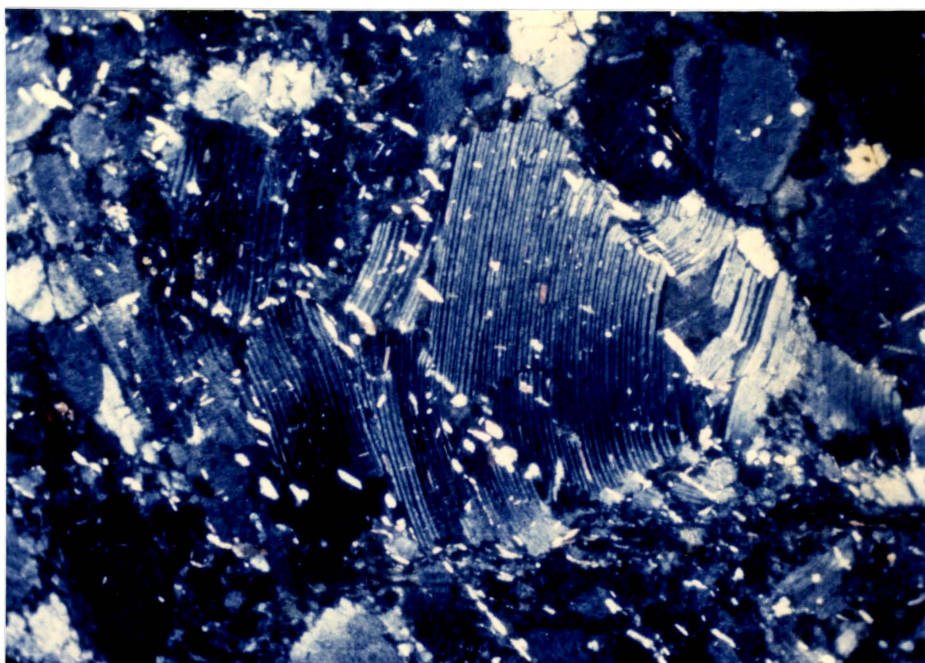
Within grain cores, narrow straight bands of recrystallized grains occur across which there is measurable lattice misorientation (Figure 39b). This misorientation is seen as either an abrupt change in extinction or, in the few crystals which possess twins, a slight change in orientation of twin lamellae. These zones correspond to the "Type III segregation bands" described by Hanmer (1981,1982).

Undulatory extinction, which is rare, is irregular due to intracrystalline microkinking (Figure 33c). Kinking generally occurs within the host crystal close to the grain boundaries. Deformation twins, deformation perthite and kink bands are also rare. Myrmekite is well developed in K-feldspars especially on the long sides of inequant grains which invariably face the finite shortening direction. Some myrmekite occurs in all K-feldspar grains.

The deformation of feldspars in area 5 has been described in the previous section under progressive development of strain features. The strain features in feldspar in area 6 are essentially equivalent to those of area 5. Mantle recrystallization (Figure 40a) and myrmekite (Figure 40b) are common. Deformation features in the core grains are rare; the abundance being dependant on the abundance of large feldspar porphyroclasts in the sample. Recrystallization of K-feldspars has resulted in new mantle grains of a different (plagioclase) composition.

Figure 34a. Fractured feldspar porphyroclast displaying bent deformation twins and minor kink banding. Fractures are infilled with muscovite quartz and fine grained plagioclase. Field of view 1.3mm. P115.

Figure 34b. Shear fractures in K-feldspar which are offsetting deformation twins. Fractures may be infilled with abraded fragments of the host grain. Field of view 1.3mm. P115.




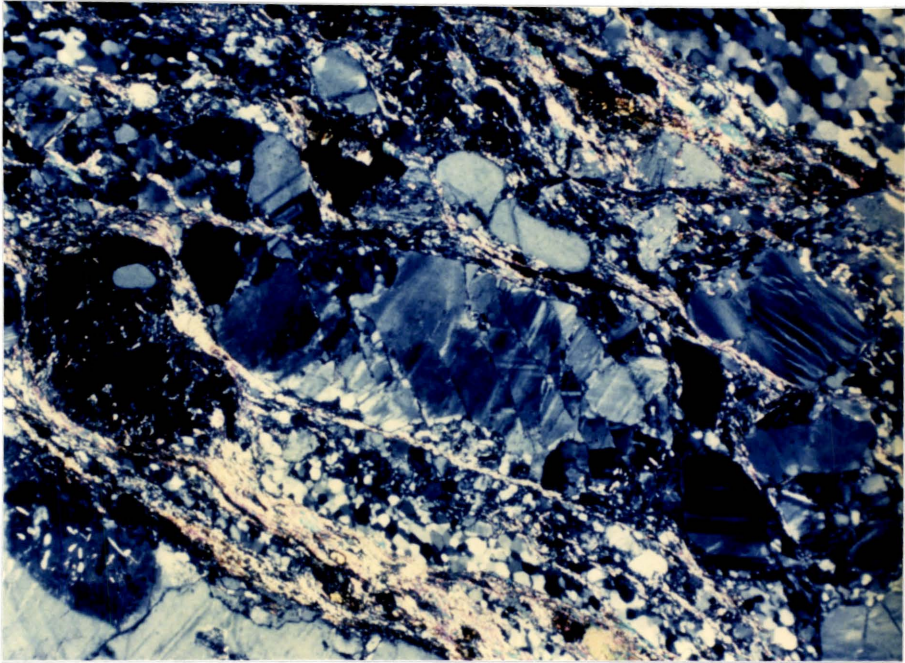


Figure 35. Strain features in feldspar from area 2. The large K- feldspar grain in the center of the photomicrograph shows rotation of fragments along shear fractures to produce "dominoes". Internal strain features include undulatory extinction and deformation twina. Adjacent plagioclase grain is being replaced by hydrous minerals. Quartz grain included in the plagioclase grain is unstrained. Myrmekite can be seen growing into the large K-feldspar grain in the corner of the photo. Field of view 3.25mm. P231.



COLLEGE



UNIVERSITY OF TORONTO CANADA

Figure 36. Perthite flames produced during deformation of a K-feldspar augen. Flames are oriented approximately normal to the foliation. The grain has been fractured internally. Field of view 3.25mm. P347.

Figure 37. Feldspar fracturing and separation along the foliation in an ultramylonite from area 3A. Slide has been stained for both Ca (pink) and K (yellow). Individual strings of connected augen are restricted to a single feldspar composition. Late shear fractures crosscut the ultramylonite normal to the foliation. Plane light. field of view 6.5mm. P269.

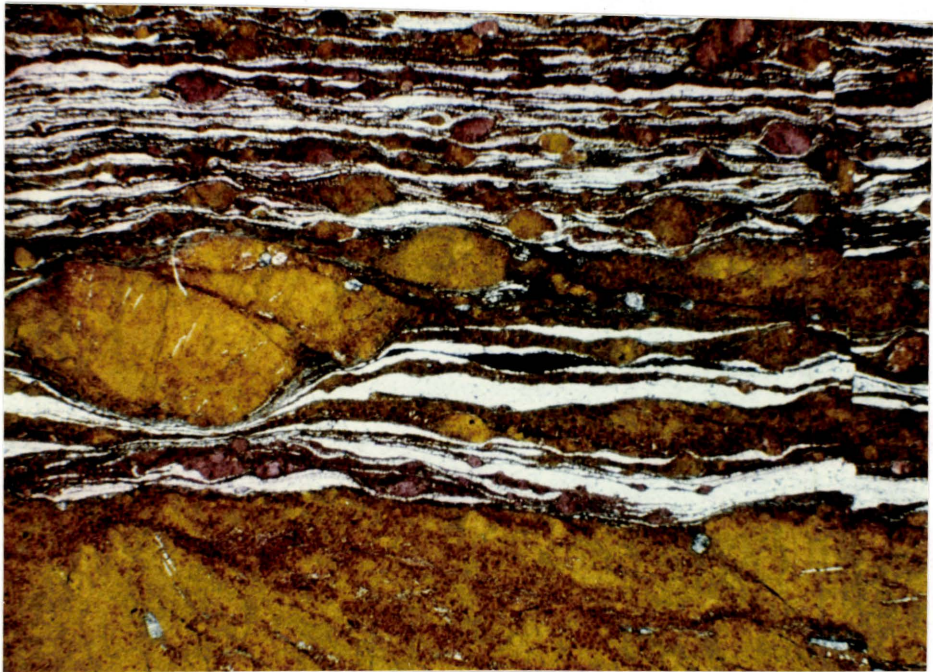
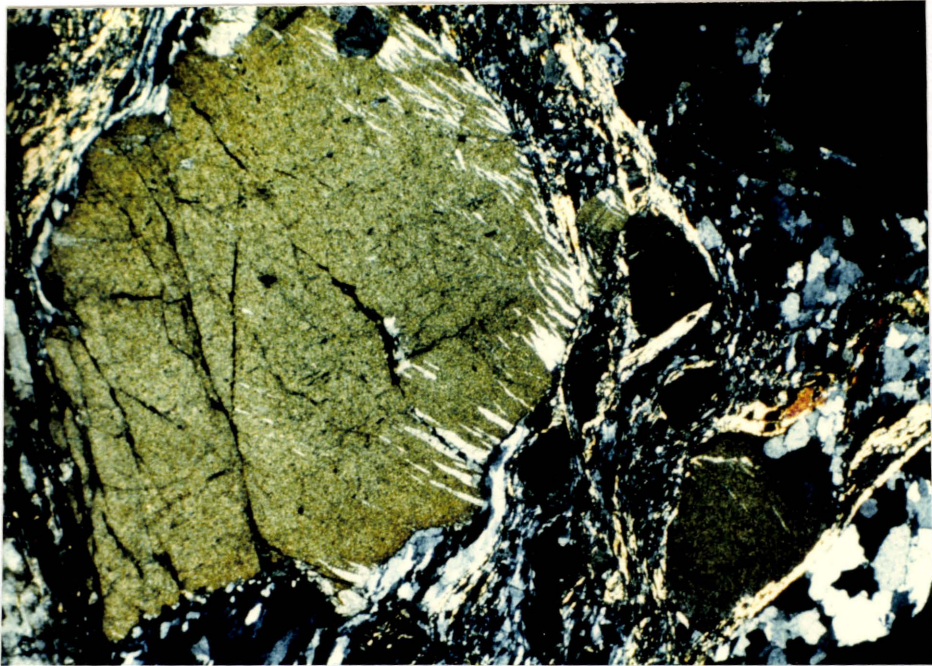


Figure 38a. Deformation twins in a plagioclase augen within a mylonite from area 3A. Field of view 3.25mm. P102.

Figure 38b. Fracturing and kink banding leading to "crinkled" extinction in plagioclase. Field of view 1.3mm. P102.

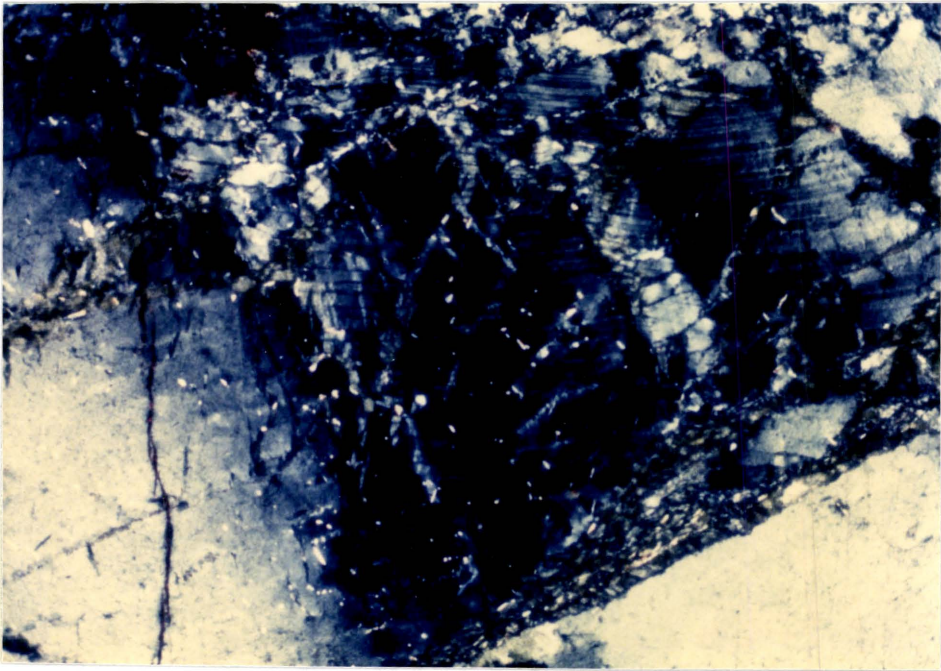
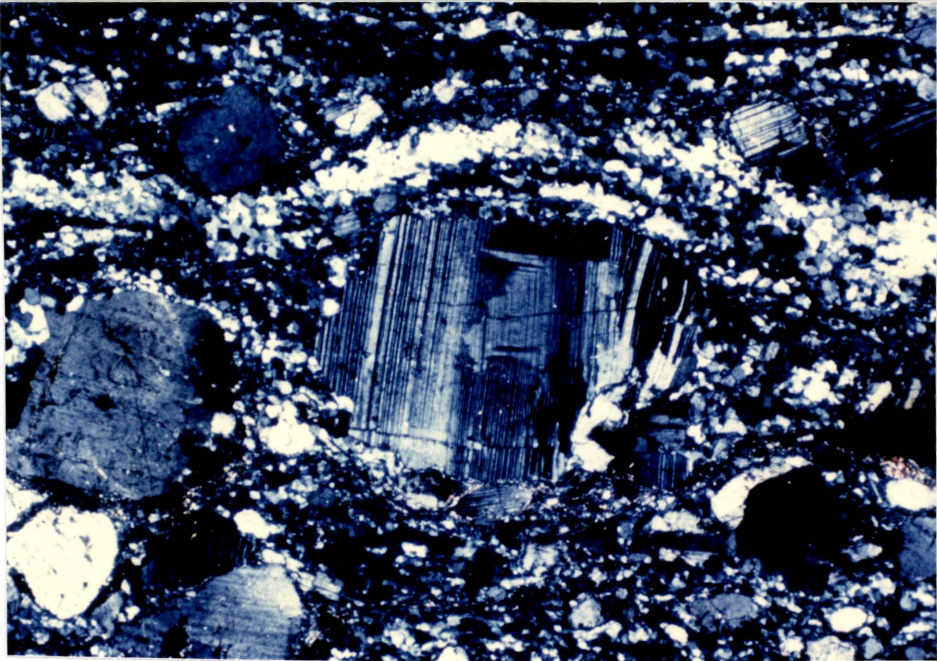


Figure 39a. Well developed core and mantle structure in a feldspar within an augen ultramylonite leading to a bimodal distribution in feldspar grain size. Field of view 1.3mm. P460.

Figure 39b. Recrystallization along a dislocation wall in plagioclase similar to Type III segregation bands described by Hanmer (1982). Grain misorientation across the band is indicated by the misorientation in twinn lamellae. Field of view 1.3mm. P10.

Figure 39c. Irregular undulatory extinction in orthoclase. Field of view 1.3mm. P10-1.

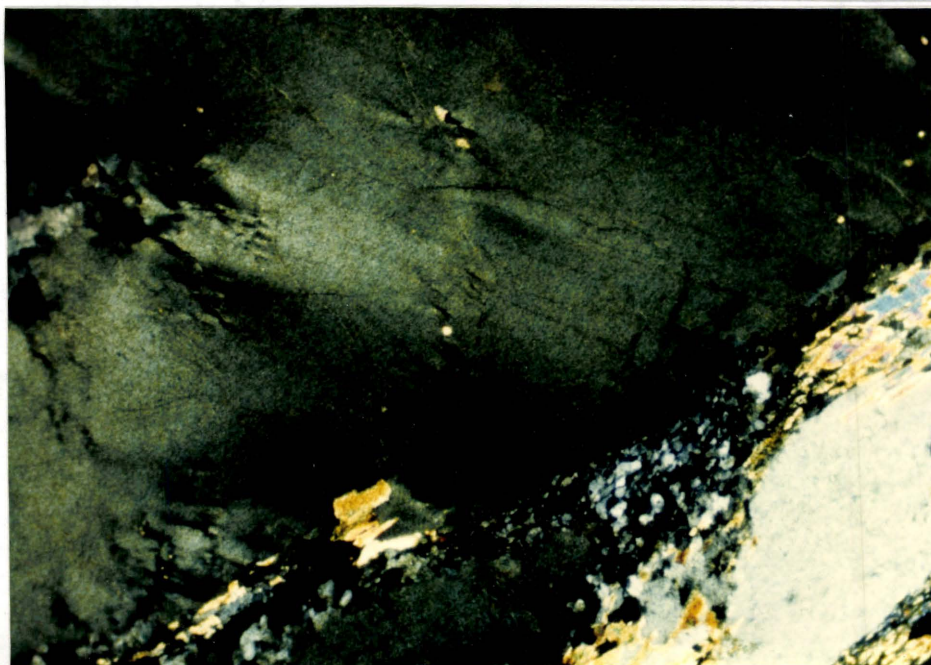
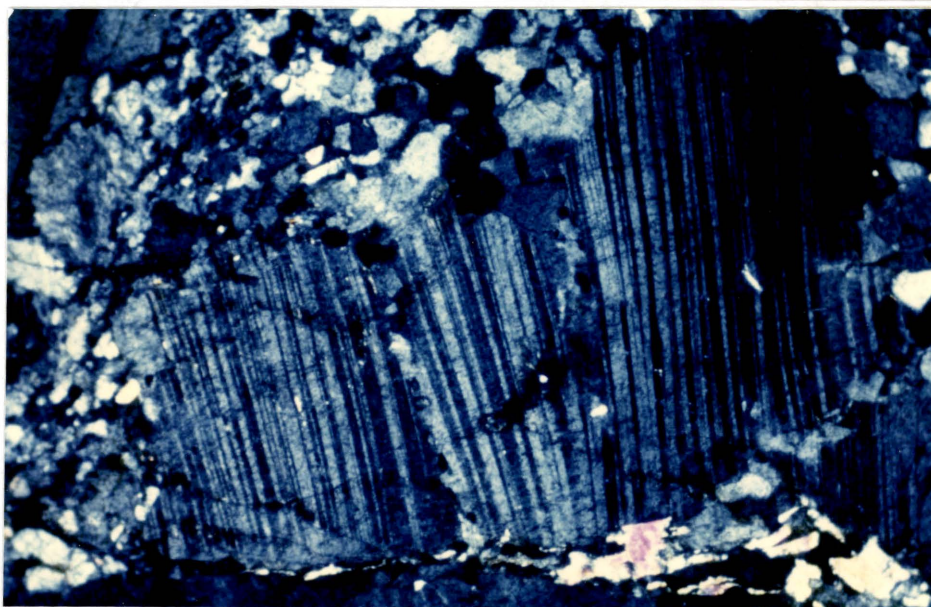
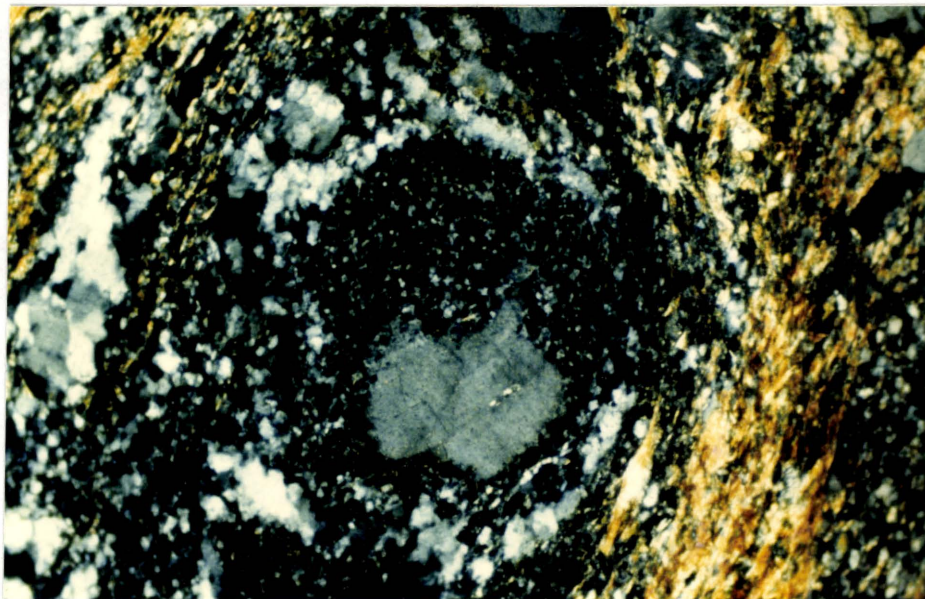
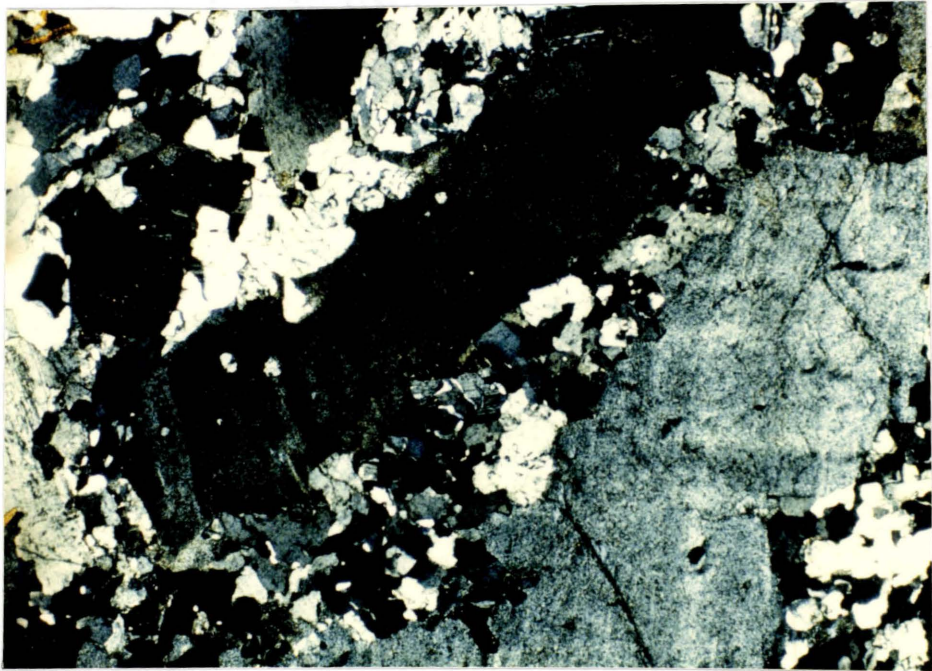
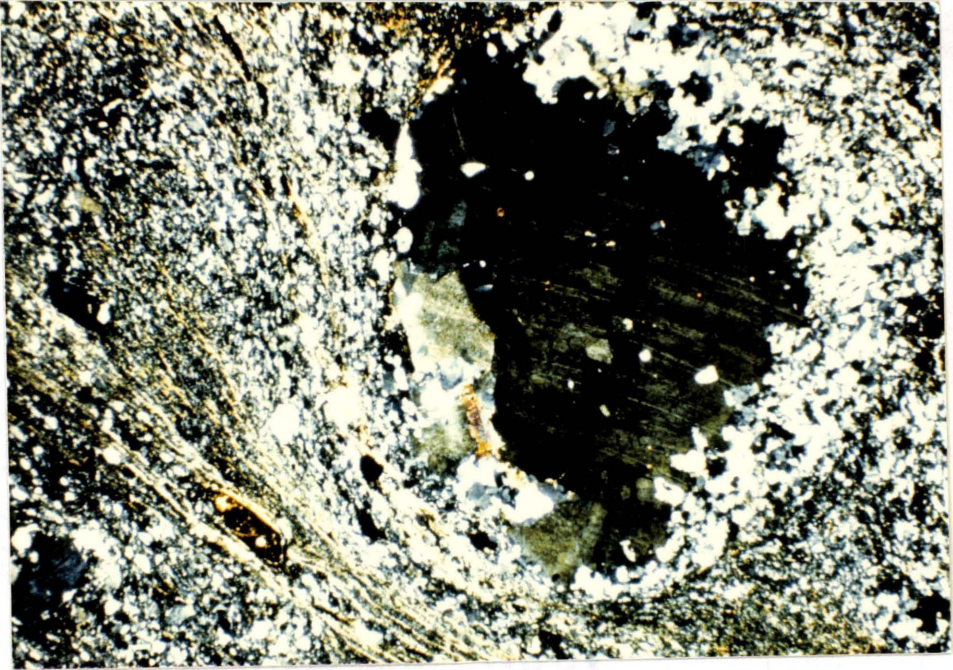


Figure 40a. Core and mantle structure in a K-feldspar within an ultramylonite from area 6. The recrystallized grains in the mantle have a different composition than the core. Field of view 6.5mm. P527.

Figure 40b. Recrystallization and myrmekite growth in feldspar from area 6. Field of view 3.25mm. P529.



In the southwestern corner of area 6, feldspar grain shapes become more inequant, the long axes of which define the foliation and control the quartz ribbon orientation. The feldspar cores display undulatory extinction and do show some fracturing with no offset (Figure 31b). These fractures show a strongly preferred orientation normal to the foliation.

Feldspar Fracture Distribution

A large number of feldspar fractures were measured in each sample studied. Some of the results of these measurements are shown in figure 41. The size of fractures and their importance as a deformation mechanism in feldspars decreases from northwest to southeast, becoming of minor importance within area 3. Southeast of area 3 fractures are generally minute and insignificant. In area 2, most fractures measured separated fragments which had been offset by shearing. Many of these fractures occur in conjugate sets, but fractures which are antithetic to the sense of movement on the C-surfaces are much more abundant than sympathetic fractures (Figure 41a,b). According to White et al. (1982), antithetic offset results from the rotation of fragments in the same sense as the major shearing direction causing movement along fractures which formed initially as tensile fractures. Conversely, fractures showing a sympathetic sense

of movement to the major shearing direction, formed originally as shear fractures. Subsequent rotation of these fracture fragments is in the opposite sense to that of the tension fracture fragments (Figure 42). Many of the fractures showing the same sense of rotation as the major shearing direction contain fine grained matrix material indicating that a small amount of separation has occurred. Thus, the majority of the fractures occurring in feldspars in area 2 originated as tensile fractures. This accounts for the large number of fractures showing antithetic movement.

Along the northern boundary of the shear zone in area 3A, the majority of fractures showing offset are sympathetic to the sense of movement on C-surfaces (Figure 41c,d). This change in fracture pattern therefore corresponds to a slight change in the behavior of feldspars from area 2 to area 3. In all cases, sympathetic fractures make a smaller angle with the shear foliation than do antithetic fractures. Values for sympathetic fractures vary from 0 to 50 degrees while those for antithetic fractures vary from 20 to 70 degrees.

Very few fractures from the southern side of the mylonite zone in area 3 and none from area 5 and 6 show evidence of displacement. The orientation of fractures from the first two of these areas are equivalent to those of offset fractures of either shear or tensile origin (Figure 41e,f,g).

Figure 41a-i. Rose diagrams of feldspar fracture orientations. All sections measured are subvertical in orientation with northwest to the left, southeast to the right in all diagrams. Fractures were measured relative to the foliation which occupies a vertical position in all diagrams. Dashed lines separate antithetic (dextral) fractures from sympathetic (sinetral) fractures.

Fig. 41 a
P231
N = 82

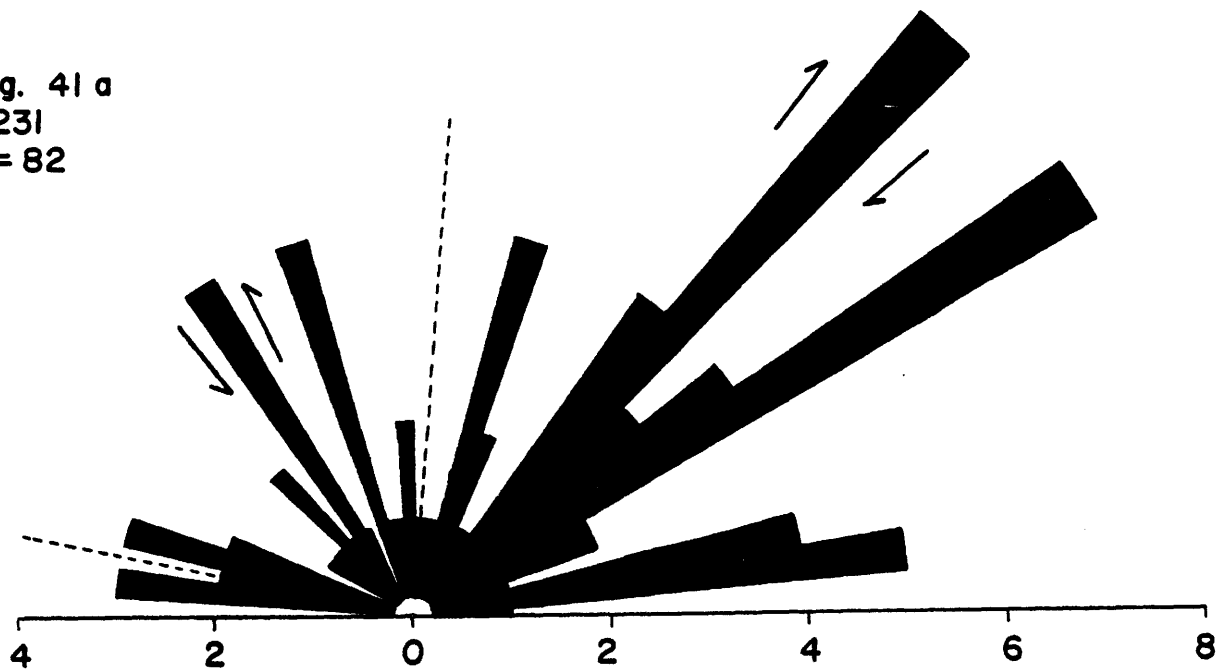


Fig. 41 b
P368
N = 86

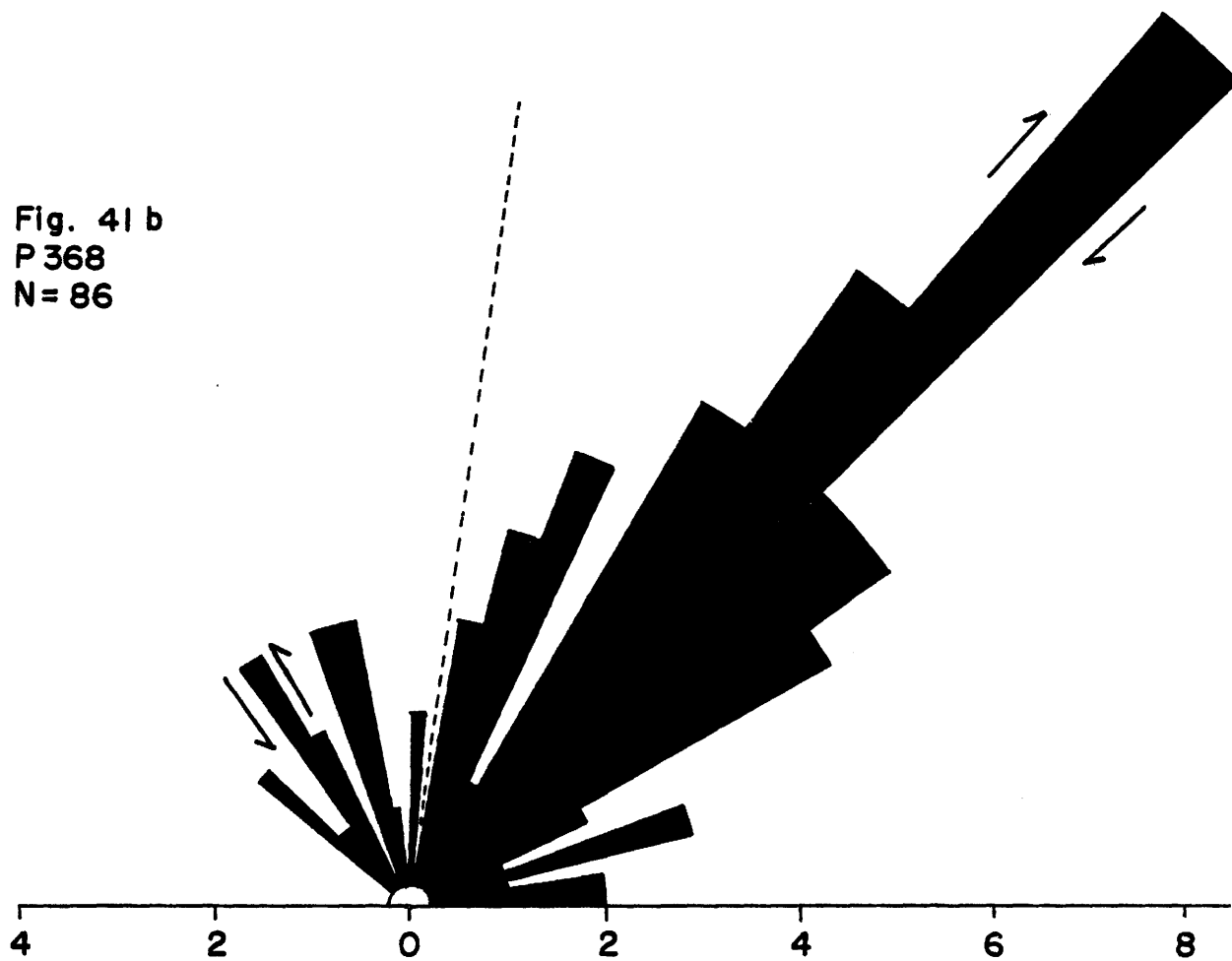


Fig. 4l c
P102
N= 56

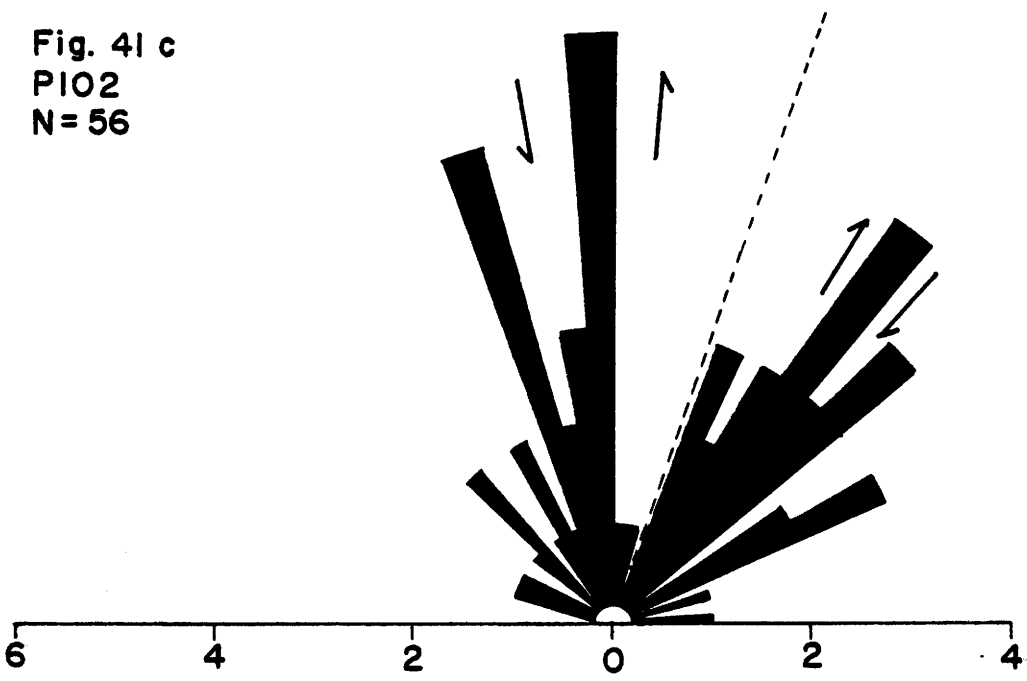


Fig. 4l d
P269
N=137

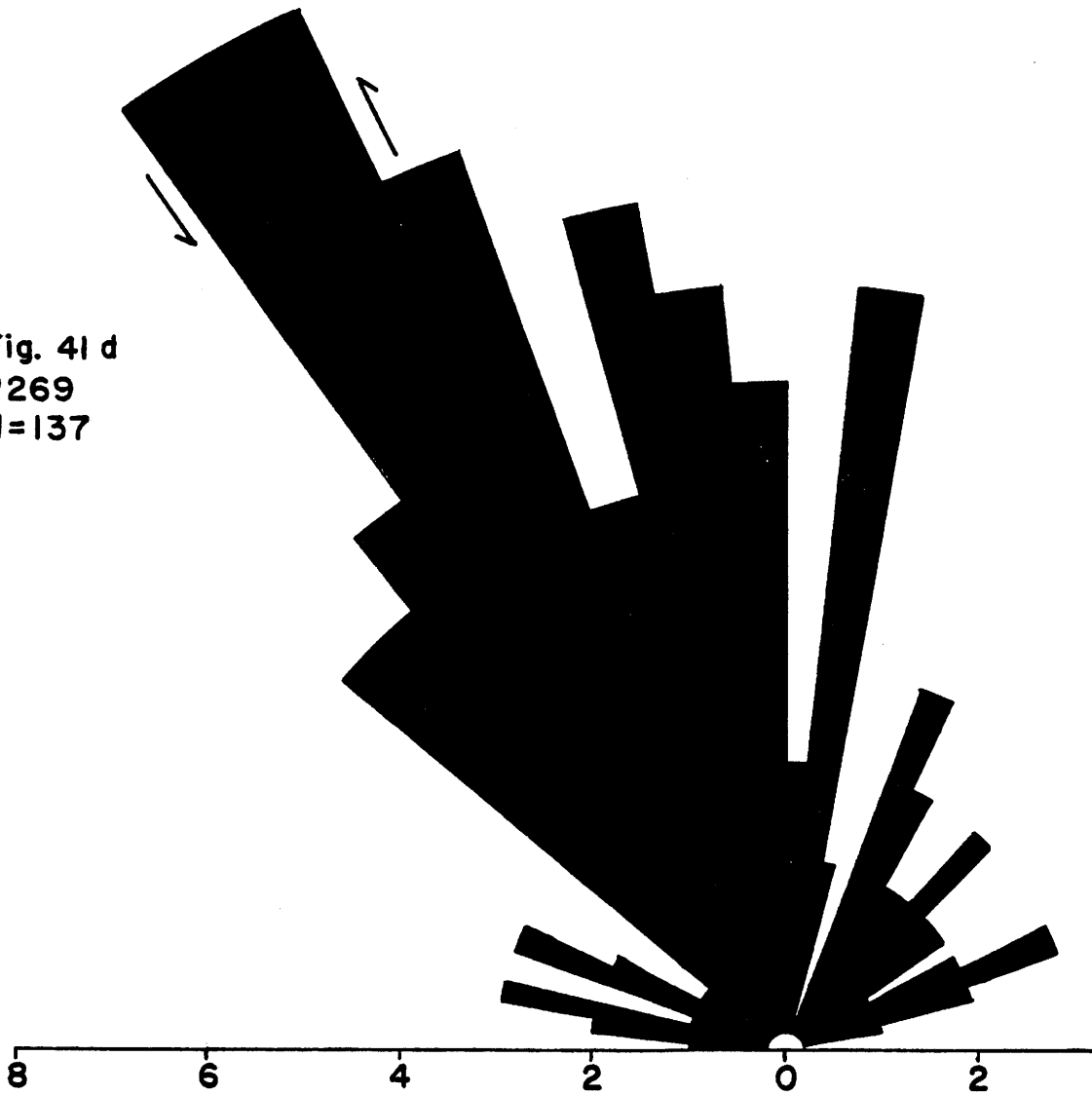


Fig. 41 e
P10-1
N=108

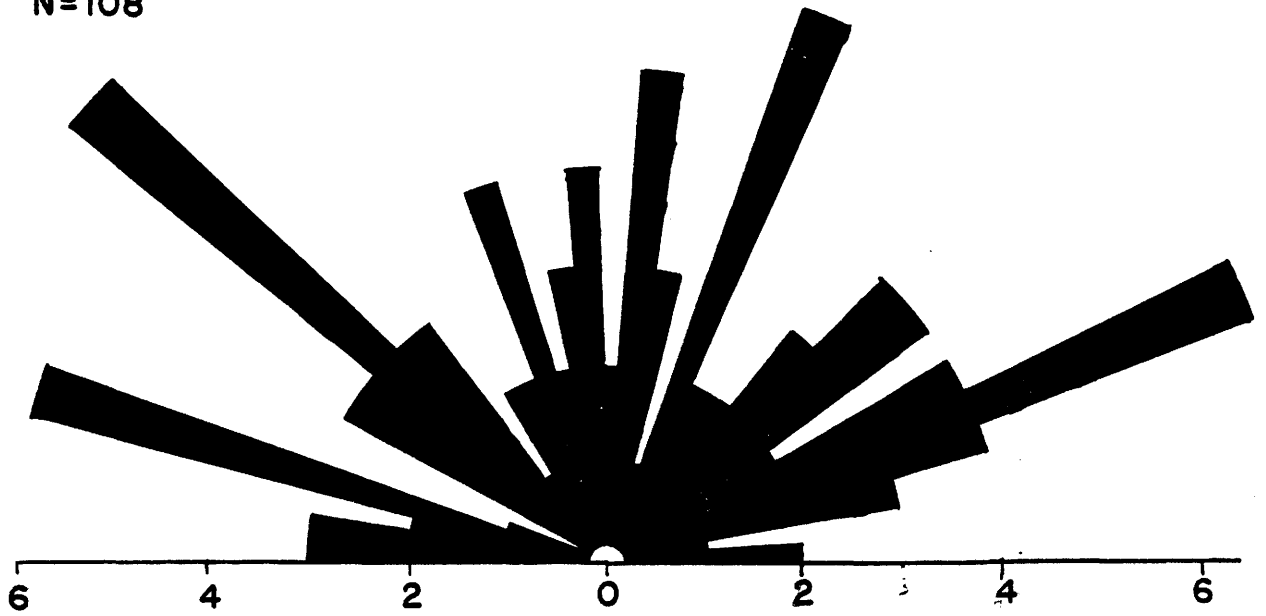


Fig. 41 f
R95
N=101

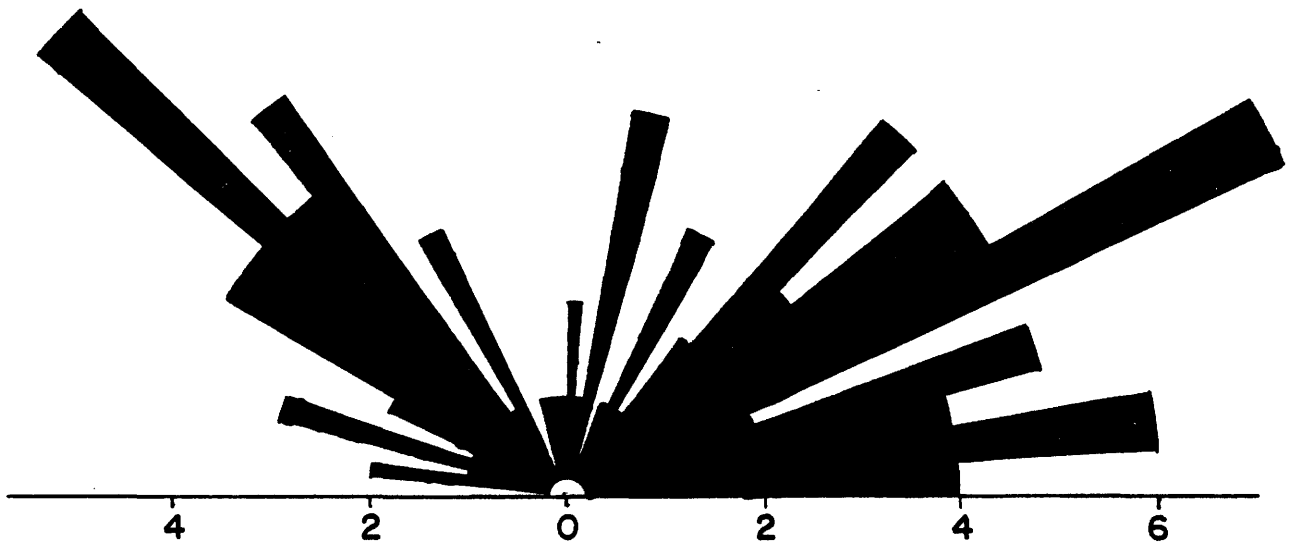


Fig. 41 g
P35 A
N= 183

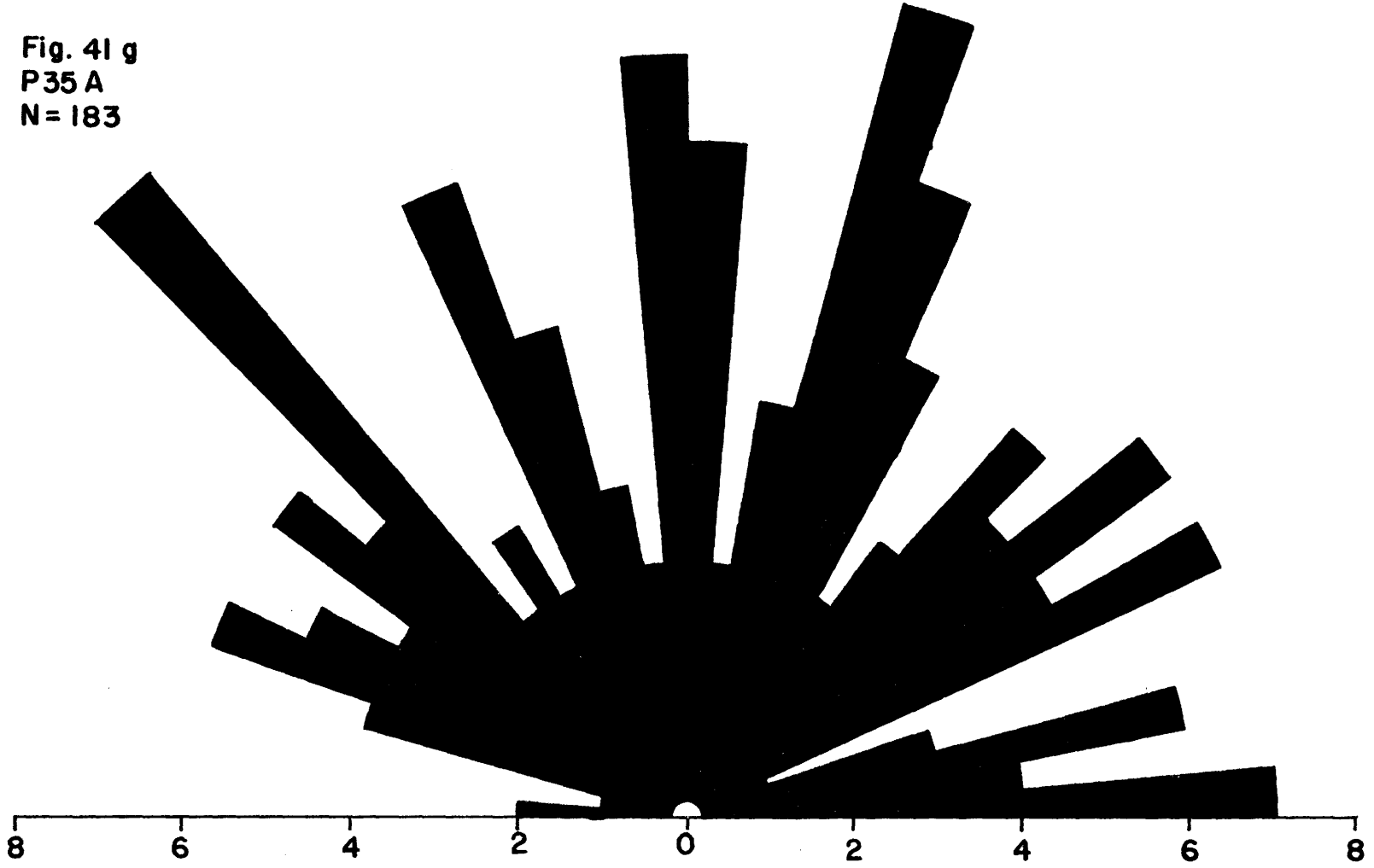


Fig. 4l h
P529
N=100

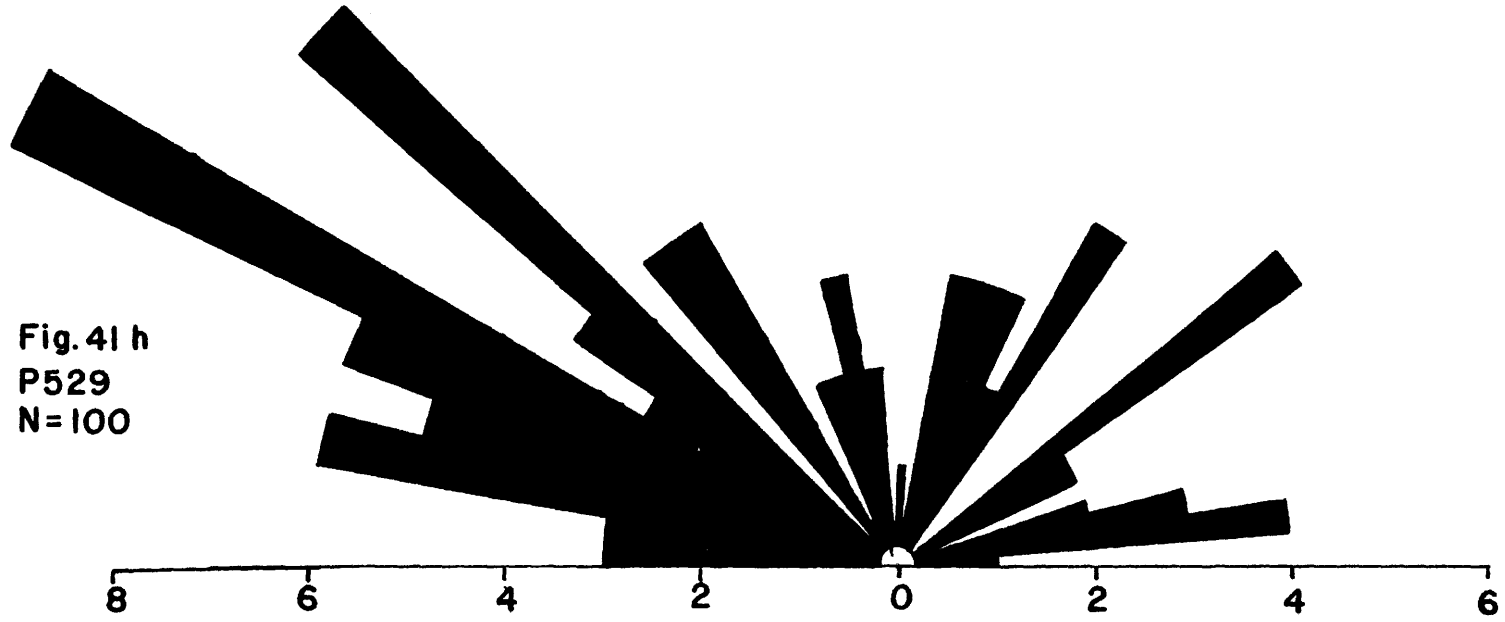
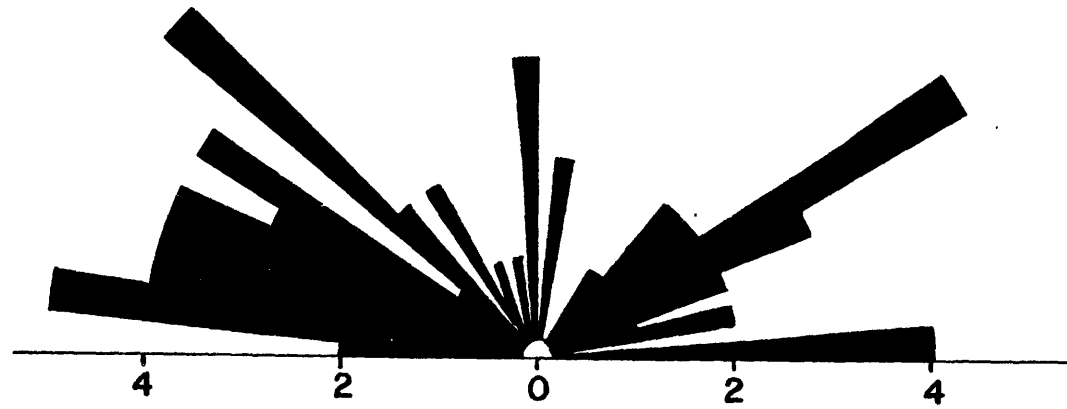


Fig. 4l i
P527
N=66



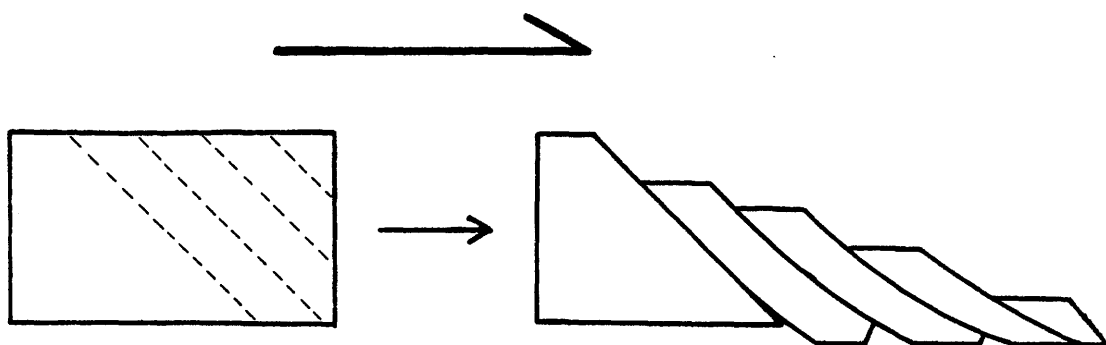
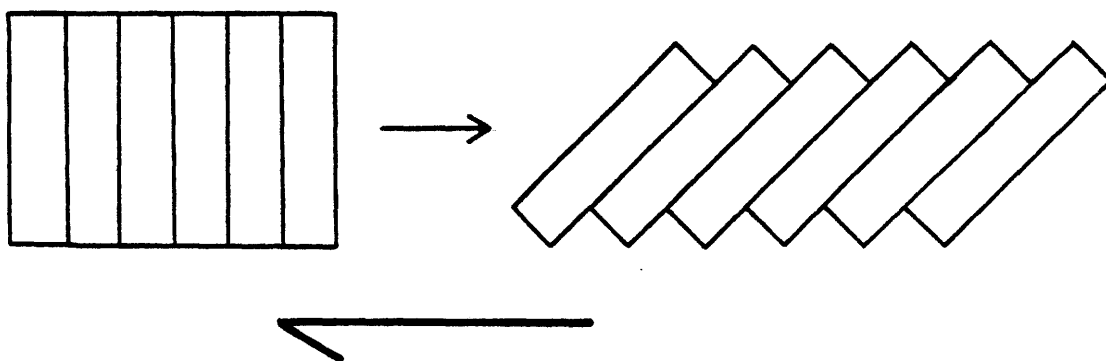
a**b**

Figure 42. a) Shear fracture rotation. b) Tensile fracture rotation. (after White et al., 1982).

The orientation of fractures from area 6 (Figure 41h,i) are in a tensile fracture position, oriented normal to the foliation direction. Since the dominant type of deformation in these areas is one involving crystal plastic (ductile) processes, these fractures are probably a late feature produced following uplift to a higher crustal level during thrusting.

Discussion of Feldspar Microstructures

Recently there has been a great surge in interest in the behavior of feldspars during deformation in ductile shear zones. A large volume of recent literature now exists which deals largely with microstructural strain features in these minerals (eg. White, 1975; Marshall & McLaren, 1977; Tullis & Yund, 1977, 1980; Debat et al., 1978; Borges & White, 1980; Boullier, 1980; Brown, 1980; Vidal et al., 1980; Hanmer, 1981, 1982; White et al., 1982; Fitzgerald et al., 1983; Vernon et al., 1983; Andrews, 1984; Jensen & Starkey, 1985; Olsen & Kohlstedt, 1985; White & Mawer, 1986).

Unlike quartz, which begins to behave in a ductile fashion at the onset of greenschist facies metamorphic conditions, feldspars remain strong, deforming largely in a brittle fashion, well into amphibolite grade. This behavior is well illustrated in the rocks described here. By far the

most apparent strain features in feldspars observed from areas 1 to 3 are microfracturing and microfaulting. In areas 3 to 6, recrystallization becomes the dominant process.

Feldspar fractures from a mylonite formed in lower greenschist grade metamorphic conditions (300-400°C) have been described by Boullier (1980). She found that under these conditions, only tensile fractures are produced in a position normal to the stretching lineation. These fractures are wide and usually filled with quartz and/or albite. Andrews (1984) also described fractures produced during shearing under greenschist facies conditions (350 to 500°C) but found the majority of these to be sympathetic shear fractures.

Therefore it appears that the transition from tensile to shear fracture dominance in feldspars corresponds to a slight increase in metamorphic grade. As the grade of metamorphism increases, the number of fractures showing displacement decreases (Debat et al., 1978) and the bulk strain becomes accommodated by grain boundary sliding in recrystallized grains.

The deformation of feldspar at lower greenschist to lower amphibolite facies conditions is accomplished through continued fracturing and physical separation leading to grain size reduction. This process continues with increasing strain until the grains reach what appears to be an equilibrium size. Once the equilibrium size has been reached, further

straining does not appear to change it very much. The formation of fractures is independent of aspect ratio (Boullier,1980). All feldspar grains which are larger than the equilibrium size, regardless of shape, will fracture. Grain size populations in which the entire range of sizes is evenly represented is an indication that grain size reduction has occurred through fracturing.

Deformation by crystal plastic processes in feldspar begins under conditions of amphibolite facies metamorphism (White,1975; Hanmer,1982; Olsen & Kohlstedt,1985). Many of the strain features produced by these processes are similar to that described for quartz but several important differences exist. For the minerals in which deformation mechanisms are most frequently studied, eg. quartz and calcite, no compositional change can occur during deformation. Conversely, the feldspars are very sensitive to mineralogical changes. A second important difference lies in the fact that most feldspars are solid solutions and therefore, in their most stable form, have a highly ordered crystal structure. During deformation, the internal energy of a feldspar grain can be increased through chemical changes and lattice disordering as well as through the formation of dislocations. Deformation under conditions below amphibolite facies (~500°C) occurs while feldspars are still in their ordered state (White,1975). The higher the An content of the

feldspar, the higher the degree of ordering within the crystal. Much higher temperatures are required to plastically deform anorthite than albite. Pure albite is not a solid solution and therefore, like quartz, begins to show signs of recovery (i.e. subgrain formation) under greenschist facies conditions. An equivalent deformation feature in highly ordered plagioclase to one seen in quartz requires, and contains, much higher energy because of the extra energy needed to disorder the lattice. Plagioclase also requires much more energy to diffuse a dislocation through the lattice; 1) dislocation diffusion disrupts the order of the lattice and 2) dislocations of opposite sign tend to pair in feldspars creating a larger dislocation that must diffuse (White, 1975).

During cataclastic fragmentation of feldspars, dilation must occur within the rock. This dilation allows water to enter the system, thus making it available to react with the deforming feldspars. This availability of fluids is capable of increasing diffusion rates by several orders of magnitude, leading to the formation of deformation perthite and myrmekite. The same sort of process can occur, although at a vastly different scale, as the number and ordered configuration of dislocations within the deforming mineral increases. Increasing the temperature within the system, increases the rate of formation of these features by 1)

increasing the rate of diffusion and 2) by allowing more diffusion pathways (dislocation pathways) to form within the mineral. This accounts for the increase in the penetration distance, and intracrystalline formation, of deformation perthite toward the southeast of the area.

The development of dislocation walls, which lead to the formation of undulatory extinction, deformation bands, bent twins or kink bands, is the same as that described for quartz with the exception of the much higher energy required. Once these dislocation walls have formed, they provide a pathway for diffusing atoms, i.e. deformation enhanced diffusion. Recrystallization along these boundaries (Figure 39b) can then be accomplished by the nucleation and growth of new grains.

Recrystallization along grain boundaries, leading to the formation of a core and mantle structure, is initially accomplished through nucleation and growth of new grains (White, 1975). The formation of new feldspar grains having a different composition than the host grain (Figure 40a,b) or new untwinned grains derived from a twinned host are evidence that this process has occurred. Once recrystallization starts, much of the strain can be accommodated through grain boundary sliding. This relieves some of the stress on the host grain resulting in fewer intracrystalline strain features. The creation of voids resulting from grain boundary

sliding and rotation, allows the ingress of fluids so that the process may continue (White,1975).

Once the temperature becomes high enough that sufficient energy is available for feldspars to exist in a stable but disordered state, the rate of dislocation diffusion increases dramatically and the crystal behaves, like quartz, in a truly ductile fashion. The critical temperature at which this occurs, varies depending on feldspar composition. Commonly, necessary temperatures are those which occur under upper amphibolite to granulite facies metamorphic conditions (Olsen & Kohlstedt,1985; Jensen & Starkey,1985; White & Mawer,1986). Recrystallization under these circumstances occurs, as in quartz, through grain boundary migration and subgrain rotation.

Feldspar deformation which has occurred through either nucleation and growth or subgrain rotation will have a bimodal distribution of grain size. The change from an even distribution to a bimodal distribution of feldspar grain sizes can be seen in the study area within area 3. Therefore the change in the behavior of feldspar from largely brittle to largely ductile occurs across the mylonites of the Johnnie Lake Shear Zone.

KINEMATIC ANALYSIS

Introduction

A large number of fabric elements exist in the rocks of this area from which the sense of movement can be deduced. Since this area is known to be within a zone of regional reverse fault movement, the reliability of some commonly used kinematic indicators can be tested.

C & S Fabrics

The concept of a C & S fabric was first introduced by Berthe et al. in 1979. They noted that an initially isotropic rock which had been disturbed by a single deformational event, had developed two different foliations which had a specific angular relationship both to each other and to the regional shear zone. Up until that time, multiple foliations had been used to indicate that the rock had been subjected to multiple episodes of deformation. Since its inception in 1979, this fabric has become widely accepted as an important kinematic indicator (Simpson & Schmid, 1983; Bell & Hammond, 1984; Lister & Snoke, 1984).

When a rock undergoes non-coaxial deformation, two different foliation surfaces may develop; 1) S-surfaces,

which are related to the accumulation of finite strain and 2) C-surfaces, which are related to areas of high localized shear strain. S and C surfaces develop with a specific angular relationship to one another and to the shear zone itself. The existence of both of these surfaces within a single rock constitutes a C & S fabric.

S-surfaces define the plane of preferred mineral orientation and thus the schistosity within a rock. During the initial stages of deformation these surfaces correspond to the XY plane of the finite strain ellipsoid and contains the maximum extension direction. Both pressure shadows at the extremities of feldspar porphyroclasts and the 001 cleavages of phyllosilicates tend to lie within this plane.

C-surfaces, which form initially at 45 degrees to the S-foliation, maintain a constant orientation during progressive deformation. These planes are active slip surfaces which contain a mineral lineation or slickenstriations at all stages of development. This lineation defines the stretching direction.

During progressive deformation, the angle between C- and S-surfaces decreases from 45 degrees by rotation of S-surfaces. On a map scale, the configuration of S-surfaces conforms to the Ramsay and Graham (1970) model for the development of schistosities within shear zones. Associated with this change is an increase in the number of C-surfaces.

This increase is due to: 1) the creation of new shear planes with increasing strain and 2) the activation of S-surfaces as they rotate into parallelism with C-surfaces (Berthe et al., 1979). As ultramylonite is approached, S- and C-surfaces are essentially parallel and equivalent surfaces. At this stage the finite extension direction is oblique to both C- and S-surfaces. Both S-surfaces and X rotate about the Y axis but the S-surfaces rotate more rapidly than X (Berthe et al., 1979). Because of this the use of the angular relationship between S and C planes to determine quantitative strain estimates should be avoided.

The most important feature of mylonites resulting from S and C relationships is the asymmetry in the fabric which is produced and maintained long after S-surfaces can no longer be recognized. In cases where the parent rock possessed a foliation from a previous deformation, the large amount of strain required to produce a mylonite is more than sufficient to completely obliterate any previous fabric. Since all mylonites form during non-coaxial deformation, all mylonites possess this asymmetry. The mylonites occurring in this study area contain some excellent examples of asymmetrical strain features. The consistency in the sense of asymmetry is by far the most reliable kinematic indicator.

Lister and Snoke (1984) have divided S-C mylonites into two categories. Type I S-C mylonites are those in which the

S-surfaces are mesoscopically visible (Figure 9a). They are observed to anastomose in and out of narrow zones of high shear strain, i.e. C-surfaces. In these rocks continuity is generally maintained across these ductile shear zones.

S-surfaces asymptotically approach C-surfaces producing a sigmoidal pattern between each C-plane. The sense of shear implied by this configuration reflects the sense of the bulk shearing direction (Figure 43).

In Type II S-C mylonites, the C-surfaces alone define the mesoscopic foliation. These occur at much higher strain levels than Type I, as C-surfaces become very closely spaced. Microscopic scale features representing S-surfaces are seen commonly in quartz aggregates between C-planes. The boundaries of quartz ribbons may be sigmoidal between C-surfaces (Figure 44) or elongated grains within the aggregate will have a preferential orientation oblique to the C foliation (Figure 26c). Commonly, different degrees of obliquity will exist between the long axes of these grains and the C-surfaces within a single thin section. The attitude of elongate grains within aggregates depends on the amount of shear strain that has accumulated since the last recrystallization. Those grains whose orientation is closest to the C-plane are the oldest, those with a high angle are the youngest. This process can continually repeat itself such that continued recrystallization can lead to a constant

resetting of the "finite strain clock" (Lister & Snoke, 1984).

In mylonites having a very high content of fine grained phyllosilicates in the matrix, S-surfaces are commonly traced by the preferential orientation of these minerals (Figure 45). Very large mica grains commonly develop into asymmetrical "mica fish" (Figure 46a; Lister & Snoke, 1984). In these grains the stable configuration is one in which the 001 cleavage of the mineral is inclined obliquely to the shearing direction so as to face the shortening direction (Figure 46a,b). Only in this orientation can these otherwise soft minerals remain intact within an ultramylonite. Any other configuration would result in destruction of the mineral through kinking, folding, cleavage fracture or slippage along the cleavage planes.

Tails on feldspar augen which are generally composed of fine grained feldspar, can also be used as a kinematic indicator. Much discussion has been focused in the past on the interpretation of these features (eg. Davidson et al., 1982; Simpson & Schmid, 1983; Hanmer, 1984) some of which seems ambiguous. Since feldspars often act as a rigid inclusion in a ductile matrix, the morphology of the tails they possess may be modified by grain rotation. The sense and amount of rotation that can occur is dependent on such things as aspect ratio, finite shear strain, porphyroclast to matrix ratio, metamorphic grade, etc. It is the variability in

rotation of these porphyroclasts which can lead to ambiguity in interpretation. Of the tailed porphyroclasts examined in the area, those occurring in mylonite as isolated inclusions in a fine grained matrix which had been deformed under ductile conditions for feldspar always indicated the same sense of shear as the other kinematic indicators in the sample. Tails are generally sigmoidal and follow the S foliation (Figures 33d & 47). As the number of porphyroclasts increases locally, they begin to influence the flow of the matrix, disturbing the regular sigmoidal pattern (Figure 47). In cases such as this, an indication of the shear sense may be derived by following the tail away from the concentration of augen. A much safer practice is to avoid using interpretations derived from local zones of high augen content. The shape of feldspar augen tails can also vary with metamorphic grade. Below the brittle-ductile transition in the behavior of feldspars, augen and their tails are produced by brittle processes. Rigid body rotation is much more important in these rocks than those of higher grade and again may lead to ambiguity in interpretation (Figure 46a).

The distribution of fractures in feldspars is another feature which, in some circumstances, can be used as a kinematic indicator. If the sense of offset can be determined for the majority of fractures, that population which is distributed at the lower angle to the mylonitic foliation

will generally have the same sense as the bulk shearing direction. Ambiguities arise where the two populations have an equivalent but opposite angular relationship with the shear plane. The size of either population has no bearing on the sense indication. These should only be used in conjunction with more reliable indicators.

Another feature which appears to be useful as a kinematic indicator is the perthite formed during deformation. Because this feature is most likely a strain induced diffusion phenomenon, it will ideally form along a direction parallel to the maximum stress direction in a typical tension fracture orientation (Figure 46b). This feature has been observed with the same spatial relationship by Debat et al. (1978). A similar feature to this, which would indicate the principal stress direction from which the sense of shear can be determined, is the deformation induced myrmekite. Like much of the perthite, myrmekite forms preferentially along grain boundaries which are oriented along the flattening plane (Simpson, 1985). Therefore grain boundaries which correspond in orientation to S-surfaces, can be identified as those showing myrmekite growth. These two features by themselves cannot be used as kinematic indicators if any evidence exists that grain rotation during or after their formation may have occurred. Much more research on deformation-induced diffusion phenomenon is necessary before these features are

commonly used as kinematic indicators but, based on a small number of empirical observations, they may be used as supportive evidence in conjunction with other, more reliable features which are confined to the matrix.

The kinematic indicators in the study area support the interpretation that deformation has been produced through regional thrusting from southeast to northwest. By far the most reliable of these indicators is the fabric asymmetry resulting from S-C relationships.

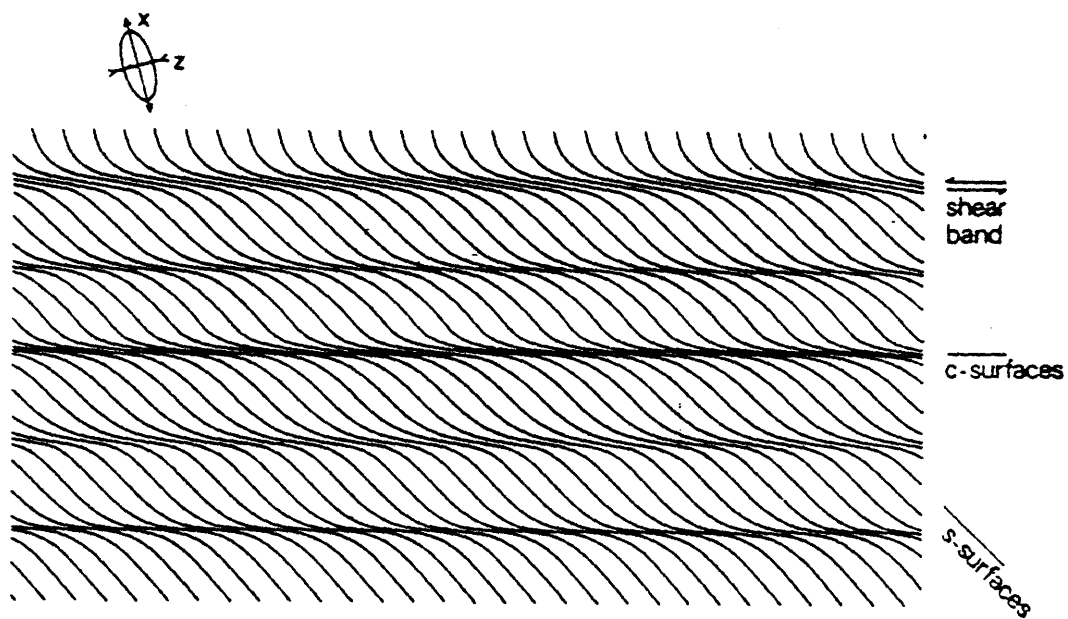


Figure 43. Illustration of a C & S Fabric. (From Lister and Snoke, 1984).

Figure 44. Sigmoidal quartz aggregate defining the S-foliation in a quartz-feldspar mylonite. Movement on C-plane is sinistral (southeast side up). Field of view 6.5mm. P115.

Figure 45. Phyllosilicate rich augen ultramylonite. The preferential orientation of micas around competent feldspar augen defines the flattening plane. Tails on feldspar augen follow the same pattern as micas. Sinistral shear is indicated. Field of view 6.5mm. P460.

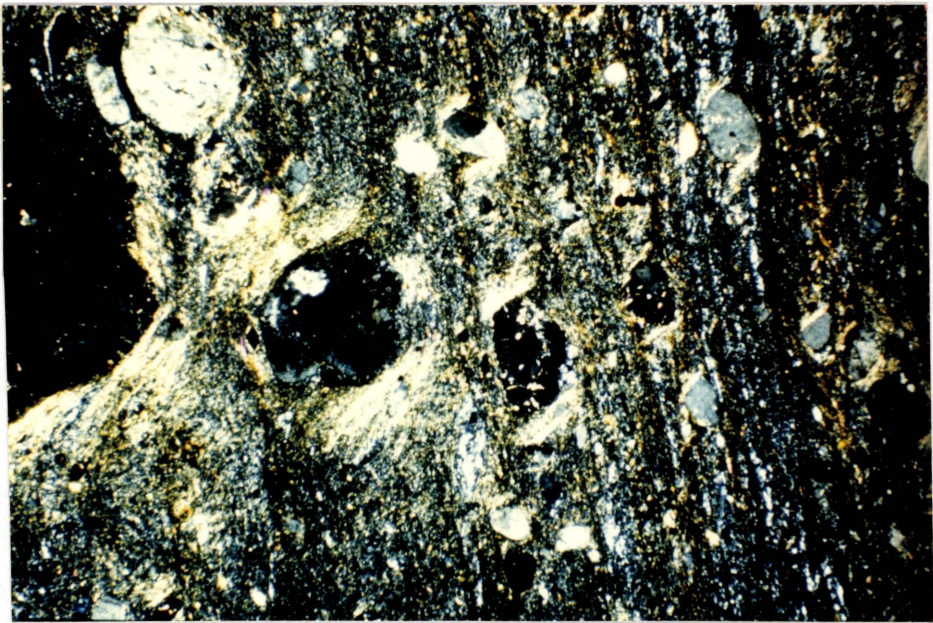
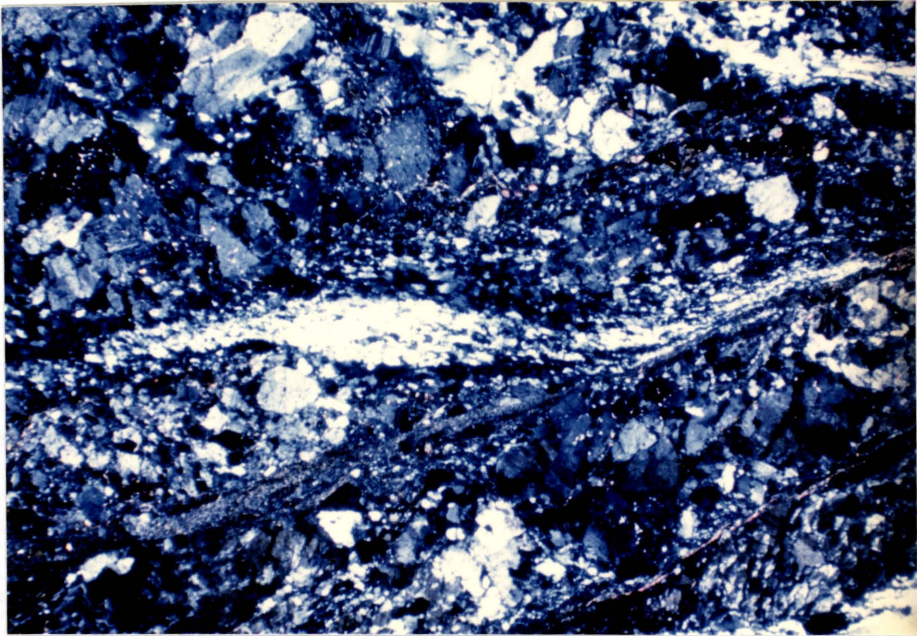


Figure 46a. Biotite "mica fish" in an ultramylonite. the 001 cleavage is oriented parallel to the XY plane of flattening. Slight assymetry of "fish" and the angular relationship between the 001 cleavage and the mylonitic foliation both indicate sinistral shear. Field of view 3.25mm. Plane light. P269.

Figure 46b. Large muscovite grain isolated between two C-planes. The 001 cleavage is parallel to the XY plane of flattening. The angle between the cleavage and the shear plane is 40 degrees. Deformation perthite in the two adjacent K-feldspar crystals show perthite growth to be in a direction normal to the 001 muscovite cleavage. Sinistral shear sense is indicated. Field of view 1.3mm. Plane light. P368.

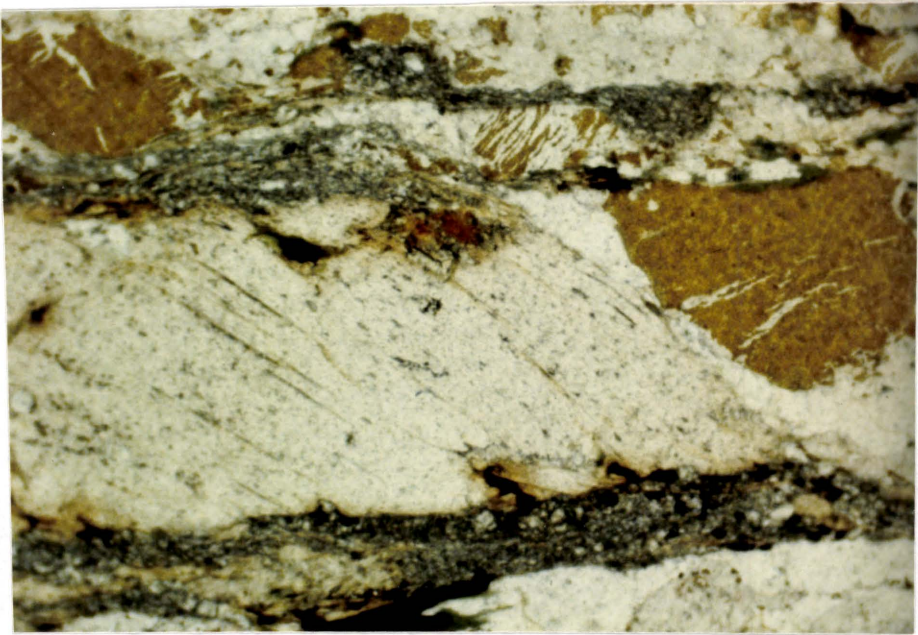


Figure 47. Polished slab of ultramylonite showing well developed tails on feldspar augen. P35a.



CHAPTER 5
STRESS, STRAIN AND METAMORPHISM

THEORY AND APPLICATION OF PALEOPIEZOMETERS

Introduction

When a rock undergoes deformation and metamorphism the crystal system within the rock will change in an attempt to re-equilibrate with its thermodynamic environment. Equilibration may occur through breakdown and recrystallization of pre-existing minerals to form new minerals, through grain growth (static annealing) or through grain size reduction (dynamic recrystallization). Experimental studies of crystal systems subjected to varying temperatures and pressures have shown that the equilibrium or steady state grain size can be directly related to the

differential stress under which the system was deformed.

The mechanism which plays a major role in recrystallization is dislocation creep. The boundary of a grain can be considered a continuous surface of dislocations. Dislocations are also found within crystals in subgrain boundaries, in deformation lamellae and in isolated point or line defects. By means of experimental calibration the density of dislocations, subgrain size, recrystallized grain size and lamellae spacing can be used to determine the flow stresses that were acting at the time of recrystallization.

Energy Controls

Energy is stored in the bonds within crystals. Lowering the number of vacant electron sites in the outer orbitals of the atoms within the crystal through bonding, increases the stability of the crystal. All crystals have boundaries in which there are necessarily vacant electron sites. The total number of vacant sites per unit volume will have an energy proportional to that of its thermodynamic environment. If vacant sites exist within the crystal, the boundary need not possess the total energy per unit volume necessary for equilibrium. In a high energy (high stress) environment more vacant sites are required per unit volume to attain thermodynamic equilibrium. The majority of vacant electron sites are located in the grain boundary. Since surface area

varies as d^2 and volume varies as d^3 , small grains can possess much more energy per unit volume than large grains. Based on this there should theoretically be a stable or steady state grain size for any given stress state.

When a rock changes from one stress state to another, re-equilibration will occur if the temperature is high enough to overcome kinetic barriers. The higher the temperature, the more rapidly equilibration will occur. This process takes place through the creation or removal of dislocations leading to recrystallization.

Diffusion of Point Defects

The rate of diffusion of any type of crystal defect is dependent on a number of factors.

- 1) Diffusion rate is directly proportional to temperature. There is a minimum temperature (excitation energy) necessary before any diffusion can proceed. Once this temperature is reached, increasing the temperature enhances the rate of diffusion.
- 2) Increasing the concentration of point defects generally increases the rate of diffusion by creating a perturbation in the crystal's electric field where defects are concentrated. Through the diffusion of these defects the crystal attempts to decrease the severity of this perturbation.
- 3) Increasing pressure inhibits the diffusion of dislocations

by introducing a volume constriction on the system. Under conditions of high pressure, more energy is required to make the necessary adjustments to the crystal lattice and allow for defect migration. Under such conditions, it appears that it would be energetically more favorable to concentrate the defects on crystal boundaries, and allow straining to proceed through grain boundary sliding.

It can therefore be seen that the strain rate of a mineral is influenced by the thermodynamic environment in which it exists by affecting both the diffusion rate and the concentration of dislocations.

Derivation of the Paleopiezometer

Based on the arguments presented it should be possible, in principle, to infer the differential stress from:

- 1) dislocation density
- 2) subgrain size
- 3) recrystallized grain size
- 4) deformation lamellae spacing

Twiss (1977) has presented the derivation of such a relationship for subgrain size and recrystallized grain size. By combining theoretical controls with experimental results, a quantitative relationship has been determined. Some of the assumptions that he has used are that:

- 1) the formation of subgrains and recrystallized grains

is an energetically favorable process.

2) the energy stored in the subgrain and recrystallized grain boundaries is equivalent to the steady state dislocation density for a given stress state. This means that a unique grain dimension (d) exists for any given stress state.

3) the smallest stable grain size is the one that develops, ie. a newly recrystallized grain will contain no internal dislocations.

For a more detailed discussion of the derivation and its inherent assumptions refer to Twiss (1977). Similar derivations to this have been carried out by various authors and the resultant paleopiezometers for quartz are listed in table 4.

Limitations

There are certain limitations which must be taken into consideration when using a paleopiezometer such as those listed in table 4. These equations assume that the grain size measured is the equilibrium grain size for the desired stress state, but this is not always the case.

An underestimate in stress results if grain growth during dynamic recrystallization is not taken into consideration. If the smallest possible recrystallized grain is the one that forms, it follows that a grain will not recrystallize until

it has reached two times this size. The mean grain size measured will be between d and $2d$. If annealing has proceeded past $2d$ and the differential stress is only maintained for a short period of time, the mean grain size measured will be a larger multiple of d . If the temperature is maintained after the stress has been relaxed, static annealing will proceed, thus increasing the grain size. Since annealing occurs most rapidly in crystals having a high dislocation density or small grain size, those textures resulting from high stress are the least likely to be preserved. Unless the system has been quenched in some way either during or immediately following the relaxation of the stress field, the grain size measured will be larger than the steady state grain size and use of this grain size results in an underestimate of the differential stress.

There are also circumstances which may result in an overestimate of the differential stress. Such would be the case if the initial grain size were small and the applied stress level was low enough that an unreasonable length of time would be necessary to allow the grain size to re-equilibrate. The same result occurs if grain growth or recrystallization is inhibited by neighboring minerals of a different composition (Twiss, 1977). Because of these limitations it is necessary to determine if the observed grain size has resulted from an increase or decrease of the

original grain size.

Paleopiezometers appear to be most useful when applied to the recrystallization associated with major thrust faults. If thrusting has occurred at, or proceeded to, a high crustal level, there is a good chance that the steady state grain size has been preserved, since temperatures could not be maintained at this level. Results from several studies (Twiss, 1977; Weathers et al, 1979; Kohlstedt & Weathers, 1980; Ord & Christie, 1984) of mylonites from major thrust belts indicate that the differential stresses involved in thrusting range from 200 to 2000 bars, with average values of ~1000 bars.

Differential stress values based on the recrystallized grain size of quartz have been determined for this area (Table 5). Calculations were done using the calibration of Christie et al. (1980). Two conclusions can be drawn from these values: 1) The differential stress decreases across the area from northwest to southeast and 2) maximum values for differential stress are much higher than those normally calculated for major thrust belts. Median values, i.e. those calculated for the center of the area, do correspond to average values calculated by other authors. The higher than average values determined for the northwestern part of the area may be the result of one or more of the following:

Table 4

Paleopiezometers for quartz

(a) Recrystallized grain size ($D, \mu\text{m}$) (MPa) = AD^{-n}

A	n	Reference
381	0.71	Mercier <u>et al.</u> (1977)
603	0.68	Twiss (1977)
4090	1.11	Christie <u>et al.</u> (1980)
3902	1.43	Christie <u>et al.</u> (1980)

(b) Subgrain size ($d, \mu\text{m}$) (MPa) = Bd^{-m}

B	m	Reference
200	1	Twiss (1977)

(c) Dislocation density (N, cm^{-2}) (MPa) = CN^p

C	p	Reference
6.3×10^{-3}	0.5	Goetze (1975)
1.64×10^{-4}	0.66	McCormick (1977)
2.47×10^{-3}	0.5	Twiss (1977)
6.6×10^{-3}	0.63	Kohlstedt <u>et al.</u> (1979)
6.6×10^{-3}	0.5	Weathers <u>et al.</u> (1979)
2.89×10^{-4}	0.67	Kohlstedt & Weathers (1980)

(d) Deformation lamellae ($s, \mu\text{m}$) (MPa) = Ds^{-1}

D	1	Reference
6.35×10^3	2.18	Koch & Christie (1981)

TABLE 5
Quartz Grain Size Paleopiezometry

Sample	Grain Size (mm)	Differential Stress (Kbar)
P204	0.005	6.8
P231	0.005	6.8
P368	0.01	3.2
P115	0.007	4.7
P139	0.01	3.2
P460	0.008	4.1
P268	0.01	3.2
P102	0.02	1.5
P10	0.02	1.5
P35	0.05	0.5
P45	0.04	0.7
P527	0.07	0.4
P54	0.07	0.4
P244	0.1	0.2

- 1) The exposed crustal level is higher than in most thrust belts;
- 2) The differential stress was higher;
- 3) The grain size reduction in this part of the area was due to brittle processes and is therefore not related to differential stress;
- 4) Calculations have not been done by other authors over as wide an area.

Of these possibilities, the fourth is the most likely. The second is unlikely since the average values calculated for this area correspond to those calculated for other zones.

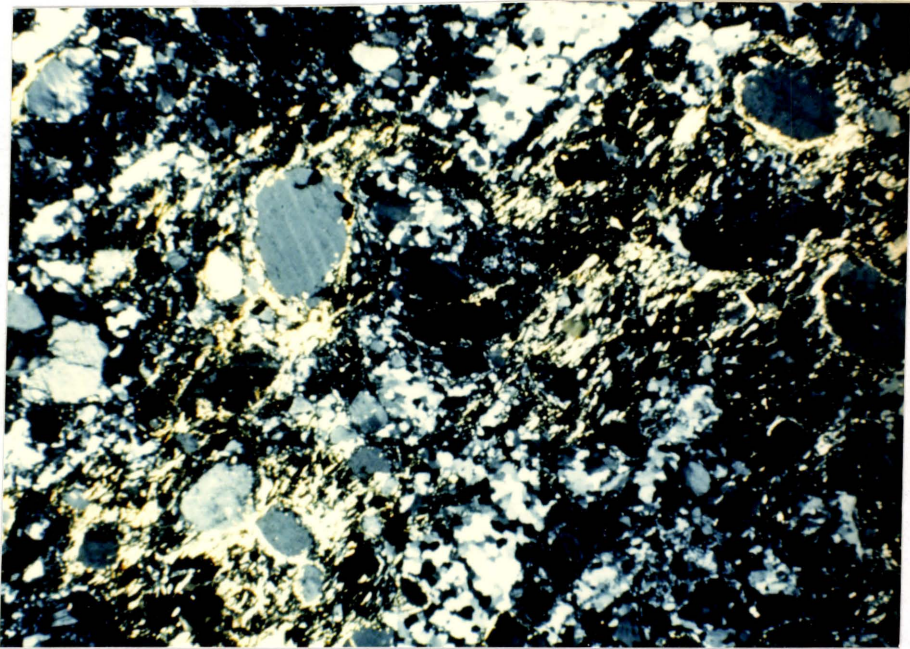
STRAIN ESTIMATE

A sample of ultramylonite from the Johnnie Lake Shear Zone has been cut along both the XZ and the XY planes in order to determine the type of strain in three dimensions. Quartz ribbon widths in the XZ section ranged from 0.2 to 0.01mm with the average width being 0.07mm. In the XY section quartz occurs as elongated grain aggregates which are on the average 2mm wide and 7mm long. The long axes of the aggregates defines the mineral lineation. These measurements give an average volume for the aggregates of 1.4mm^3 which is similar to the volume of individual quartz grains in the relatively undeformed aggregates in the rock from which the

mylonite was derived. Reducing this to an order of magnitude calculation, beginning with an initial unit cube, the strain has produced a final rhombohedron having dimensions 10mm x 1mm x 0.1mm. These numbers give a strain ratio of 100:10:1 with a k value of 1 implying that there has been very little volume loss (Ramsay, 1967). Also the intermediate dimension has changed very little from that of the original, indicating that deformation has been produced largely through simple shear. The amount of shear strain necessary to produce this transformation is 9 which corresponds to an angular shear of ~ 85 degrees. This value appears to be a reasonable estimate for shear strain in an ultramylonite (White et al., 1980).

Although these estimates are grossly oversimplified, they do appear to be reasonable and help to characterize the strain involved in the formation of these mylonites. Another feature which supports some of these conclusions is shown in figure 48. Biotite flakes which have a highly asymmetrical distribution pattern in the XZ section are seen in the XY section to be symmetric on either side of feldspar augen. All flakes are preferentially oriented parallel to the mineral lineation, rarely tapering to a point to get around obstacles created by other grains. This feature supports the conclusion that the majority of the strain has been restricted to the XZ plane with very little affect on the Y direction. If a significant pure shear component had acted in the Y

Figure 48. Symmetrical distribution of biotite flakes on either side of a feldspar augen in an XY section of ultramylonite. Field of view 6.5mm. P269.



direction, mica flakes with a component of that orientation would be expected. This does not occur. Quartz pressure shadows on feldspar augen in the XY section show similar behavior.

METAMORPHISM

This study has been confined to the granitic units occurring in the study area. Due to the restricted chemical composition of these units, a well defined metamorphic gradient is not easily determined on a mineralogical basis. In figure 49 a crude isograde map has been constructed based on the appearance or disappearance of certain minerals. The mineral assemblages for each thin section studied are outlined in table 6. The samples in table 6 are listed in order of their occurrence from northwest to southeast. In all of these assemblages, quartz + K-feldspar + plagioclase also occur.

The characteristic mineral assemblage of the northwestern boundary of the area is bio-musc-chlor-ep-sph. It is found in both the Bell Lake Granite and the Killarney Granite. Immediately north of the Johnnie Lake Shear Zone along the northern boundary of area 3, small garnet porphyroblasts are developed in the Bell Lake Granite as well as rare sillimanite. Within area 3, hornblende becomes a common

constituent in addition to the assemblage mentioned above.

The northwestern boundary of area 6 essentially coincides with the disappearance of muscovite from this assemblage. Slightly southeast of this, chlorite, epidote and sphene become scarce. Assemblages found southeast of this line are one of; qtz-ksp-plag-bio, qtz-ksp-plag-bio-hbld or qtz-ksp-plag-bio-hbld-alm. In the southeastern corner of the map area, along highway 637, is a small patch, with poorly constrained boundaries, of amphibolite retrograde from granulite. This patch marks the disappearance of biotite leaving the assemblage qtz-ksp-plag-hbld-alm. In thin section the hornblende can be seen to be a retrogressive product from the alteration of pyroxenes, of which only very small fragments remain. In outcrop this rock is massive, granular and weathers to an amber-brown colour.

Based on the thin sections examined a general increase in metamorphic grade from greenschist to granulite can be recognized from northwest to southeast. A similar increase in metamorphic grade to that indicated by the mineralogy, can be inferred from the change in the deformational behavior of quartz and feldspar.

TABLE 6

Mineral Assemblages

Sample	Bio	Musc	Chlor	Ep	Sph	Hbld	Sil	Gar
P204	x	x	x	x	x			
P121	x	x	x	x	x			
P115	x	x		x	x			
P113	x			x	x	x		
P109	x	x		x	x			
P368	x	x		x				
P361	x	x		x				
P347	x	x	x	x			x	x
P139	x	x	x	x	x			x
P102	x	x		x				
P460	x	x	x	x	x			x
P268	x	x	x	x	x			x
P269	x	x		x				x
R95	x	x		x				x
P286	x	x	x		x			x
P283	x		x	x	x			
P10	x	x				x		x
P10-1			x		x	x		x
P35	x	x	x	tr	x	x		x
P45	x	x					x	
P529	x			x	x	x		
P527	x		x	x	x			
P52	x							
P53	x	tr	tr					
P54	x	tr						
P602	x					x		
P244	x					x		x
P245						x		x

All assemblages include qtz + K-spar + plag.

tr - trace

bio- biotite; musc- muscovite; chlor- chlorite;

ep- epidote; sph- sphene; hbld- hornblende;

sil- sillimanite; gar- garnet.

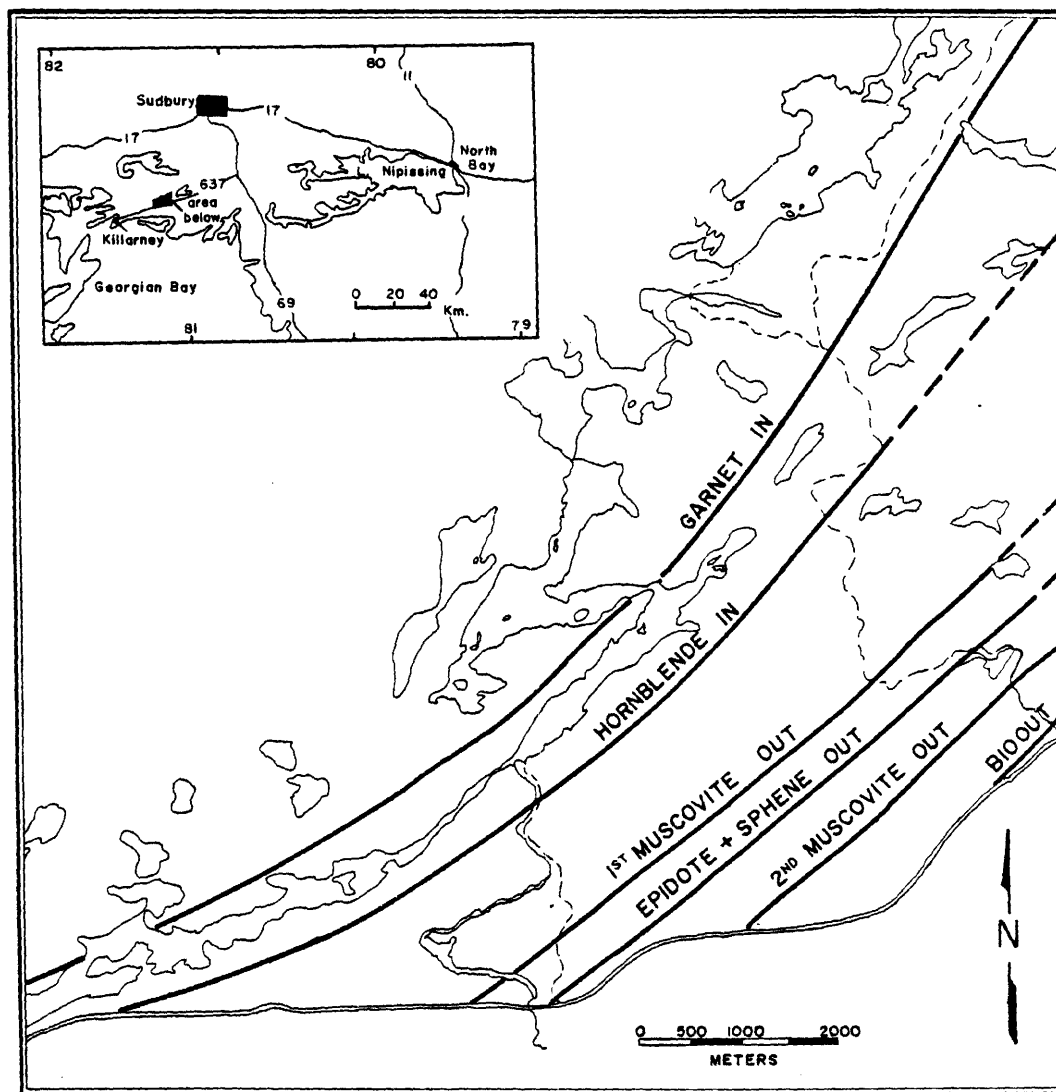


Figure 49. Isograd map based on the appearance or disappearance of minerals across the area.

Quartz

The variations in microstructural strain features in quartz, discussed in chapter 4, are indicative of an increase in metamorphic grade from northwest to southeast. In area 1 the predominant mode of deformation is brecciation which indicates that conditions during deformation were below lower greenschist facies.

As area 2 is traversed, both from northwest to southeast and from southwest to northeast, ductile deformation features become more important and brecciation of quartz no longer occurs. A core and mantle structure becomes dominant and indicates that temperatures had reached or surpassed 0.4 of the absolute melting temperature of quartz, which corresponds to lower greenschist facies or higher.

Along the northwestern boundary of area 3A, Type I quartz ribbons are the common form of quartz. These ribbons have been recognized by Simpson (1985) in rocks deformed under lower greenschist facies conditions. Within the mylonites of area 3A, Type II quartz ribbons occur and according to Simpson (1985) correspond to conditions during deformation of mid to upper greenschist grade.

In the central part of area 5 as well as in area 3B, Type IV quartz ribbons are the dominant form of quartz. This change in quartz morphology may indicate that the metamorphic grade has increased above upper greenschist. In the southern

part of area 5 and in area 6, quartz occurs as Type III ribbons. These ribbons are indicative that the metamorphic grade during deformation was at epidote-amphibolite grade or higher (Simpson, 1985).

Feldspar

The variation in microstructural strain features in feldspars and the corresponding metamorphic grade necessary for their formation has been discussed previously in chapter 4. Using these features the following increase in metamorphic grade can be inferred.

Between the northwestern limit of mapping and the northern part of area 2, the type of fracturing occurring in feldspar indicates that temperatures during deformation were below 300°C. Within the central portion of area 2, the predominance of antithetic fractures indicates that temperatures were between 300 and 400°C, lower greenschist facies, (Boullier, 1980; White, 1975). In the southern part of area 2 along the contact with area 3A, as well as a large portion of the northeastern half of area 2, some feldspars begin to show evidence of crystal plastic behavior, i.e. deformation twinning, undulatory extinction, deformation bands and kink bands. As well as this, sympathetic shear fractures are the dominant mode of deformation. The combination of these features indicates that temperatures during deformation in these areas were near 500°C, (Andrews, 1984; White, 1975).

In the center of area 3A and in area 3B, fracturing of feldspar is replaced by recrystallization through nucleation and growth as the dominant deformation mechanism. This change in mode of deformation corresponds to a change from upper greenschist to lower amphibolite grade conditions, having temperatures slightly above 500°C. This change also corresponds with the appearance of hornblende as a stable mineral.

Beginning within area 5 and increasing in importance to the southeastern limit of mapping, dynamic recrystallization occurs in feldspars indicating that deformation took place under metamorphic conditions of mid amphibolite to granulite.

DISCUSSION

Based on mineralogy and the microstructural strain features of quartz and feldspar the metamorphic grade existing during deformation ranged from below lower greenschist grade along the northwestern boundary to granulite grade at the southeastern boundary. This corresponds to an increase in temperature across the area of ~400°C. Within the area, the transition from greenschist to amphibolite facies occurs across the Johnnie Lake Shear Zone in area 3A. The extension of this isograd to the northeast swings up into the Bell Lake Granite in area 2.

The increase in metamorphic grade toward the northeast may be responsible for the decrease in abundance of glassy mylonite along the extension of the Johnnie Lake Shear Zone in area 3B. At a higher metamorphic grade the deformation is more penetrative and the strain need not localize along discrete surfaces. The crystal plastic behavior of feldspar would allow a large proportion of the strain to be accomplished through feldspar deformation. The occurrence of metasediments in this zone would also allow a large portion of the strain to be accommodated through deformation of the softer quartz rich sediments.

The increase in metamorphic grade discussed above accompanies the increase in recrystallized quartz grain size, discussed at the beginning of this chapter. The increase in grain size corresponds to a decrease in differential stress or, equivalently, to an increase in confining pressure with depth at constant maximum stress. Based on the values for differential stress derived through paleopiezometry, this would imply an increase in confining pressure across the area of about 6 Kbar. This value is reasonable for a temperature increase of 400°C. These values indicate that there is a differential erosion level of approximately 20 kilometers from northwest to southeast or, equivalently, a vertical displacement of the southeast block over the northwest block of 20 kilometers during thrusting.

Recent investigations by Indares and Martignole (1985) of the Grenville Front Zone in Quebec indicate that the metamorphic conditions during thrusting are characterized by temperatures between 500 and 650°C and pressures between 7 and 8 Kbar. Assuming that these conditions are more or less representative of the majority of the Grenville Front Zone, they agree reasonably well with the increase in temperature and pressure determined above, starting from an initial grade of below lower greenschist facies. Although varying amounts of movement have taken place along the length of the Grenville Front, vertical movements of 15 to 20 kilometers are common (Wynne-Edwards, 1972).

The direction of movement of material during thrusting follows that expected in a regional reverse fault system, passing from a deep ductile regime to a high level brittle regime through a competent cover. The competent cover is represented here by the Bell Lake Granite through which the zone would be expected to steepen. The increase in inclination of structural elements from southeast to northwest corresponds to this change in attitude.

A change in the nature of the foliation is associated with the change in attitude. In the extreme southeastern section of the map area, a single foliation defined by the long axes of both quartz and feldspar exists. This foliation dips moderately toward the southeast. Northward from this

boundary, the expression of this surface changes, becoming less penetrative until it occurs as discrete surfaces with discernible offset (C-surfaces) northwest of area 3. This change in the nature of the C-surfaces is accompanied by an increase in importance of S-surfaces in the northwest, which are similar in nature to the C-surfaces in the southeast, i.e. S-surfaces are defined by the long axes of quartz and feldspar.

At the onset of deformation, at deep crustal levels, the differential stress is low while the absolute stress and temperature are high. Thrusting causes displacement of these rocks to higher crustal levels, thus decreasing the confining pressure. In the deep, plastically deforming rocks an apparent flattening foliation is pervasive. Those rocks which are subsequently subjected to retrogressive metamorphism during thrusting, i.e. those raised to a higher crustal level, become strong with the decrease in confining pressure. With this increase in strength, the flattening foliation can no longer keep up with the progressive simple shear such that shear discontinuities develop within the rock (Robin, pers. comm.). This process corresponds to an increase in differential stress and is associated with the more brittle deformation of feldspar and a smaller recrystallized grain size in quartz.

It follows from the above discussion that the majority of

the area had an original foliation which dipped shallowly toward the southeast. These surfaces were subsequently rotated during uplift into a steeper orientation. Since the external stress remained non-coaxial and constant in orientation, a second foliation (C) was imposed over the first.

CHAPTER 6

CONCLUSIONS

Across the portion of the Grenville Front Tectonic Zone covered in this study, there has been an increase in metamorphic grade from lower greenschist to upper amphibolite or granulite grade. This metamorphic gradient involves a change in temperature of approximately 400°C and in pressure of 6 Kbar. Vertical displacement of the southeast block upward has been accomplished through reverse fault movement and is estimated to be on the order of 20 kilometers.

Deformation of the rocks which underlie this area has been produced largely through simple shear. Shear strain has been estimated to be 9 or higher in the Johnnie Lake Shear Zone and has resulted in a strain ratio of 100:10:1 with a k

value of 1. The strain in the area has not been restricted to a single narrow zone but becomes increasingly penetrative southeast of the Johnnie Lake Shear Zone. The dominant deformation mechanisms in the northwestern half of the area involve fracture and fragment rotation in feldspars and dynamic recrystallization and subsequent flow in quartz. The deformation mechanism in the southeastern half of the area has been recrystallization and subsequent flow in both quartz and feldspar. Deformation enhanced diffusion becomes an important process at upper greenschist grade metamorphism and above. Microstructural strain features in quartz and especially feldspar could potentially become important indicators of metamorphic grade during deformation.

The maximum principal stress during deformation was oriented along a horizontal line trending northwestward. The intermediate stress, also horizontal, had a northeasterly trend while the minimum principal stress was oriented vertically. The maximum principal strain direction changes from vertical to moderately inclined toward the southeast from northwest to southeast.

Asymmetry resulting from S-C relationships is the most reliable kinematic indicator.

Suggestions For Further Research

More investigation is necessary, both experimental and empirical, on the relationship between microstructural strain features in feldspars and metamorphic grade during deformation. This may prove to be an important tool in areas where the P-T conditions existing during deformation have not been sustained long enough for the mineralogy to equilibrate.

The evolution and mechanism involved in the formation of deformation induced perthite should be investigated as a potential kinematic indicator.

The role of fluids during deformation and mylonite formation at all metamorphic grades also requires further research.

REFERENCES

- Andrews, J.R. 1984. Fracture controlled feldspar shape fabrics in deformed quartzo-feldspathic rocks. J. Struct. Geol. 6, 183-188
- Barlow, A.E. 1893. Relations of the Laurentian and Huronian rocks north of Lake Huron. Geol. Soc. Am. Bull. 4, 313-332.
- Bell, R. 1878. Geology in the neighbourhood of Shiboananing. Geol. Surv. Can. Report on Progress 1876-77, 208-210.
- Bell, R. 1891. Sudbury Mining District. Geol. Surv. Can. Ann. Rep. V, Part F, 95p.
- Bell, R. 1898. Report on the geology of the French River sheet, Ontario. Geol. Surv. Can. Ann. Rep. IX, Part I, 29p.
- Bell, T.H. and Etheridge, M.A. 1973. Microstructures of mylonites and their descriptive terminology. Lithos 6, 337-348.
- Bell, T.H. & Hammond, R.L. 1984. On the internal geometry of mylonite zones. J. Geol. 92, 667-686.
- Berthe, P., Choukroune, P. & Jegouzo, P. 1979. Orthogneiss, mylonite and non-coaxial deformation of granites: the example of the South Armorican shear zone. J. Struct. Geol. 1, 31-42.
- Borges, F.S. and White, S.H. 1980. Microstructural and chemical studies of sheared anorthosites, Roneval, South Harris. J. Struct. Geol. 2, 273-280.
- Bouchez, J.-L. 1977. Plastic deformation of quartzites at low temperature in an area of natural strain gradient. Tectonophysics 39, 25-50.
- Boullier, A.M. 1980. A preliminary study on the behavior of brittle minerals in a ductile matrix: example of zircons and feldspars. J. Struct. Geol. 2, 211-217.
- Boullier, A.M. and Bouchez, J.-L. 1978. Le quartz en rubans dans les mylonites. Bull. Soc. Geol. Fr. 20, 877-882.

- Brooks, E.R. 1964. Nature and origin of the Grenville Front north of Georgian Bay, Ontario. Unpublished Ph.D. thesis, Univ. Wisconsin, Madison, Wisconsin.
- Brooks, E.R. 1967. Multiple metamorphism along the Grenville Front, north of Georgian Bay, Ontario. Geol. Soc. Am. Bull. 78, 1267-1280.
- Brooks, E.R. 1976. The Sudbury Basin, the Southern Province, The Grenville Front and the Penokean Orogeny: discussion. Geol. Soc. Am. Bull. 87, 954-958.
- Brown, W.L., Macaudiere, J. and Ohnenstetter, M. 1980. Ductile shear zones in a meta-anorthosite from Harris, Scotland: textural and compositional changes in plagioclase. J. Struct. Geol. 2, 281-287.
- Burg, J.P. 1986. Quartz shape fabric variations and c-axis fabrics in a ribbon-mylonite: arguments for an oscillating foliation. J. Struct. Geol. 8, 123-131.
- Burg, J.P. and Laurent, Ph. 1978. Strain analysis of a shear zone in a granodiorite. Tectonophysics 47, 15-42.
- Card, K.D. and Lumbers, S.B. 1977. Sudbury-Cobalt. Ont. Dept. Mines, Geol. Compilation Series, Map 2361.
- Carreras, J., Estrada, A. and White, S.H. 1977. The effects of folding on the c-axis fabric of a quartz mylonite. Tectonophysics 39, 3-24.
- Christie, J.M. 1963. The Moine thrust sone in the Assynt region, northwest Scotland. Univ. Calif. Pubs. Geol. Sci. 40, 345-440.
- Christie, J.M. and Ord, A. 1980. Flow stress from microstructures of mylonites: examples and current assessment. J. Geophys. Res. 85, 6253-6262.
- Christie, J.M., Ord, A. and Koch, P.S. 1980. Relationship between recrystallized grain size and flow stress in experimentally deformed quartzite (abstract). EOS Trans. Am. Geophys. Un. 61, 377.
- Collins, W.H. 1916. The age of the Killarney granite. Geol. Surv. Can., Museum Bull. 8, 31p.
- Collins, W.H. 1925. North shore of Lake Huron. Geol. Surv. Can. Memoir 143, 160p.

- Culshaw, N.G. and Fyson, W.K. 1984. Quartz ribbons in high grade granite gneiss: modifications of dynamically formed quartz c-axis preferred orientation by oriented grain growth. J. Struct. Geol. 6, 663-668.
- Davidson, A. 1986. A New Look at the Grenville Front in Ontario. GAC-MAC Joint Annual Meeting, Ottawa '86, Field Trip 15.
- Davidson, A., Culshaw, N.G. and Nadeau, L. 1982. A tectono-metamorphic framework for part of the Grenville Province, Ontario: in Current Research, Part A, Geol. Surv. Can. paper 82-1A, 175-190.
- Debat, P., Soula, J.-C., Kubin, L. and Vidal, J.-L. 1978. Optical studies of natural deformation microstructures in feldspars (gneiss and pegmatites from Occitania, southern France). Lithos 11, 133-145.
- Deer, W.A., Howie, R.A. and Zussman, J. 1966. An Introduction to the Rock Forming Minerals. Logman. 528p.
- Derry, D.R. 1950. A Tectonic Map of Canada. GAC Proc. 3, 39-53.
- Dollase, W. 1962. Geology of the Tyson Lake Area, Ontario. Unpublished M.Sc. thesis, Univ. Wisconsin, Madison, Wisconsin.
- Evans, D.J. and White, S.H. 1984. Microstructural and fabric studies from the rocks of the Moine Nappe, Eriboll, NW Scotland. J. Struct. Geol. 6, 369-389.
- Fitzgerald, J.D., Etheridge, M.A. and Vernon, R.H. 1983. Dynamic recrystallization in a naturally deformed albite. Textures and Microstructures 5, 219-237.
- Frarey, M.J. 1985. Proterozoic geology of the Lake Panache-Collins Inlet area, Ontario. Geol. Surv. Can. paper 83-22, 61p.
- Frarey, M.J. and Cannon, R.T. 1969. Notes to accompany a map of the geology of the proterozoic rocks of the Lake Panache-Collins Inlet map areas, Ontario. (41I/3, H/14). Geol. Surv. Can. paper 68-63, 5p.

- Gapais, D. & White, S.H. 1982. Ductile shear bands in a naturally deformed quartzite. Textures and Microstructures 5, 1-17.
- Ghosh, S.K. and Ramberg, H. 1976. Reorientation of inclusions by combination of pure shear and simple shear. Tectonophysics 34, 1-70.
- Goetze, C. 1975. Sheared lherzolites: from the point of view of rock mechanics. Geology 3, 172-173.
- Hanmer, S. 1981. Segregation bands in plagioclase: non-dilatational quartz veins formed by strain enhanced diffusion. Tectonophysics 79, T53-T61.
- Hanmer, S. 1982. Microstructure and geochemistry of plagioclase and microcline in naturally deformed granite. J. Struct. Geol. 4, 197-213.
- Hanmer, S. 1984. The potential use of planar and elliptical structures as indicators of strain regime and kinematics of tectonic flow. Curr. Res. Geol. Surv. Can. paper 84-1B, 133-142.
- Henderson, J.R. 1967. Structural and Petrological relationships across the Grenville Province - Southern Province Boundary, Sudbury District, Ontario. Unpublished Ph.D. thesis, McMaster Univ., Hamilton, Ontario.
- Henderson, J.R. 1972. Deformation of the Chief Lake batholith, Ontario, Canada. 24th Int. Geol. Cong., Montreal, Sec. 3, 505-515.
- Higgins, M.W. 1971. Cataclastic Rocks. Prof. Pap. USGS 687.
- Hobbs, B.E., Means, W.D. and Williams, P.F. 1976. An Outline of Structural Geology. Wiley. 571p.
- Indares, A. and Martignole, J. 1985. The Montreal - Val d'Or Geotraverse. Field Guidebook. Friends of the Grenville. October 4-5-6, 1985.
- Jensen, L.N. and Starkey, J. 1985. Plagioclase microfabrics in a ductile shear zone from the Jotun Nappe, Norway. J. Struct. Geol. 7, 527-539.
- Jones, W.A. 1930. The petrography of the rocks in the vicinity of Killarney, Ontario. Univ. Tor. Studies, Geol. Ser. 29, 39-60.

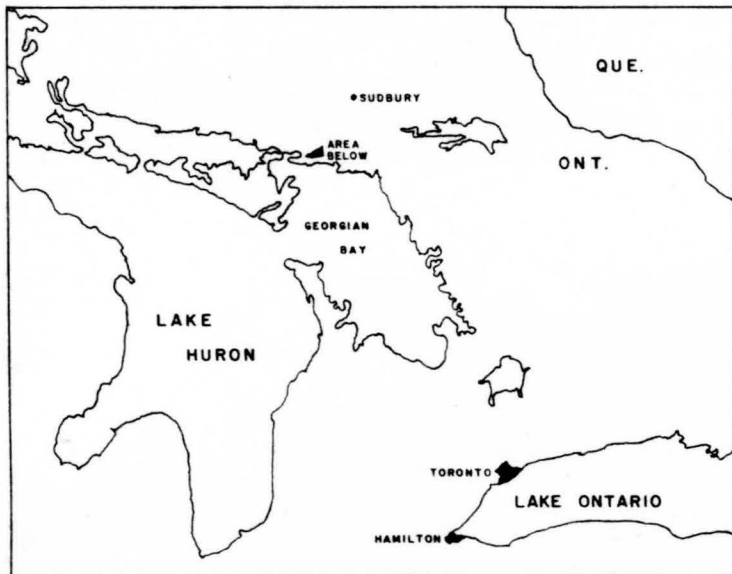
- Koch, P.S. and Christie, J.M. 1981. Spacing of deformation lamellae as a paleopiezometer (abstract). EOS Trans. Am. Geophys. Un. 62, 1030.
- Kohlstedt, D.L. and Weathers, M.S. 1980. Deformation-induced microstructures, paleopiezometers, and differential stresses in deeply eroded fault zones. J. Geophys. Res. 85, 6269-6285.
- Kohlstedt, D.L., Cooper, R.F., Weathers, M.S. and Bird, J.M. 1979. Paleostress analysis of deformation-induced microstructures: Moine thrust zone and Ikertog shear zones. in Analysis of Actual Fault Zones in Bedrock, USGS Open File Report 79-1239, Menlo Pk., Calif., 349-425.
- Lapworth, C. 1885. The highland controversy in British geology: its causes, course and consequences. Nature 32, 558-559.
- Lawson, A.C. 1929. Some Huronian problems. Geol. Soc. Am. Bull. 40, 361-383.
- Lister, G.S. and Price, G.P. 1978. Fabric development in a quartz-feldspar mylonite. Tectonophysics 49, 37-78.
- Lister, G.S. & Snoke, A.W. 1984. S-C mylonites. J. Struct. Geol. 6, 617-638.
- Lumbers, S.B. 1978. Geology of the Grenville Front Tectonic Zone in Ontario. in Currie, A.L. and Mackasey, W.D., eds., Toronto '78, Field Trips Guidebooks, GAC, 347-371.
- Marshall, D.B. and McLaren, A.C. 1977. Deformation mechanisms in experimentally deformed plagioclase feldspars. Phys. Chem. Minerals 1, 351-370.
- Mawer, C.K. 1986. What is a mylonite? Geoscience Canada 13, 33-34.
- McCormick, J.W. 1977. Transmission electron microscopy of experimentally deformed synthetic quartz. Unpublished Ph.D. thesis, Univ. Calif., Los Angeles.
- Mercier, J.C., Anderson, D.A. and Carter, N.L. 1977. Stress in the lithosphere: inferences from the steady state flow of rocks. Pure Appl. Geophys. 115, 199-226.

- Murray, A. 1849. Report of Alexander Murray, Esq., Asst. Geologist, Geol. Surv. Can. Ann. Rep. for 1847-48, 93-124.
- Murray, A. 1857. Report of Alexander Murray for the year 1856. Geol. Surv. Can. Rep. of Prog. for the years 1853-56, 145-188.
- Nicolas, A. and Poirier, J.P. 1976. Crystalline Plasticity and Solid State Flow in Metamorphic Rocks. Wiley. 444p.
- Olsen, T.S. and Kohlstedt, D.L. 1985. Natural deformation and recrystallization of some intermediate plagioclase feldspars. Tectonophysics 111, 107-131.
- Ord, T.S. and Christie, J.M. 1984. Flow stresses from microstructures in mylonitic quartzites of the Moine thrust zone, Assynt area, Scotlant. J. Struct. Geol. 6, 639-654.
- Poirier, J.P. 1980. Shear localization and shear instability in materials in the ductile field. J. Struct. Geol. 2, 135-142.
- Quirke, T.T. 1917. Espanola District, Ontario. Geol. Surv. Can. Memoir 102, 87p.
- Quirke, T.T. and Collins, W.H. 1930. The disappearance of the Huronian. Geol. Surv. Can. Memoir 160, 112p.
- Ramsay, J.G. 1967. Folding and Fracturing of Rocks. McGraw-Hill. 568p.
- Ramsay, J.G. 1980. Shear zone geometry: a review. J. Struct. Geol. 2, 83-99.
- Ramsay, J.G. & Graham, R.H. 1970. Strain variation in shear belts. Can. J. Earth Sci. 7, 786-813.
- Ramsay, J.G. and Huber, M.I. 1983. The Techniques of Modern Structural Geology. Volume 1: Strain Analysis. Academic Press. 307p.
- Ransom, D.M. 1971. Host control of recrystallized quartz grains. Min. Mag. 38, 83-88.

- Robin, P.-Y.F. and Jowett, E.C. 1986. Computerized density contouring and statistical evaluation of orientation data using counting circles and continuous weighting functions. Tectonophysics 121, 207-223.
- Shelley, D. 1972. Syntectonic recrystallization and preferred orientation of quartz. Geol. Soc. Am. Bull. 83, 3523-3524.
- Simpson, C. 1985. Deformation of granitic rocks across the brittle-ductile transition. J. Struct. Geol. 7, 503-511.
- Simpson, C. & Schmid, S.M. 1983. An evaluation of criteria to deduce the sense of movement in sheared rocks. Geol. Soc. Am. Bull. 94, 1281-1288.
- Stockwell, C.H. 1982. Proposals for the time classification and correlation of Precambrian rocks and events in Canada and adjacent areas of the Canadian shield; Part 1: A time classification of Precambrian rocks and events. Geol. Surv. Can. paper 80-19, 135p.
- Streckeisen, A.L. 1976. To each plutonic rock its proper name. Earth Sci. Rev. 12, 1-34.
- Tullis, J. 1978. Mylonites - natural and experimental; Processes and conditions of mylonite formation as inferred from experimental deformation studies. Geol. Soc. Am. short course, March 7,8,1978, Boston, Mass., 18p.
- Tullis, J. and Yund, R.A. 1977. Experimental deformation of dry Westerly granite. J. Geophys. Res. 82, 5705-5718.
- Tullis, J. and Yund, R.A. 1980. Hydrolytic weakening of experimentally deformed Westerly granite and Hale albite rock. J. Struct. Geol. 2, 439-451.
- Twiss, R.J. 1977. Theory and applicability of a recrystallized grain size paleopiezometer. Pure Appl. Geophys. 115, 227-244.
- Vernon, R.H., Williams, V.A. & D'Arcy, W.F. 1983. Grain size reduction and foliation development in a deformed granitoid batholith. Tectonophysics 92, 123-145.

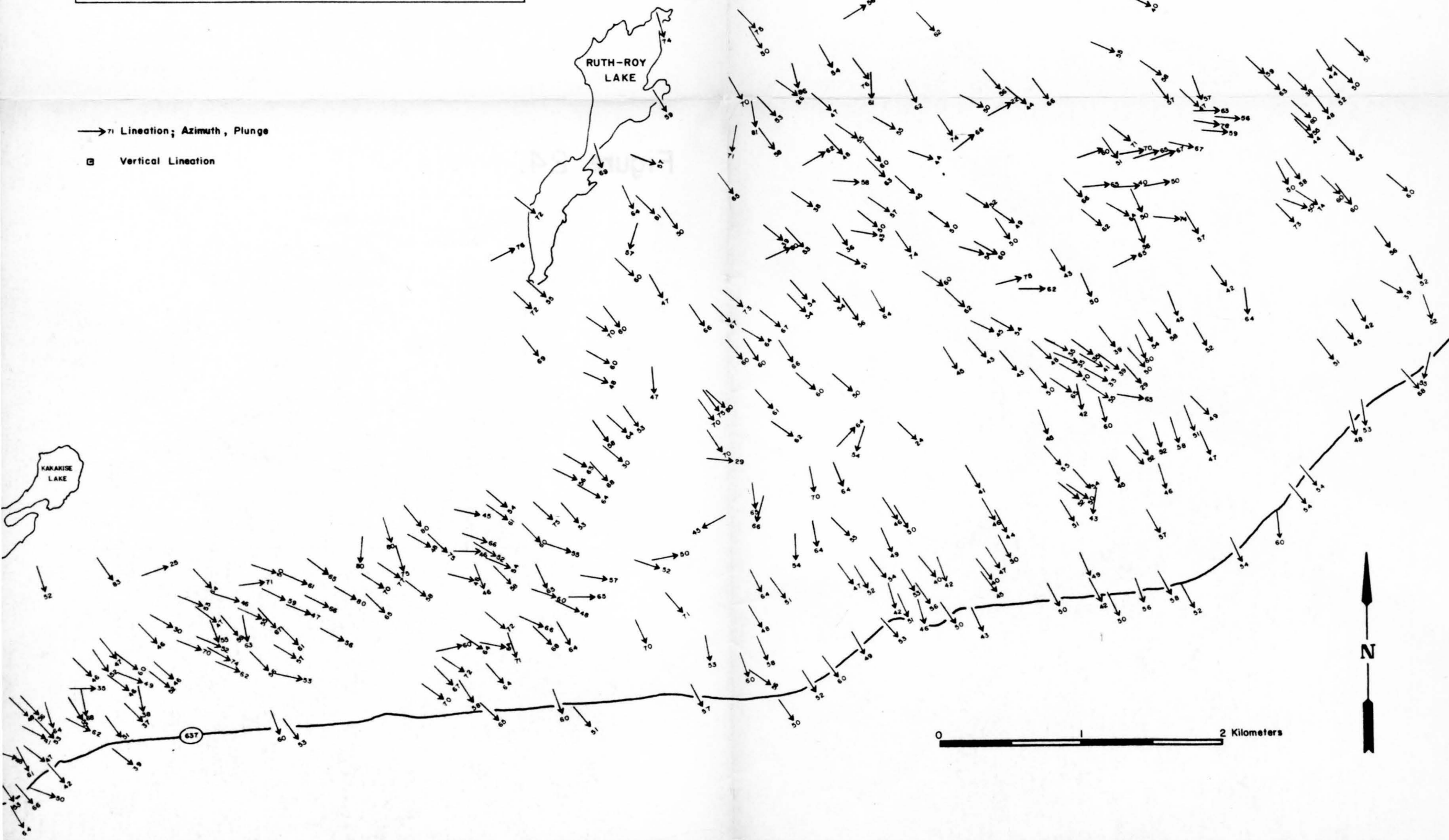
- Vidal, J.-L., Kubin, L., Debat, P. and Soula, J.-C. 1980. Deformation and dynamic recrystallization of k-feldspar augen in orthogneiss from Montagne Noire, Occitania, Southern France. Lithos 13, 247-255.
- Weathers, M.S., Bird, J.M., Cooper, R.F. and Kohlstedt, D.L. 1979. Differential stress determined from deformation-induced microstructures of the Moine thrust zone. J. Geophys. Res. 84, 7495-7509.
- White, S. 1975. Tectonic deformation and recrystallization of oligoclase. Contrib. Mineral. Petrol. 50, 287-304.
- White, S. 1976. The effects of strain on the microstructure, fabrics and deformation mechanisms in quartzite. Phil. Trans. R. Soc. Lond. Ser. A. 283, 69-86.
- White, J.C. and Mawer, C.K. 1986. Extreme ductility of feldspars from a mylonite, Parry Sound, Canada. J. Struct. Geol. 8, 133-143.
- White, S.H., Burrows, S.E., Carreras, J., Shaw, N.D. & Humphreys, F.J. 1980. On mylonites in ductile shear zones. J. Struct. Geol. 2, 175-187.
- White, S.H., Evans, D.J. and Zhong, D.-L. 1982. Fault rocks of the Moine thrust zone: microstructures and textures of selected mylonites. Textures and Microstructures 5, 33-61.
- Wilson, M.E. 1918. The subprovincial limitations of Precambrian nomenclature in the St. Lawrence basin. J. Geol. 26, 325-333.
- Wynne-Edwards, H.R. 1972. The Grenville Province. in Variations in Tectonic Styles in Canada, R.A. Price and R.J.W. Douglas, eds., Geol. Assoc. Can. Spec. Pap. 11, 263-334.

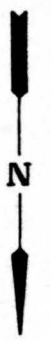
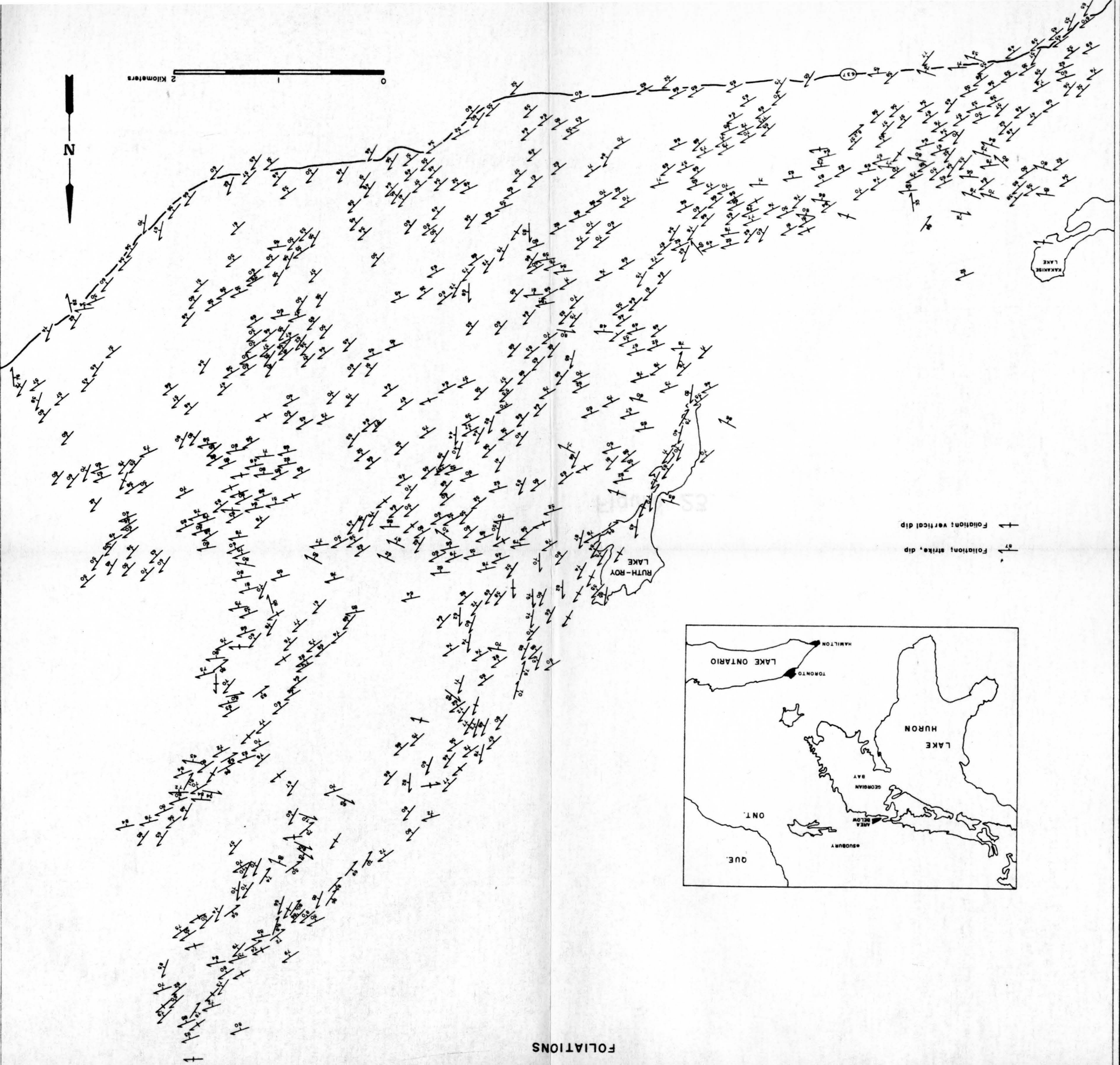
LINEATIONS



→ 71 Lineation; Azimuth, Plunge

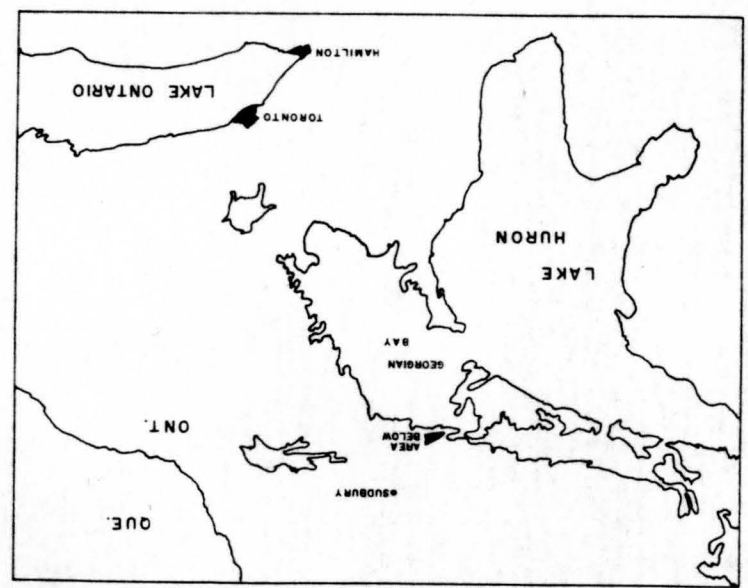
□ Vertical Lineation



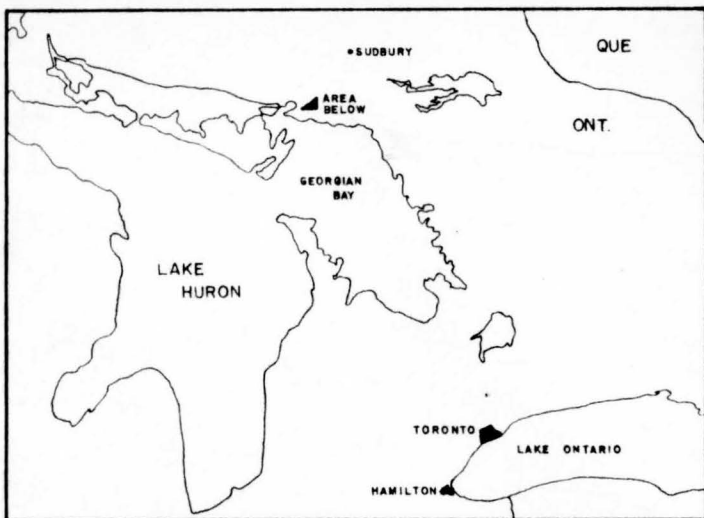


0 1 2 Kilometers

———> Foliation: vertical dip
 ———> Foliation: strike, dip



FOLIATIONS



METASEDIMENTS

- Qz** Quartzite
- Arg** Argillite
- Qsg** "Streaky Biotite Gneiss"
- Pqb** Quartz-Biotite Paragneiss

- Contact
- Shear Zone
- Sample number and location

INTRUSIVE UNITS

PLUTONIC ROCKS

- Fg** Fine Grained Granite
- BLG** Bell Lake Granite: Porphyritic granite, granodiorite or quartz-monzonite
- Kg** Killarney Granite:
 - Kg1** Granite, granodiorite:
 - Kg2** Quartz-monzonite
- Tld** Terry Lake Diorite
- To** Tonalite
- Ag** Augen Gneiss

DYKES

- Dd** Diabase Dyke
- Pd** Pegmatite Dyke

UNITS OF UNKNOWN ORIGIN

- Qf** Quartzo-feldspathic Gneiss
- Am** Amphibolite:
 - Am1** Retrograde from granulite facies
- B** Breccia

